Post-modification of Poly(trimethylene carbonate) Derivatives with Ester Free Type and Their Physical and Biological Properties

TAN LEE YAE

A thesis submitted in fulfillment of the requirements for

the degree of

Doctor of Philosophy (Engineering)

September 2022

Materials Science

Nara Institute of Science and Technology

(NAIST)

Post-modification of Poly(trimethylene carbonate) Derivatives with Ester Free Type and Their Physical and Biological Properties

TAN LEE YAE

A thesis submitted in fulfillment of the requirements for

the degree of

Doctor of Philosophy (Engineering)

September 2022

Nara Institute of Science and Technology

Contents

Chapter 3

Synthesis of New Ester-free Poly(trimethylene carbonate) Bearing Cinnamyl Moiety for Biomaterials Applications

Chapter 4

Aromatic Urea PTMC Derivatives for Drug-Release Control Application

General Introduction

Biodegradable polymer has been gaining attention in medical realm, potential to be applied in clinical materials such as drug delivery system[1], vascular engineering[2], cardiac therapy[3], etc. Its biodegradability takes advantageous over current non-biodegradable medical implants. There is no post-surgical procedure required after healing functions as it will be degraded and eliminated metabolically from the body. For instances, the percutaneous transluminal coronary angioplasty (PTCA) with stents and balloon catheters has revolutionized into drug-eluting stent (DES) and drug-eluting balloon (DEB) by using polymeric coating materials and antiproliferative drug to overcome inflammatory response, delayed endothelization, and subacute stent thrombosis (ST) , simultaneously[4]. Synthetic suture also has been developed to be used bioresorbable polymer such as poly(glycolide acid) (PGA) with improved mechanical properties and less inflammatory reactions has found general acceptance[5].

To investigate the medical application, essential properties in term of mechanical properties, thermal stability, biocompatibility, interaction of biodegradable polymer with physiological environment are accountable. For instances, biomaterial used for bone scaffold replaces in cortical bone should have mechanical strength between 100 and 230 MPa[6]. In order to be used as cardiac stent, expansion behavior and radial strength are focused. Commercial bioresorbable stent (i.e Absorb GT1, Elixir, DESlove, etc) exhibit push ability ranges from 34%

to 45% with radial strength in term of pressure between 1.1 atm to 1.6 atm[7]. The desired properties of biomaterial depend on the specific clinical needs.

Up-to-date, there are diversity of biodegradable polymers have been investigated including poly(lactic acid) (PLA), poly(glycolide acid) (PGA), polycaprolactone (PCL) in biomedical applications[8] (**Figure 1**). With the concern of toxicity of degradation-byproduct, PLA as well as PGA degraded into lactic acid and glycolide acid which can be finally incorporated into Krebs cycle and are ultimately expired as CO_2 by the lung or urine. Quantitative data with regard to the acute toxicity of glycolic acid and lactic acid are respectively summarized in **Table 1**[9]. There is study that reported these implants could involve transient local fluid accumulation and decrease in pH from fast degrading polymer may readily override the buffering capacity of the surrounding tissue, particularly in tissue with poor vascularization[10]. If the level of glycolic acid exceeds the capacity of maternal blood buffers to neutralize the acid, may lead to maternal metabolic acidosis[11]. Like other acids of moderate intensity, the free acid become irritant especially on the skin, eyes or mucous membranes.

Table 1. Toxicological Evaluation of Glycolic Acid and of Lactic Acid

Compound	Species	Application	LD mg/kg
glycolic acid	Rat	Oral	LD_{50} 1950
glycolic acid	Rat	Intravenous	LD_{50} 1000
glycolic acid	Guinea pig	Oral	LD_{50} 1920
D,L-lactic acid	Rat	Oral, s.c.	LD_{50} 3730
D,L-lactic acid	Rat	i.p	LD_{50} 2000
D,L-lactic acid	Mouse	oral	LD_{50} 4875
D,L-lactic acid	Mouse	s.c.	LD_{50} 4875
D,L-lactic acid	Rabbit	Oral	LD_{50} 500
D,L-lactic acid	Guinea pig	Oral	LD_{50} 1810

[a] s.c. = subcutaneous; i.p. = intraperitoneal

Alongside mentioned poly(ester)s, poly(carbonate)s particularly poly(trimethylene carbonate) (PTMC) is a potential candidate in clinical applications due to its low toxicity, biocompatibility, biodegradability. It is advantageous that its versatility to introduction various kind of functionality on the side chain of monomer to tune its properties for more advanced applications. The most common synthetic pathway for functional monomer trimethylene carbonate (TMC) is using the versatile 2,2-bishydroxy(methyl)propionic acid (bis-MPA) as precursor to direct functionalization[12].

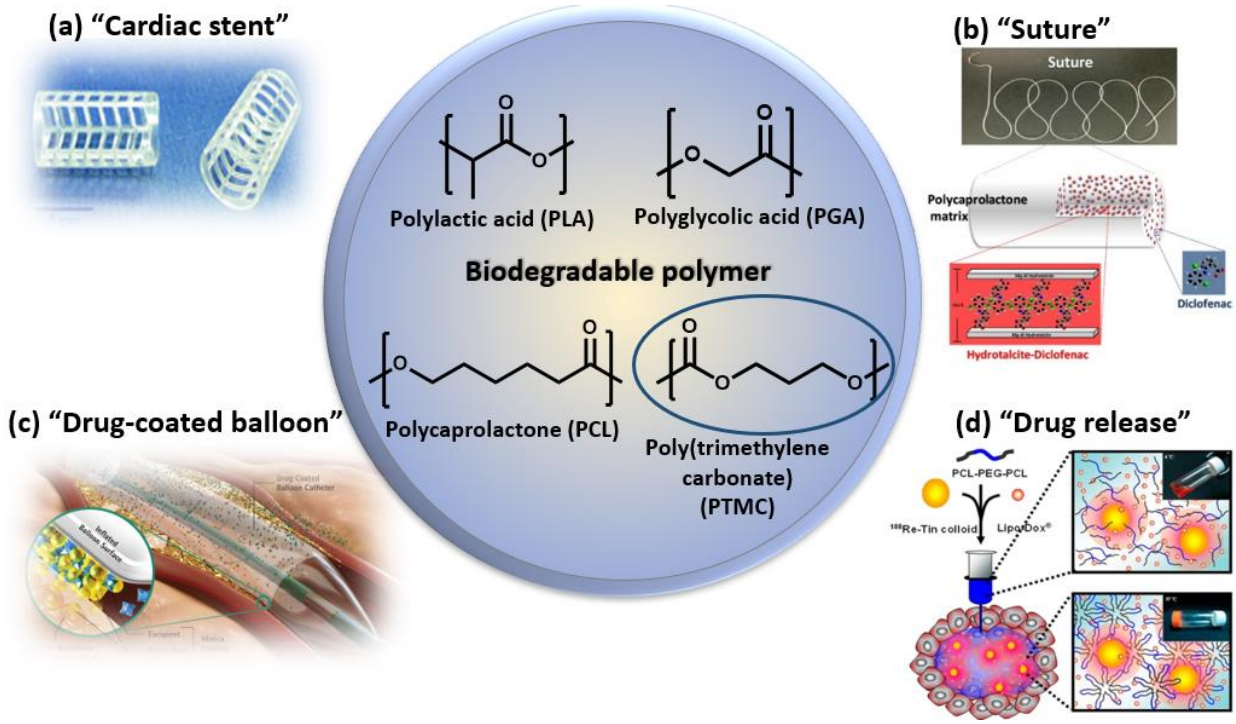

Figure 1. Well-known biodegradable polymers used in medical applications. (a) A prototype stent fabricated from poly(LLA-*co*-GA-*co*-TMC)[13] (b) Concept of anti-inflammatory fibre of PCL[14] (c) Drug-coated balloon technique and mechanism of action[15] (d) PCL-PEG-PCL solution loaded with Lipo-DOX and Re-Tin colloid[16].

Currently, the functionalities such as alkyl[17], acryl[18], alkene[19], alkyne[20], halogen[21],

amino[20], and urea[22] moieties have been cooperated into side chain of TMC monomer. With this effort, properties such as thermal stability, enable the attachment of relevant therapeutic and biological molecules for clinical application have been achieved. For instances, cinnamate-functional 5-methyl-5-cinnamoyloxymethyl-1,3-dioxan-2-one with a molecular weight of 6000 g mol^{-1} (ĐM = 1.87) had a T_g of 42 °C[23]. Antoine et al. had synthesized guanidinium-rich PTMC to explore the impact of these polymer design on their siRNA complexation and cell transfection performance[24].

Up-to-date, the published functionalized TMC has been focused on ester-based structure due to ease of synthetic route[25]. However, I have concern for acidic residues by – product could possibly occur in the body after degradation. Alternative ways to functionalization of TMC is gaining attention to replace either ester-based PTMC or polyesters. Thus, in our group we focused on the ester-free functionalization for fabrication diverse PTMC derivatives as we believe the ether linkage is promising to be generation no acidic compounds after decomposition[26]. In previous works, several potential groups have successfully introduced into PTMC via ether-linkage. Ajiro et al. reported that oligoethylene glycol (OEG) was used for functionalization of PTMC, showing significant thermosensitivity performance at body temperature, which is promising to be essential material in biomedical application[27]. Also, introduction of aromatic ring and alicyclic substituents have increased glass transition temperature, T_g of PTMC from -29°C up to 4°C and -6 respectively[28,29]. Improvement in

mechanical properties by incorporating BTB to form crosslinked film with OEG-TMC was performed[30]. Nobuoka et al. reported that a block copolymer composed of TMC and TMC derivatives with OEG was used to study cilostazol drug eluting by adjusting composition ratio of the block polymer[31].

By far, the efforts on modification PTMC has been achieved by functionalization at monomer level before polymerization. However, it is important to note that not all pendant functionalities such as amine, carboxylic acids and alcohols are compatible with the ring-opening polymerization (ROP). In this case, one of the alternatives to ease without compromise the polymerization efficiency is to functionalize polycarbonates via post-modification pathway[32]. For instances, Hedrick et al. utilized monomer bearing with pentafluorophenyl activated ester pendant groups that remain intact during the acid catalyst polymerization, and further modified with amines and alcohols in high yield in a post-modification step[32]. Also, Dove and co-workers studies reported polymerizing of cyclic monomers with allyl pendant group and further modified with host of thiols through thiol-ene 'click' chemistry[33,34]. A significant number of publications related to the post-modification of cyclic carbonates, particularly with ester-based containing group.

The extension of the versatility of the PTMC to a broader set of functionalities is desired. Several functional groups are attractive to improve PTMC performance. Functional

group such as aromatic ring, urea derivatives, etc have capability to improve physical properties of polymer through intermolecular interaction such as $\pi - \pi$ interaction, and hydrogen bonding. There are many examples of synthetic polymers comprising of aromatic rings including poly(ethylene terephthalate), polycarbonate, polystyrene and high performance polymers imparted excellent mechanical properties to these plastics[35,36]. With these inspirations, our group have synthesized variety of aromatic derivatives of TMC with exploring its thermal performance, showed potential to improve physical properties[37]. Endo and co-workers have reported to use styrene derivative into the monomer 5-ethyl-5-[(p-vinylphenyl)methoxymethyl]-1,3-dioxane-2-one(St6CC) to form cross-linked polymer (**Figure 2**) [38]. This could be motivation to utilize styrene moiety (aromatic bearing with vinyl) for further post-modified with potential functional group as shown in **Figure 3** and **Figure 4**.

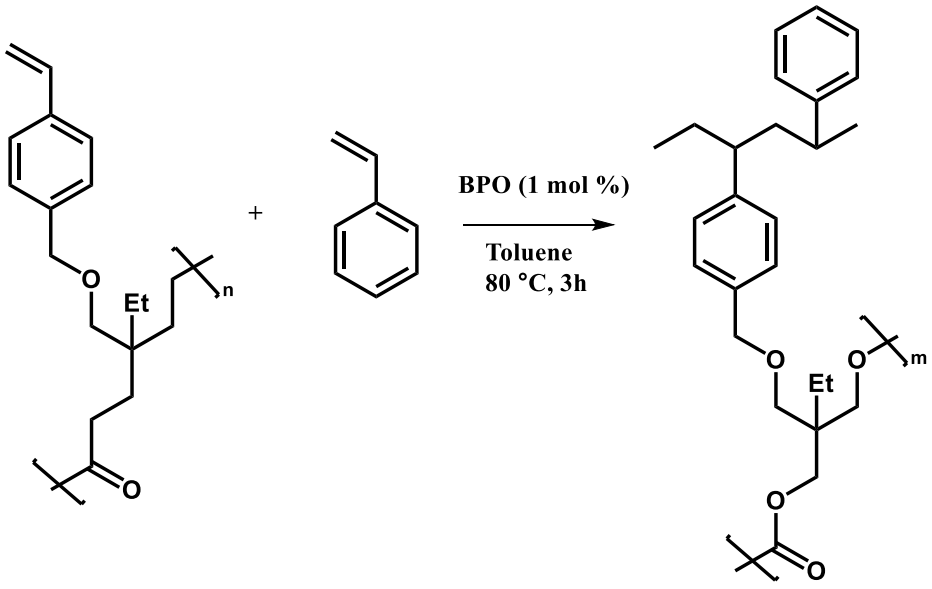

Figure 2. Radical cross-linking of poly(st6CC).

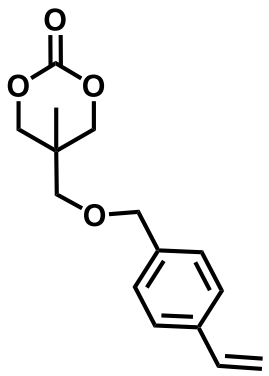

Figure 3. Styrene moiety of TMC derivative.

Notably, functional group containing NH- and C=O groups could be beneficial in term of mechanical properties and therapeutic interaction. Polyurethanes comprising of hard segments formed by di-urethane groups able to interact through hydrogen bonding. The strong quadruple H-bonding interaction between UPy side groups acts as supramolecular crosslinkers enabling the TPU elastomer to have improved mechanical properties (tensile strength up to 25 MPa and toughness ~100 MJ m^{-3})[39]. Besides, it is reported that urea-type moiety bearing with thiol (-NHC(=X)NH_2) (X=O or NH) group could effective in promoting oxidative protein folding which is essential to acquire its biological functions[40]. The capability of urea to interact with proteins by non-covalent interactions allows for increasing solubility of proteins to suppress aggregation. Hydrogen bonding also may provide the drug carriers with enhanced drug-loafing efficiency, promising in drug delivery systems. Fengting and co-workers. developed cross-linked PPV-nanogel with hydrogen-bonded doxorubicin complex with incorporate additional driving force for assembly, such as hydrophobic and π−π interactions

that provide a hydrophobic microenvironment to stabilize the hydrogen bonds, facilitates higher drug loading efficiency (82%)[41]. Thus, it is attractive to include functional group containing NH- and C=O groups such as urea group into PTMC.

Furthermore, to be used as biomaterial implant, antimicrobial performance is required to prevent bacterial infection, implant failure and even death of the patients. The bactericidal coating can be applied to kill the bacteria when they come into contact with the implant surface, inhibit bacterial adherence[42]. These including antimicrobial peptides, metals, nitric oxide and quaternary amines are effective in biocidal performance. Antimicrobial metals such as silver, cobalt, aluminum, and copper have been showed antibacterial ability. However, they might be toxic to human body due to the released metal ions when they are corroded in physiological condition. The microbe-resistant surface can be constructed by using certain anti fouling substances to coat the implant surface. The strategies include superhydrophobic, non-charged or highly hydrated surfaces, which do not favor the attachment of bacteria[43]. PEG and zwitterionic polymers can effectively resist bacterial attachment because of the dynamic motion and steric repulsion of the hydrated polymer chains. Design of these antifouling surfaces is rather complicated as the microorganisms have complex mechanism to enable their attachment to the surfaces[44].

Recently, cinnamyl derivatives and natural-based resources such as thymol showed

antibacterial effect on inhibited the growth of *Staphylococcus sp., Micrococcus sp., Bacillus sp.* and *Enterobacter sp.*[45,46]. Current progress has been made by incorporation either thymol or ester-based cinnamaldehyde as antimicrobial agent with copolymer of PLA/PTMC to fabricate as composite film for food packaging application[47,48]. However, presence of ester-based, numerous steps of functionalization synthetic pathway, low molecular weight and thermal performance are still needed to be developed[47,49]. In this study, ester-free cinnamyl derivatives of TMC (**Figure 4**), ease functionalization steps are explored with incorporation of thymol as antimicrobial function. Also, the cinnamyl structure could possibly induced cycloaddition in double bond to form cyclobutane moiety for crosslinking between PTMC polymer chain. It is known that cyclobutane widely present in bioactive small molecules and natural products serves as a vital medical chemistry[50]. With this perspective, the synthesis of cyclobutanes is highly inspired yet it is still challenging to artificially synthesize due to its highly strained fused cyclobutanes. In general, it could be performed by using [2+2] cycloaddition[51], radical cyclization[52,53], 1,2-rearrangement reactions[54]. Especially, [2+2] cycloaddition possessed facile and versatile methods such as photocatalysis, organocatalysis enable the direct preparation of unsymmetric cyclobutanes through hetero-coupling of two different alkenes.

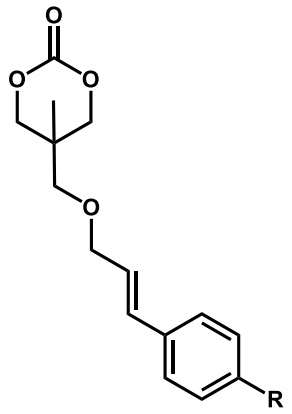

Figure 4. Cinnamyl moiety of TMC derivatives.

Herein, the objective of the present study is focused on the functionalization of ester free type PTMC derivatives with aromatic derivatives for improving physical properties, as well as further post-modification with for intermolecular interaction. The scope of research studies (**Scheme 1**) was categorized in 4 chapters as following:

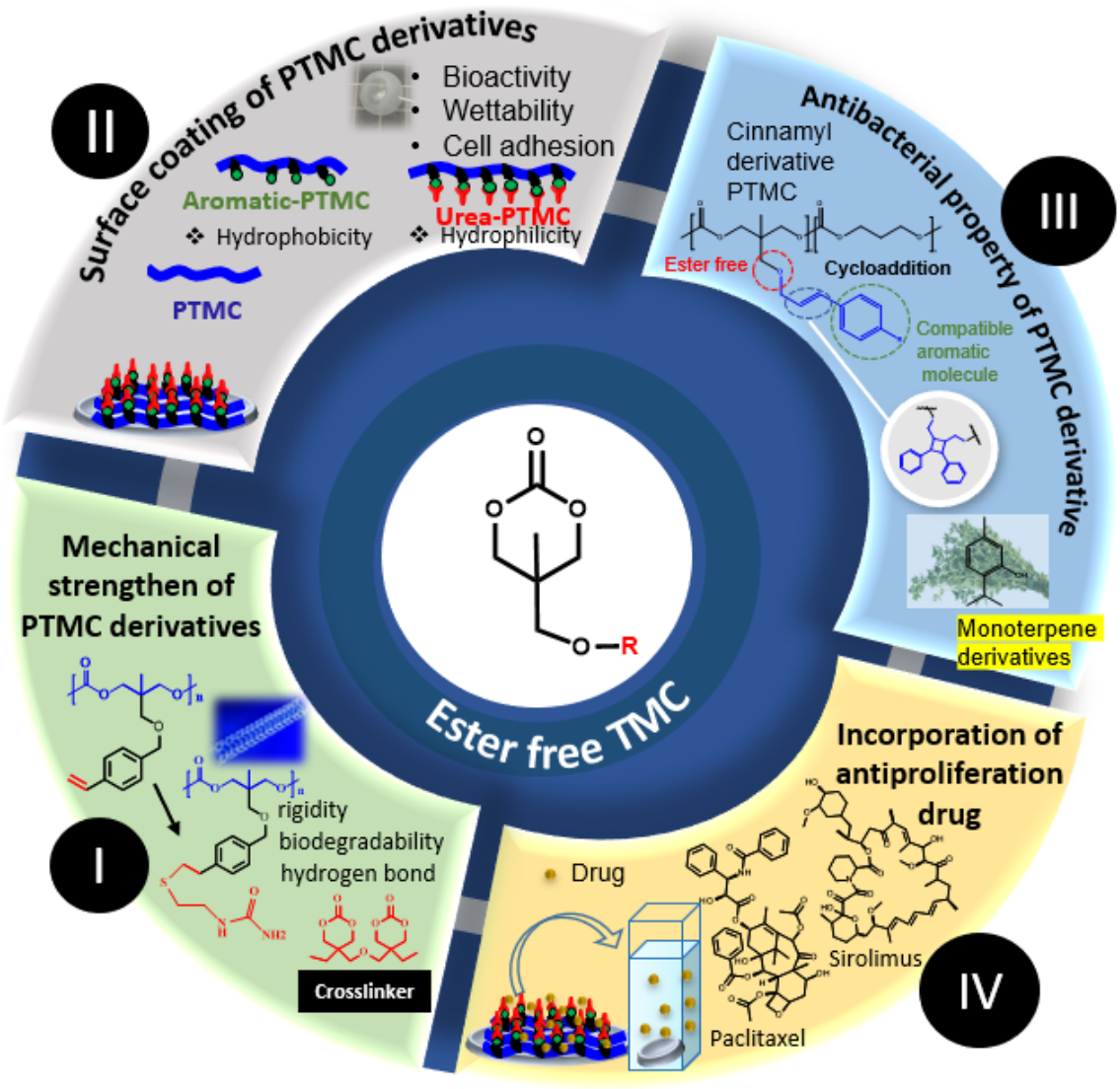

Scheme 1. Overview illustration of post-modification of PTMC derivative research.

In Chapter 1, I aim to fabricate thermally and mechanically-strengthen ester-free PTMC derivatives film with the corporation of crosslinker. Styrene moiety TMC was synthesized as precursor for further post-modified with urea group through facile thiol-ene reaction. Also, 2,2'-bis(trimethylene carbonate-5-ly)-butyl ether (BTB) was used as a crosslinker for forming PTMC derivatives film. Herein, the series of crosslinked polymer film with styrene moiety and urea pendant was examined for promising performances such as thermal stability, mechanical

properties, swelling ratio, degradation behavior in details in this chapter.

In Chapter 2, the objective is to utilize potential functional group such as urea post-modified into PTMC as biomaterial coating for study the bioactivity and biological interaction such as cell adhesion behavior. Ester-free linear homopolymer of 5-methyl-5-(((4-vinylbenzyl)oxy)methyl)-1,3-dioxan-2-one and further post-modified into 1-(2-((4-(((5-methyl-2-oxo-1,3-dioxan-5-yl)methoxy)methyl)phenethyl)thio)ethyl)urea PTMC was performed and used as a biomaterial coating. The surface properties such as morphology, wettability, protein adsorption and cell adhesion were studied in order to examine the effect on presence of urea-moiety on the PTMC side chain after post-modification.

In Chapter 3, the design of cinnamyl derivatives which comprises of vinyl aromatic was promising to functionalize into TMC for antibacterial property as well as post-modification of cycloaddition through the alkene moiety in the cinnamyl derivatives. Diverse design of ester-free cinnamyl PTMC derivatives was synthesized in order to study its inherent benefit of its structure. Copolymerization with PTMC as macroinitiator was used to increase molecular weight as well as physical properties. The polymer was incorporated with essential oil, thymol to study antibacterial performance. Cycloaddition with potential cinnamyl derivatives also have studied in this chapter.

In Chapter 4, the merit of urea group introduction into PTMC polymer was further studied in term of drug release control by coating 1-(2-((4-(((5-methyl-2-oxo-1,3-dioxan-5-yl)methoxy)methyl)phenethyl)thio)ethyl)urea PTMC on the stainless steel with incorporation with drugs sirolimus and paclitaxel. These drugs are used as medication to help prevent blockage (restenosis) were applied with the polymer to study the effect of functional group on the drug releasing rate as well as cell adhesion.

Overall, as comparing to previous research this study has remained to extend the effort to reduce the toxicity of biodegradable polymer to be safe for human body use by using ether linkage to introduce promising functional group into PTMC side chain, yet we motivated to develop more advanced functionality that is difficult to prepare before polymerization. In this study has pioneered post-modification of ester-free PTMC, which is particularly attractive as it allows to be used to prepare a library of functional polymers with relative ease, avoiding the need to optimize multiple monomer syntheses and polymerization conditions. By this, the merits such as efficient synthetic pathway, diverse improvement of polymer properties can be achieved with ease.

References

1 Y. K. Sung and S. W. Kim, *Biomater Res*, **2020**, 24, 12.

2 L. Gui, L. Zhao, R. W. Spencer, A. Burghouwt, M. S. Taylor, S. W. Shalaby and L. E. Niklason, *Tissue Eng Part A*. **2011**, 17, 1191–1200.

3 D. Wee, Y. Toong, H. W. Toh, J. Chen, K. Ng, P. En, H. Wong, H. L. Leo, S. Venkatraman, L. P. Tan, H. Y. Ang and Y. Huang, *Int. J. Mol. Sci.* **2020**, 21, 3444.

4 R. v. Jeger, S. Eccleshall, W. A. Wan Ahmad, J. Ge, T. C. Poerner, E. S. Shin, F. Alfonso, A. Latib, P. J. Ong, T. T. Rissanen, J. Saucedo, B. Scheller and F. X. Kleber, *JACC Cardiovasc Interv.*, **2020,** 13, 1391–1402.

5 B. Joseph, A. George, S. Gopi, N. Kalarikkal and S. Thomas, *Int J Pharm.* **2017,** 524, 454–466.

6 S. Prasadh and R. C. W. Wong, *Oral. Sci. Int.*, **2018,** 15, 48–55.

7 T. Qiu and L. Zhao, *Vessel Plus*, **2018**, 2, 12.

8 K. R. Kunduru, A. Basu and A. J. Domb, *Encyclopedia of Polymer Science and Technology*, 2016, 1–22.

9 D. Pappalardo, rn Mathisen and A. Finne-Wistrand, *Biomacromolecules*, **2019**, 20, 4, 1465–1477.

10 O. Böstman and H. Pihlajamäki, *Biomaterials*, **2000**, 21, 2615–2621.

11 E. W. Carney, N. L. Freshour, D. A. Dittenber and M. D. Dryzga, *Toxicol Sci*, **1999**, 50,

117–126.

12 S. Tempelaar, L. Mespouille, *Chem. Soc. Rev.*, **2013**,42, 1312-1336

13 J. Dong, L. Liao, L. Shi, Z. Tan, Z. Fan, S. Li and Z. Lu, *Polym Eng Sci*, **2014**, 54, 1418–1426.

14 O. Catanzano, S. Acierno, P. Russo, M. Cervasio, M. del Basso De Caro, A. Bolognese, G. Sammartino, L. Califano, G. Marenzi, A. Calignano, D. Acierno and F. Quaglia, *Mater. Sci. Eng. C*, **2014**, 43, 300–309.

15 R. v. Jeger, S. Eccleshall, W. A. Wan Ahmad, J. Ge, T. C. Poerner, E. S. Shin, F. Alfonso, A. Latib, P. J. Ong, T. T. Rissanen, J. Saucedo, B. Scheller and F. X. Kleber, *JACC Cardiovasc Interv*, **2020**, 13, 1391–1402.

16 T. T. Hoang Thi, L. H. Sinh, D. P. Huynh, D. H. Nguyen and C. Huynh, *Front. Chem.*, **2020**, 8, 19–19.

17 C. Bartolini, L. Mespouille, I. Verbruggen, R. Willem, P. Dubois, *Soft Matter*, **2011**, 7, 9628-9637.

18 N. Nemoto, F. Sanda and T. Endo, *J. Polym. Sci., Part A-1: Polym. Chem.*, **2001**, 39, 1305–1317.

19 F. He, C. F. Wang, T. Jiang, B. Han and R. X. Zhuo, *Biomacromolecules*, **2010**, 11, 3028–3035.

20 R.C. Pratt, F. Nederberg, R.M. Waymouth and J.L. Hedrick. *Chem. Commun*, **2008**, 114-

116.

21 D. P. Sanders, K. Fukushima, D. J. Coady, A. Nelson, M. Fujiwara, M. Yasumoto and J. L. Hedrick, *J Am Chem Soc*, **2010**, 132, 14724–14726.

22 S. H. Kim, J. P. K. Tan, F. Nederberg, K. Fukushima, J. Colson, C. Yang, A. Nelson, Y. Y. Yang and J. L. Hedrick, *Biomaterials*, **2010,** 31, 8063–8071.

23 M. Helou, G. Moriceau, Z.W. Huang, S.C. Marion, S.M. Guillaume. *Polym. Chem.*, **2011**,2, 840-850.

24 A.Frère, M.Kawalec, S.Tempelaar, P.Peixoto, E.Hendrick, O.Peulen, B.Evrard, P.Dubois, L.Mespouille, D.Mottet, and G.Piel. *Biomacromolecules* **2015** 16, 769-779.

25 S. Tempelaar, L. Mespouille, O. Coulembier, P. Dubois and A. P. Dove, *Chem. Soc. Rev*., 2013, **42**, 1312–1336.

26 N. Chanthaset and H. Ajiro, *Materialia* **2019**, 5, 100178.

27 H. Ajiro, Y. Takahashi and M. Akashi, *Macromolecules*, **2012**, 45, 2668–2674.

28 H. Nobuoka, R. Miyake, J. Choi, H. Yoshida, N. Chanthaset and H. Ajiro, *Eur. Polym. J.*, **2021**, 160, 110782.

29 H. Nobuoka, H. Ajiro, H. Nobuoka and H. Ajiro, *Macromol. Chem. Phys*, **2019**, 220, 1900051.

30 H. Nobuoka and H. Ajiro, *Chem. Lett.*, **2018**, 48, 245–248.

31 H. Nobuoka, M. Nagasawa, N. Chanthaset, H. Yoshida, Y. Haramiishi and H. Ajiro, *J.*

Polym. Sci., **2020**, 58, 2347–2354.

32 A. Yuen, C. Bernard, U. Lyon, A. Veloso, A. Y. Yuen, A. Bossion, D. Mecerreyes, J. L. Hedrick, A. P. Dove and H. Sardon, *Polym. Chem*. **2018.**

33 A. W. Thomas and A. P. Dove, *Macromol. Biosci.*, **2016**, 16, 1762–1775.

34 S. Tempelaar, L. Mespouille, P. Dubois and A. P. Dove, *Macromolecules*, **2011,** 44, 2084–2091.

35 P. Zinck, F. Bonnet, A. Mortreux and M. Visseaux, *Prog. Polym. Sci.*, **2009**, 34, 369–392.

36 D. Shukla, Y. S. Negi, J.S. Uppadhyaya and V. Kumar, *Polym. Rev.*, **2012**, 52, 189–228.

37 H. Nobuoka and H. Ajiro, *Tetrahedron Lett.*, **2019,** 60, 164–170.

38 T. Miyagawa, M. Shimizu, F. Sanda and T. Endo, *Macromolecules*, **2005**, 38, 7944–7949.

39 J. Hu, R. Mo, X. Jiang, X. Sheng and X. Zhang, *Polym. Chem.*, **2020**, 11, 2585-2594.

40 S. Okada, M. Matsusaki, K. Arai, Y. Hidaka, K. Inaba, M. Okumura and T. Muraoka, *Chem. Commun.***, 2019**, 55, 759–762.

41 T. Senthilkumar, F. Lv, H. Zhao, L. Liu and S. Wang, *ACS Appl. Bio Mater*. **2019**,2,6012-6020.

42 P.L. Harrison, M.A.A. Rahman, K. Miller and P.N. Strong. *Toxicon*. **2014**, 88, 115-137.

43 D. Campoccia, L. Montanaro and C. R. Arciola, *Biomaterials***, 2013**, 34, 8533–8554.

44 L. G. Harris, S. Tosatti, M. Wieland, M. Textor and R. G. Richards, *Biomaterials*, **2004**,

25, 4135–4148.

45 V. Moleyar and P. Narasimham, *Int. J. Food Microbiol.*, **1992,** 16, 337–342.

46 A. Marchese, I. E. Orhan, M. Daglia, R. Barbieri, A. di Lorenzo, S. F. Nabavi, O. Gortzi, M. Izadi and S. M. Nabavi, *Food Chem.*, **2016**, 210, 402–414.

47 Y. Qin, J. Yang and J. Xue, *J. Mater. Sci.*, **2015**, 50, 1150–1158.

48 J. P. Chesterman, F. Chen, A. J. Brissenden and B. G. Amsden, *Polym. Chem.*, **2017**, 8, 7515–7528.

49 C. Hui, Z. Wang, Y. Xie and J. Liu, *Green Synthesis and Catalysis***, 2022**.

50 S. Poplata, A. Tröster, Y. Q. Zou and T. Bach, *Chem. Rev.*, **2016**, 116, 9748–9815.

51 N. Zhao, S. Yin, S. Xie, H. Yan, P. Ren, G. Chen, F. Chen and J. Xu, *Angewandte Chemie International Edition*, **2018**, 57, 3386–3390.

52 C. Shu, A. Noble and V. K. Aggarwal, *Angewandte Chemie International Edition*, **2019**, 58, 3870–3874.

53 R. Meier and D. Trauner, *Angewandte Chemie International Edition*, **2016**, 55, 11251–11255.

Chapter 1

Synthesis and Preparation of Crosslinked Films with Ester-free Poly(trimethylene carbonate) Bearing Aromatic Urea Moiety

1.1 Introduction

Recently, biodegradable polymers which to be used in biomaterials have become potential development and attentions. Many efforts have been focused on custom designing and synthesizing polymers with tailorable properties that can appropriately match the unique and particular requirements of each individual clinical application. Some of the important performance such as degradation period should matching the healing process, mechanical performance able to withstand on indicated application, non-toxic degradation products to avoid inflammatory or adverse effects upon implantation in the body [1]. **Table 1-1** showed the mechanical performance of well-known biodegradable polymer used in biomaterial application [2,3]. Polyglycolide (PGA) is known as one of the first biodegradable synthetic polymer to be applied in clinical application. PGA possesses excellent high tensile modulus with approximately 6 ─ 7 GPa and highly crystalline polymer. Its glass transition temperature ranges from 35 ─ 40 °C and melting point is greater than 200 °C. Due to its remarkable stiffness, it has been used as bone internal fixation

devices (Biofix ®). However, its limitation due to its low solubility and short degradation period with lose its strength in 1 ─2 months and losses mass with 6 to 12 months, make it difficult to be fabrication processing[2]. Another major candidate is poly(lactic acid) (PLA) that having two optically active forms: L-lactide and D-lactide. Generally, L-lactide is the naturally occurring isomers, polymerization forming poly(L-lactide) (PLLA). It has glass transition temperature approximately 60 ─ 65 °C and melting point around 175 °C. PLLA possesses good tensile strength and high modulus which is approximately 2 ─ 4 GPa, leading it suitable to be used in load bearing applications[3]. Poly(DL-lactide) (PDLLA) is random distribution of both L-lactide and D-lactide units which attribute amorphous nature of polymer. It has glass transition temperature of 55 ─ 60 °C and lower strength (~19 GPa). Compared to PGA, PLA polymer which is being hydrophobic, slower its degradation rate. Similar to PGA, PLA undergo bulk erosion that degrade via citric acid cycle. There is concern about the acidic degradation products that leading the urge to develop other biodegradable polymer candidate that inherent low toxicity and acidity upon degradation in human body [4].

Table 1-1. Mechanical performance of well-known biodegradable polymer used in biomaterial application [2,3].

Polymer	Strength (MPa)	Elongation at break (%)	Modulus (GPa)
PLA	65	2-6	2-4
PGA	90-110	1-2	6-7
PCL	23	> 4000	0.34─0.36
PTMC	1	60	0.03

Poly(trimethylene carbonate) (PTMC) has received attractive attention for its exceptional biocompatibility, flexibility and low toxicity. Unlike the aliphatic polyesters, the unique of degradation in term of non-acidic degradation by-product, degradation via surface erosion mechanism opens new era for biodegradable in biomedical field. It has glass transition temperature around -20 °C and being an elastomeric and poor mechanical performance, its application on medical field restricts on drug delivery vehicles, implant material for soft tissue regeneration [5,6].

The potential of PTMC could be expanded to more practical application relies on the mechanical properties and create more functionalities to meet current medical demand. There are several approaches to alter and modify the properties of PTMC including copolymerization with PLA[7,8], increase its molecular weight[9], functionalization PTMC with ester-based moiety[10,] Joanna et al. developed poly(lactide-*co*-glycolide-*co*-trimethylene carbonate) terpolymer with mechanical property, stress at break > 50 MPa that promising to be used for stent application[7]. Unfortunately, there are some drawbacks incurred such as acidic pH upon decomposition[11] and difficulties in processing process[12].

Regards of side effects of ester-based structure of current biodegradable polymer, development of more advanced and biocompatible biomaterial is surged. Herein, our group was pioneered ester-free PTMC derivatives which have the virtues of profound functionalities while no acid generation during degradation. For instances, introduction of various ether-linkage of aromatic pendant group derivatives on PTMC has successfully enhanced the physical properties[13].

Importantly, we have synthesized PTMC bearing with oligo(ethylene glycol) which has proved not only the biocompatibility but the thermosensitivity at body temperature, further strengthen the characteristics of PTMC[14]. Also, the cyclopolymer based ester-free PTMC, derived from styrenic difunctional monomers PTMC has been reported in order to control orientation and stereochemical[15].

Integration functionality to the end chains is a straightforward way to alter or introduce physical and chemical functions of PTMC. Attaching functional pendant groups into backbone of PTMC provide the possibility of polymer modifications and further extend more biomedical applications. For instance, Lizundia *et al*, explored addition of aromaticity into polyester afforded improved thermal and mechanical characteristics with considerable degradability[16]. Additionally, considering that the urea-type group could associate with interfacial bonding, investigation of the incorporation of urea-type group on PTMC on the effect of the stiffness and hydrophilicity are interested[17]. Tunable stiffness and hydrophilicity have claimed to influence the cell behaviour and adherence depend on type of cell tissues and physiological responds. The attached functional side groups could contribute to the macromolecular self-assembly behaviour via polymer intermolecular interaction. π-π Interactions between two aromatic compounds, urea functionality, and S-S crosslinked thiols are versatile substituents to interact with each other, producing tailor-made crosslinking polymer with tunable bulk properties. Utilization of reactive terminal moiety (i.e. alkyl[18], alkyne[19], halide[20], epoxy group[21]) is prerequisite for further introduce a different

functional group. Among the important and efficient click chemistry, comprising thiol-ene[22], alkyne-azide cycloaddition[21], Michael addition[22], Diels-Alder[23], epoxide-amine reactions[24], etc are facile with high conversion. Notably, thiol-ene reaction is of great interest owing for their stability and robust crosslinker are valuable for medical, biomaterial and nano-engineering applications. It is revealed that synthetic thiol bearing with urea group able to mimic the bio-conjugation for tracking cellular events, drug delivery, enzyme function, etc[25].

In this study, I aimed to prepare the novel biodegradable films with ester free structures for the possible biomedical application as shown in **Figure 1-1**. The network structure by crosslinking, π–π interaction of aromatic groups, and the hydrogen bonding by urea groups were designed, in order to overcome the mechanical strength of PTMC, as well as the thiol modification approach. 2,2'-bis(trimethylene carbonate-5-ly)-butyl ether (BTB) was used as a crosslinker, and the amount of crosslinkers was also varied to tune the properties. The degradation behaviour, thermal properties, mechanical properties and water consumption of introduction vinylbenzyl- and thiol-urea group into ester-free PTMC was discussed.

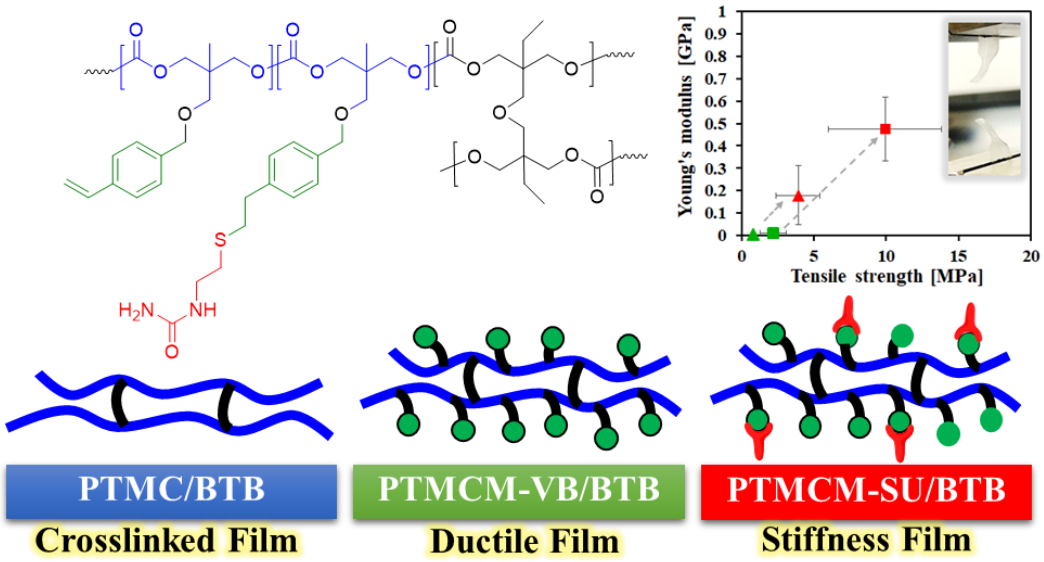

Figure 1-1. Preparation of crosslinked PTMC derivatives film.

1.2 Experimental Section

1.2.1 Materials

Trimethylolethane, ethyl chloroformate, di(trimethylopropane), 1,8-diazabicyclo[5.4.0]-7-undecene (DBU) and benzyl alcohol (BnOH) were purchased from Tokyo Chemical Industry (TCI), Japan. Azobisisobutyronitrile (AIBN) was purchased from Kanto Chemical Co. Potassium hydroxide pellet (KOH), potassium cyanate (KOCN) and 1M hydrochloric acid (HCl) were purchased from Nacalai Tesque. 4-Vinylbenzyl chloride and 2,2-dimethoxy-2-phenylacetophenone (DMPA) were purchased from Sigma-Aldrich. Trimethylamine was purchased from Fujifilm Wako Pure Chemical Corporation (WAKO), Japan. Anhydrous dimethyl

sulfoxide (DMSO), dimethylformamide (DMF), tetrahydrofuran (THF), ethyl acetate, hexane, isopropanol, sodium chloride, dichloromethane (DCM) were used without purification.

1.2.2 Synthesis of 2-methyl-2-(((4-vinylbenzyl)methoxy)methyl)1,3-propanediol (diol-styrene)

A solution of 25.6 g (0.21 mol) trimethylolethane in 85 ml of anhydrous DMSO, KOH pellet 11.9 g (0.21 mol) were added into reaction flask under nitrogen atmosphere. The mixture was kept at 0°C, then 15 ml (0.11 mol) of 4-vinylbenzyl chloride was added dropwise. The reaction mixture was allowed to stir at room temperature for 4 h. The mixture was then quenched with 5MHCl under ice bath followed by extraction with ethyl acetate and brine. The organic phase was retained, dried over $MgSO_4$ and evaporated in vacuo. The crude was purified by column chromatography through ethyl acetate/ hexane (5:1) system. The product fraction was dried to give a white solid yield 14.66 g (58%). ^{1}H NMR (400Hz, $CDCl_3$) (**Figure 1-1a**): δ 7.40 (d, J = *8.4 Hz* 2H, -C_6H_4-), 7.27 (d, J = *8.4 Hz* 2H, -C_6H_4-), 6.71 (dd, J = 18 Hz , H, -CH=CH_2), 5.75 (d, J = 16.8 Hz H, -CH=CH_2), 5.24 (d, J = 11.2 Hz, H, -CH=CH_2), 4.50 (s, 2H, -$OCH_2C_6H_4$-), 3.72 (dd, J = 10.8 Hz, 2H, CH_2OH), 3.60 (dd, J = 10.8 Hz, 2H, CH_2OH), 3.46 (s, 2H, -CH_2O-), 2.33 (brs, 2H,-OH), 0.82 (s, 3H, -CH_3). IR: ν (cm^{-1}) 3356, 3283 (-OH); 1624 (C=C); 1105 (C-O). ESI MS: m/z: calcd for $C_{14}H_{20}O_3Na$, 259.1310 $[M+Na]^+$;found: 259.1319.

1.2.3 Synthesis of 5-methyl-5-(((4-vinylbenzyl)methoxy)methyl)-1,3-dioxanone (TMCM-VB)

TMCM-VB was synthesized by introducing the solution of diol-styrene (13.8 g, 0.058 mol) in anhydrous THF (58 ml) and ethyl chloroformate (16.6 ml, 0.17 mol) under nitrogen atmosphere. Next, the mixture was kept at 0°C and trimethylamine (24 ml, 0.17 mol) was added dropwise. The mixture was stirred for 4 hand then quenched with 1 M HCl and extraction with DCM and water. The organic phase was then dried with $MgSO_4$ and evaporated in vacuo. The crude was recrystallized in hexane/isopropanol to obtain 10.02 g (0.04 mol) of white crystals TMCM-VB (yield: 66%).^{1}H NMR (400Hz, $CDCl_3$) (**Figure 1-1b**): δ 7.40 (d, *J* = 8 Hz, 2H, -C_6H_4-), 7.25 (d, *J* = 6.8 Hz, 2H, -C_6H_4-), 6.72 (dd, *J* = 17.6 Hz, H, -CH=CH_2), 5.76 (d, *J* = 17.2 Hz, H, -CH=CH_2), 5.28 (d, *J* = 11.6 Hz, H, -CH=CH_2), 4.50 (s, 2H, -$OCH_2C_6H_4$-), 4.36 (d, *J* = 10.8 Hz, 2H, CH_2OC=O), 4.08 (d, *J* = 10.8 Hz, 2H, CH_2OC=O), 3.40 (s, 2H, -CH_2O-), 1.10 (s, 3H, -CH_3). IR: v (cm^{-1}) 1744 (C=O); 1624 (C=C); 1100 (C-O). ESI MS: m/z: calcd for $C_{15}H_{18}O_4Na$, 285.1103 $[M+Na]^+$; found: 285.0970.

1.2.4 Synthesis of 2,2´-bis(trimethylene carbonate-5-yl)-butylether crosslinker (BTB) and 1-(2-mercaptoethyl)urea (SU)

The synthetic method of 2,2´-bis(trimethylene carbonate-5-yl)-butylether crosslinker (BTB)[26] and 1-(2-mercaptoethyl)urea (SU)[27] were synthesized as the references. The synthesis was

confirmed by ^{1}H NMR as shown in **Figure S1-1** and **Figure S1-2**.

1.2.5 Film preparation with TMC and BTB (PTMC/20%BTB)

PTMC/20%BTB film was performed under nitrogen atmosphere. DBU and BnOH were used as catalyst and initiator, respectively. TMC (1.5 g) and BTB (0.88 g) was dissolved in 7.35 ml of DCM. After that, DBU and benzyl alcohol were added and transferred to a Teflon mold. The mixture was left for overnight and followed by gently vacuum drying to remove the solvent. The obtained cross-linked film was flexible and transparent.

1.2.6 Film preparation with TMCM-VB and BTB (PTMCM-VB/20%BTB and PTMCM-VB/50%BTB)

PTMCM-VB/20%BTB and PTMCM-VB/50% BTB were prepared with the same procedure as above description by using the TMCM-VB monomer with 20% of BTB and 50% BTB, respectively. IR: v (cm^{-1}) 1744 (C=O); 1624 (C=C); 1233 (C-O in polymer backbone); 1100 (C-O in side chain).

1.2.7 Film modification by thiol–ene reaction of PTMCM-VB/20%BTB (PTMCM-SU/20%BTB) by DMPA

The PTMCM-VB/20%BTB (0.3 g) was modified by thiol-ene reaction using SU (0.673 g, 0.057 mol) in DMF/H_2O 25 ml:10 ml. DMPA (0.008 g, 0.03 mmol) as UV initiator was feed into the

reactor under nitrogen atmosphere. Next, the mixture was kept at 0°C under ice bath for 4 hours. The film was then rinsed with DMF and water to get rid excess unreacted SU. The film was vacuum drying at 60°C to yield the PTMCM-SU/20%BTB. ^{13}CP MAS (400 Hz): 7.94 (-CH_3CH_2), 17.35((-$CH_3CCH_2CH_2$),23.65(-$CH_2C(CH_2)_2$), 31.70(-CH_2S), 36.57(-CH_2CH_2S), 40.27(-CH_2NH), 72.02(-$OCH_2C(CH_2O)CH_2$), 114.50(CH_2=CH), 127.43(-C_6H_4-), 137.54(-C_6H_4-, CH=CH_2), 143.76(C(O)NH_2), 155.63(-OC=O). ELEM.ANAL. C, 64.97%; H, 7.06%; N, 0.95%.

1.2.8 Film modification by thiol–ene reaction of PTMCM-VB/20%BTB (PTMCM-SU/20%BTB) by AIBN

The PTCM-VB/20%BTB (1.80 g) was modified by thiol-ene reaction using SU (4.12 g, 0.034 mol) in 80 ml DMF. AIBN (0.020 g, 0.12 mmol) as thermal initiator was feed into the reactor under nitrogen atmosphere. Next, the mixture was kept at 80°C for overnight. The film was then rinsed with DMF and water to get rid excess unreacted SU. The film was vacuum drying at 60°C to yield the PTMCM-SU/20%BTB. ^{13}CP MAS (400 Hz): 7.94 (-CH_3CH_2), 17.35((-$CH_3CCH_2CH_2$), 23.65(-$CH_2C(CH_2)_2$), 31.70(-CH_2S), 36.57(-CH_2CH_2S), 40.27(-CH_2NH), 72.02(-$OCH_2C(CH_2O)CH_2$), 114.50(CH_2=CH), 127.43(-C_6H_4-), 137.54(-C_6H_4-, CH=CH_2), 143.76(C(O)NH_2), 155.63(-OC=O). ELEM.ANAL. C, 61.58%; H, 6.86%; N, 2.63%. IR: v (cm^{-1}) 3385 (N-H); 1744 (C=O); 1740 (C=O in polymer backbone); 1667 (C=O in SU

group). Similarly, PTMCM-TB/50%BTB was modified by SU to obtain PTMCM-SU/50%BTB as above description.

1.2.9 Degradation behavior

PTMCM/20%BTB was demonstrated with 3 replicates (6 mm × 2 mm × 0.5 mm). Sample was soaked in 2 ml of lipase solution (5mg/ml), HCl solution (0.01M), and NaOH solution (0.01M). The films were monitored weight simultaneously at 4, 7, 30, 60 and 90 days and calculated as the following equation.

$$\text{Degradation rate} = \frac{Wi - W_d}{W_i} \times 100\%$$

Where w_i; initial weight before soaking and w_d; dried weight of the films at specific day.

1.2.10 Thermal resistance

The thermal stability of the polymeric film was determined by a thermo-gravimetric analyser TGA-50 (Shimadzu) under nitrogen atmosphere with 10°C/min flow rate to 500°C. Differential scanning calorimetry (DSC) spectra were also analysed by a Hitachi DSC6200 in the atmosphere with temperature ramp rate 10°C/min in range 70°C—200°C.

1.2.11 Mechanical properties

A mechanical strength of the polymeric films was evaluated by using EZ-SX texture analyzer

(Shimadzu) at room temperature (25 °C). The specimens with flat dumbbell-shape were tested at least three replicates.

1.2.12 Water retention capacity

The swelling ratio (S.R) of films was determined as the following equation:

$$\text{S.R.} = \frac{W_s - W_d}{W_d} \times 100\%$$

Where w_s; the weight of swollen film in PBS solution (24 h), w_d; dried films (n=3)

1.3 Results and Discussion

1.3.1 Monomer synthesis and polymeric film preparation

The results cast a new light on a novel ester-free TMC monomer by introduction of vinyl aromatic functionality for thiol-ene click reaction as shown in **Scheme 1-1a**, although the similar monomer has been previously reported as St6CC carbonate monomer, involved ethyl group and styrene side chain in order to obtain cross-linked polymer network via radical cross-linking[28]. Compared to the previous study, this study possessed methyl group at the side chain, which could favorable to be used for suppression of protein adsorption purpose due to more hydrophilicity induced. Also, the synthetic monomer was obtained within two steps of nucleophilic substitution and cyclization. With a simple synthetic process, TMCM-VB monomer was derived from 4-vinylbenzyl chloride and trimethylolethane by Williamson ether

reaction. After cyclization reaction, the chemical structure was confirmed by ^{1}H NMR spectrum (**Figure 1-2**). The spectrum showed three signals at 5.27, 5.77, and 6.72 ppm which is attributed to the vinylic protons of TMCM-VB. In order to fabricate the films, TMCM-VB monomer was then incorporated with BTB at different ratio (**Scheme 1-1b).** The films with alter crosslinker content, 20% and 50% of BTB were denoted as PTMCM-VB/20%BTB and PTMCM-VB/50%BTB, respectively. According to determine chemical group, a FT-IR peak at 1744 cm^{-1} was appeared in both monomer and polymeric films which attributes from the C=O stretching due to TMC base. While, an ester bond of polymer backbone was also approved a band around 1233 cm^{-1} of C-O stretching. TMCM-VB, PTMCM-VB/20%BTB and PTMCM-VB/50%BTB were confirmed the functionality of pendant groups such as vinyl aromatic and ether linkage with the intense peaks at 1100 cm^{-1} of C-O stretching and 1630 cm^{-1} of C=C. To confirm the presence of CH_2 and CH_3, the signals around 2860 cm^{-1}, 2960 cm^{-1} were observed and had slightly intense after polymerization. Alternatively, the standard film was prepared from unmodified TMC monomer (commercial) and 20% of BTB as PTMCM/20%BTB.

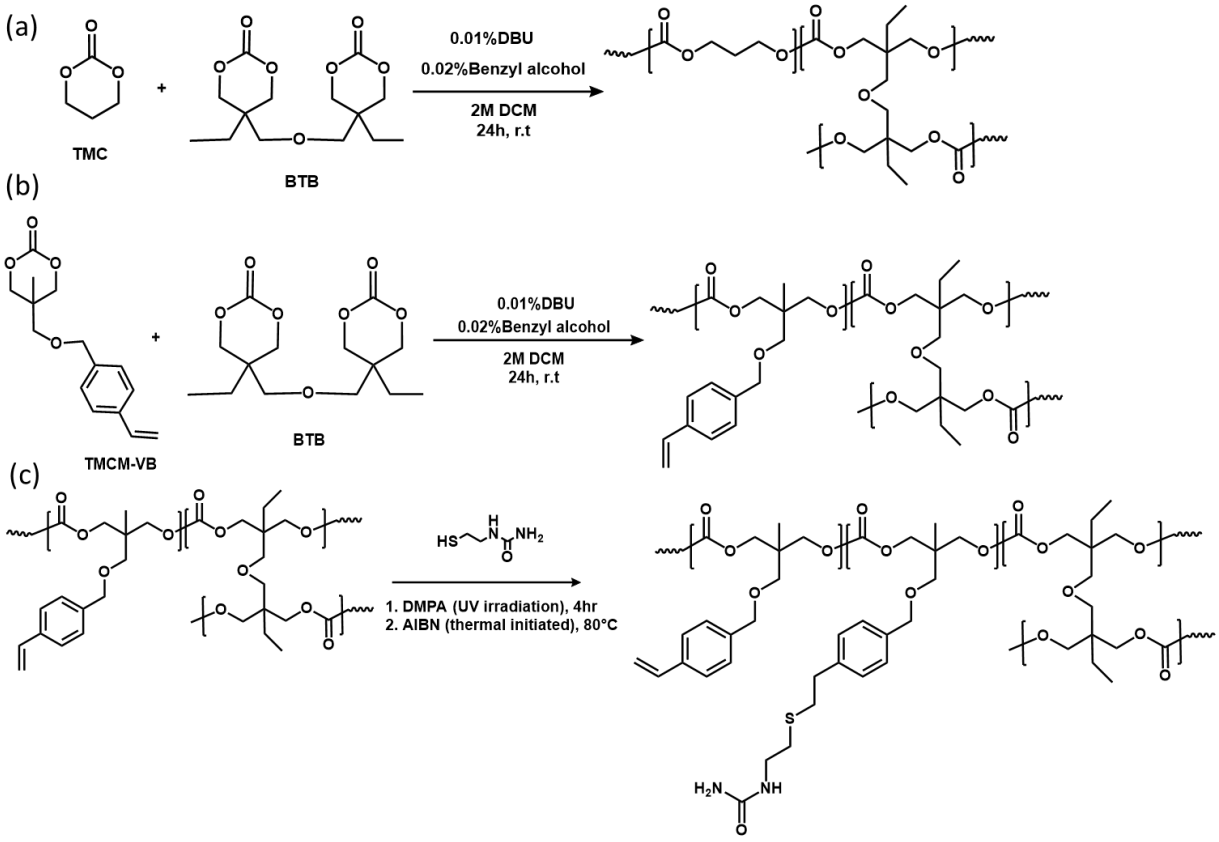

Scheme 1-1. Preparation of PTMC/20%BTB film (a), preparation of PTMCM-VB/20%BTB and TMCM-VB/50%BTB films (b), and proposed post-modification pathway for attachment urea group into PTMCM-VB/20%BTB and PTMCM-VB/50%BTB (c).

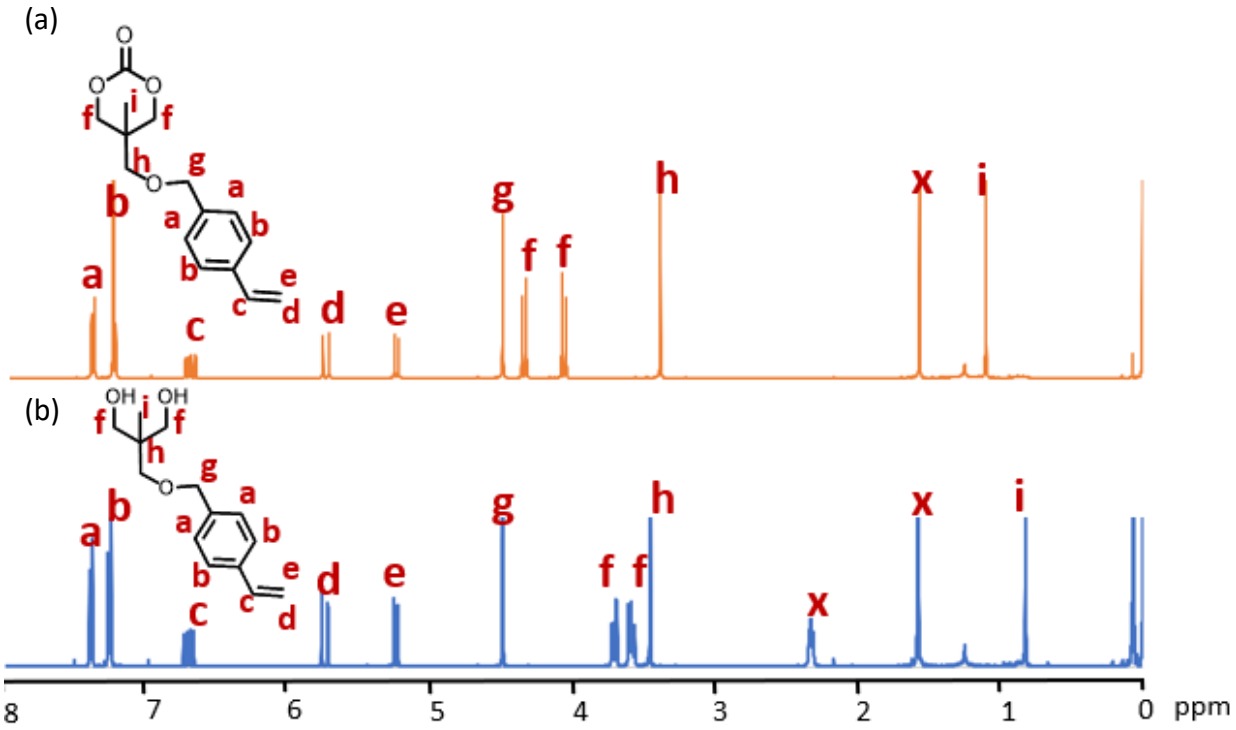

Figure 1-2. ^{1}H NMR spectra of TMCM-VB (a) and diol-styrene (b) ($CDCl_3$, 400 MHz, r.t).

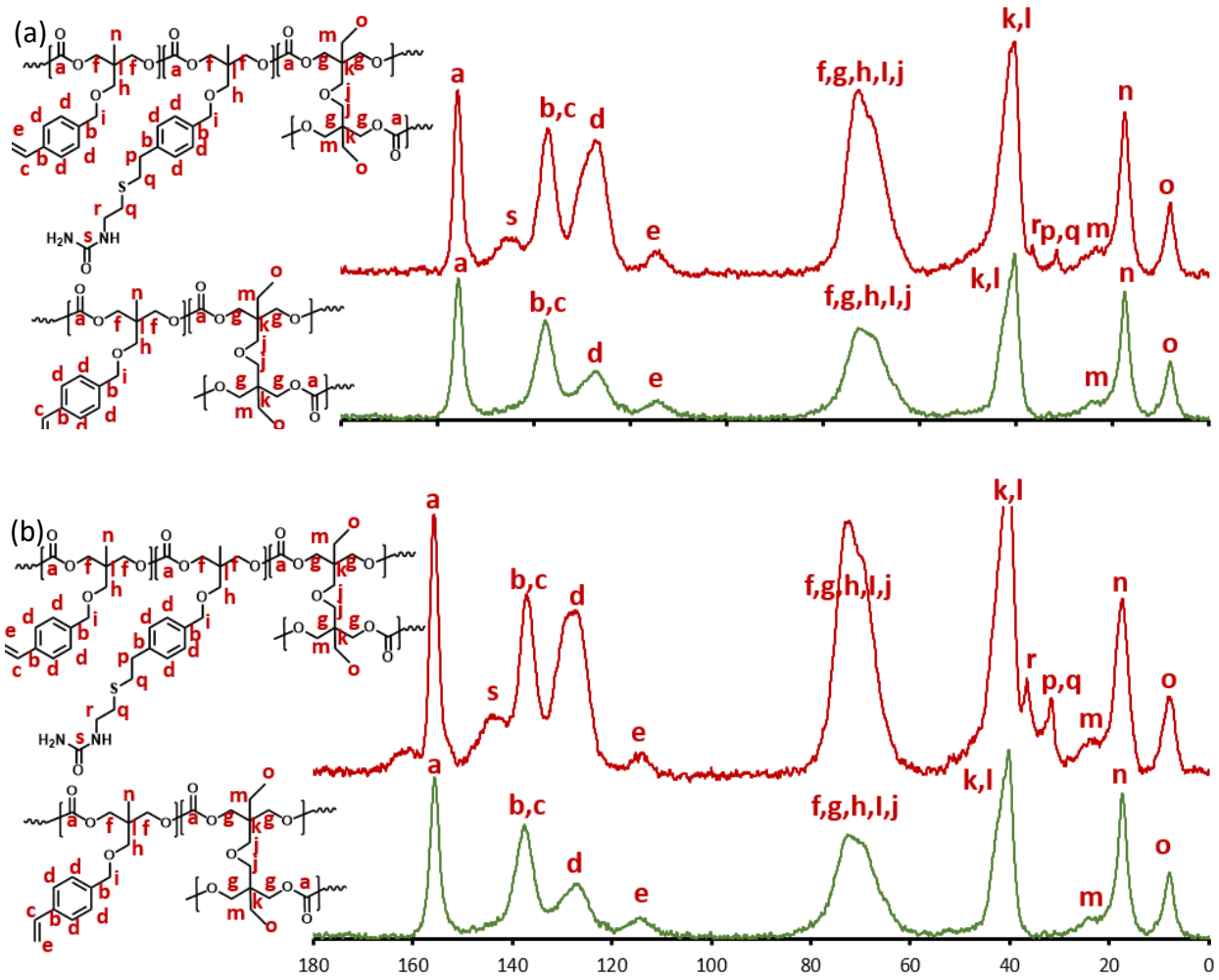

Figure 1-3 ^{1}H NMR of UV irradiation by DMPA (a) and thermal-initiated by AIBN (b).

One concern about the improving of stiffness, showing the merits of the urea functional group not only bioactive binding but also hydrogen bonds. It could be carried out in both UV irradiation by DMPA and thermal-initiated by AIBN (**Scheme 1-1(c)).** Both reactions were confirmed by ^{13}CPMAS corresponding the presence of urea group with chemical shifts 23.65, 31.70, 36.57 and 43.76 ppm (**Figure 1-3a and 1-3b).** In order to examine the reaction reactivity, elemental analysis was carried out to quantified percentage of urea group attached on the polymer side chain. Based on the result, thermal-initiated by AIBN displayed higher reactivity, 30%

compared to UV irradiation by DMPA, 11% (**Table 1-2).** Therefore, the modification of PTMCM/20%BTB and PTMCM/50%BTB at vinyl groups with thiol-urea (SU) were carried out by thermal-initiated by AIBN, denoted as PTMCM-SU/20%BTB and PTMCM-SU/50%BTB respectively. This study also reported the findings about quantitative determination by elemental analysis, resulting 30 % and 38 % of SU attachment onto the PTMCM-VB/20%BTB and PTMCM-VB/50%BTB films, respectively **(Table 1-3).** Since the successfully obtained the target polymer materials, we move to evaluate various properties next.

Table 1-2: Elemental analysis and modification reactivity for post modification of PTMCM-VB/20%BTB film under UV irradiation and thermal-initiated conditions.

Sample	**Experimental weight %**			**Modification %**
	Carbon	Hydrogen	Nitrogen	
UV irradiation	64.97	7.06	0.95	11
Thermal-initiated	61.58	6.86	2.63	30

Table 1-3: Elemental analysis and modification reactivity for post modification of PTMCM-VB/20%BTB and PTMCM-VB/50%BTB under thermal-initiated conditions.

Sample	**Experimental weight %**			**Modification %**
	Carbon	Hydrogen	Nitrogen	
PTMCM-VB/20%BTB	61.58	6.86	2.63	30
PTMCM-VB/50%BTB	60.56	7.27	2.31	38

1.3.2 Degradation study

To persuade the biomaterials, the degradation behavior of the film was studied and shown in **Figure 1-4 and Table 1-4.** In this experiment, the main polymeric structure PTMCM-

VB/20%BTB film was assessed in degradation study under various circumstances such as lipase enzyme solution, 0.01M HCl solution, and 0.01M NaOH solution. As the result of weight loss, degradation loss % were examined at every 4, 7, 30, 60, and 90 days as in lipase condition accordingly 8.30% ± 2.24, 8.40% ± 1.78, 6.67% ± 0.49, 9.75% ± 0.40 and 7.53% ± 0.29 respectively. Rate in acid condition was 6.83% ± 1.13, 6.24% ± 1.83, 11.82% ± 0.82, 16.25 % ± 1.31, and 20.69% ± 1.25 respectively. While, alkaline condition was consecutively 7.57% ± 3.09, 10.61% ± 1.28, 18.54% ± 0.45, 24.44 % ± 2.24 and 32.60% ± 2.26 respectively. The film in lipase showed less than 10% degradation loss within 90 days whereas the acid and base condition was over 20 and 30%. It is important to note, that the present film exhibited lower degradation against the lipase compared with another. The stable degradation of lipase conditions in this case could be due to the crosslinker effect and the initial weight loss could be due the PTMC surface erosion process. Also, this may support the crucial modification on the PTMC side chain with ether linkage. Jan and his coworkers studied the non-functionalized PTMC possessed faster erosion rate in enzymatic lipase condition than immersed in media varying in pH from 1 to 13, non-enzymatic hydrolysis[29]. This variation could be explained to the presence of crosslinker as well as functionalization. Depend on type of biomaterial application, stability in degradation during healing process is promising to be used to maintain the thermodynamic properties and mechanical integrity of the material.

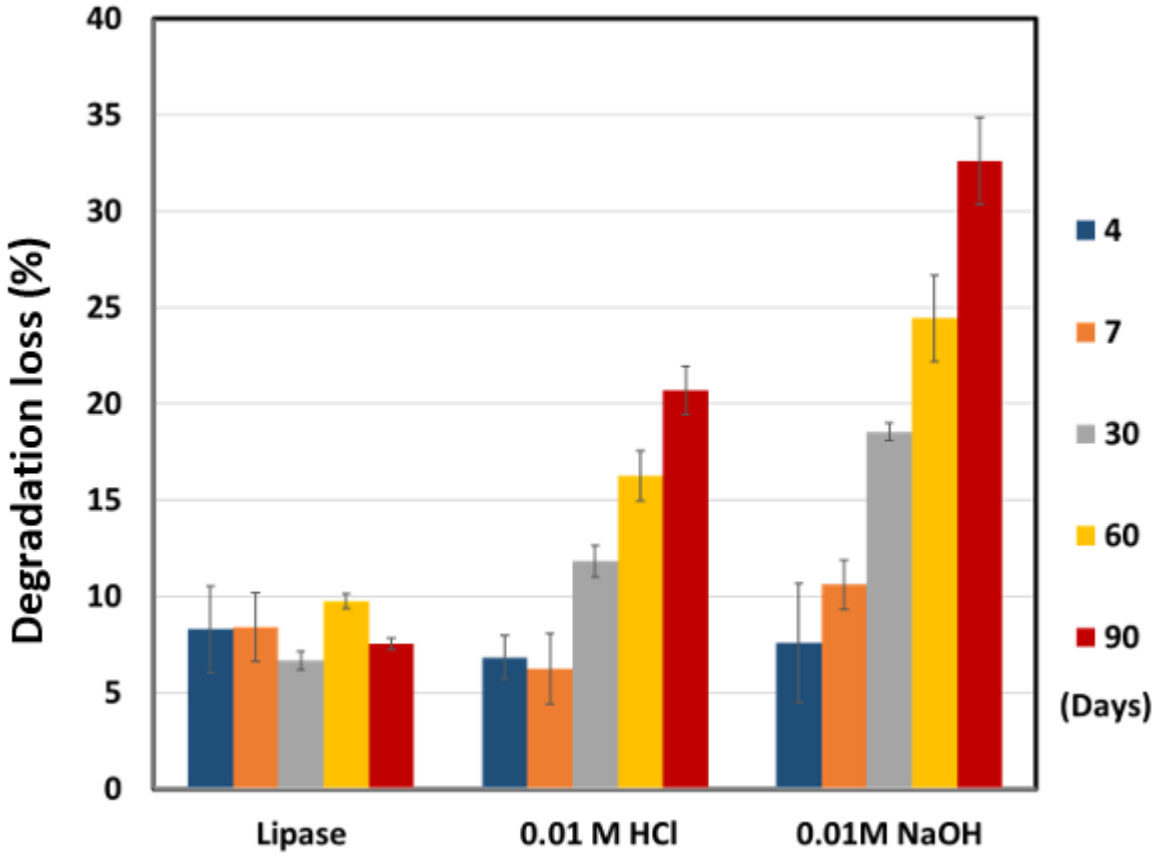

Figure 1-4. Degradation behavior of PTMCM-VB/20%BTB against lipase, HCl and NaOH solution for 4, 7, 30, 60, and90 days. (left to right).

Conditions	Lipase	HCl	NaOH
4 days			
7 days			
30 days			

60 days			
90 days			

Table 1-4. Images of degradation behavior of PTMCM-VB/20%BTB against lipase, HCl and NaOH solution for 4, 7, 30, 60, and 90 days.

1.3.3 Thermal stability

As considering the sterilization and processing-related temperature, thermal stability of polymeric materials is considered. Herein, TGA thermograms and measurements of the synthetic films were evaluated in the relevant temperature profile (**Figure 1-5(a)).** In this case, the onset decomposition temperatures at 10% weight loss (T_{10}) were reported as 203°C for PTMCM/20%BTB film, 241—243°C for PTMCM-VB/20%BTB and PTMCM-VB/50%, and 249—276°C for PTMCM-SU/20%BTB and PTMCM-SU/50%BTB. As the results, this suggests that all polymeric films are able to withstand temperatures above 200°C. PTMCM/20%BTB film had lower T_{10} than PTMCM-VB/20%BTB and PTMCM-VB/50%BTB films, I speculated that this might be due to the incorporation of vinyl benzyl group. In the case of PTMCM-VB/20%BTB and PTMCM-VB/50%BTB, both exhibited curves depicted one step of loss region and the similar T_{10} values, which was approximately 240°C and no further weight loss after 430°C. The shift temperature of weight loss was illustrated that the thermal stability enhanced when side-chain

modified PTMC was introduced. The similar discussions were reported by polymer composition, which it may relate with the type of covalent or noncovalent bonds, degree of unsaturation, functional groups, molecular weight, branch degree, cross-linking, and crystallinity[30,31]. Accordingly, it is well-known that aromatic component in the polymer structure can improve the thermal stability. Hence, a presence of aromatic functional group possessing high resonance energy contributes to higher thermal stability. Conversely, there is no significant change in T_{10} for increased BTB ratio. While the post modification of urea functional group (SU) enhanced the T_{10} to 276°C. It was postulated that the existence of intermolecular interaction between the SU group and polymeric matrix. The decomposition curve displayed multiple stage, assumed because of mixture of bi-functional PTMCM-VB and PTMCM-SU present in the polymeric film as well as microphase separation due to BTB concentration. However, PTMCM-SU/50% BTB comparatively no significant change when introduced SU group.

Glass transition temperature (T_g) of the polymeric films were studied by DSC as shown in **Figure 1-5(b)**. The T_g values of PTMC/20% BTB, PTMCM-VB/20%BTB, PTMCM-VB/50%, PTMCM-SU/20%BTB and PTMCM-SU/50%BTB were –19°C, –17°C, –4°C, 6°C and 21°C, respectively. As comparison with PTMC/20%BTB standard, presence of vinyl aromatic of PTMCM-VB/20%BTB has no significant change in T_g. The induction of aromaticity possibly needed to be considered the pronouncement of π - π interaction as well as the bulkiness of aromaticity. On the other hand, an increasing of crosslinker ratio from 20% to 50% resulted in

improvement of T_g to – 4°C. This implies that high density may behave as if there are limitations of segmental mobility. Therefore, it requires more energy as higher temperature shifting since higher crosslink density[31]. For the PTMCM-SU/20%BTB and PTMCM-SU50%BTB films, the existence of SU moieties leaded a pronounced effect on T_g values due to the intermolecular interaction between SU groups with polymer main chain by hydrogen bonding.

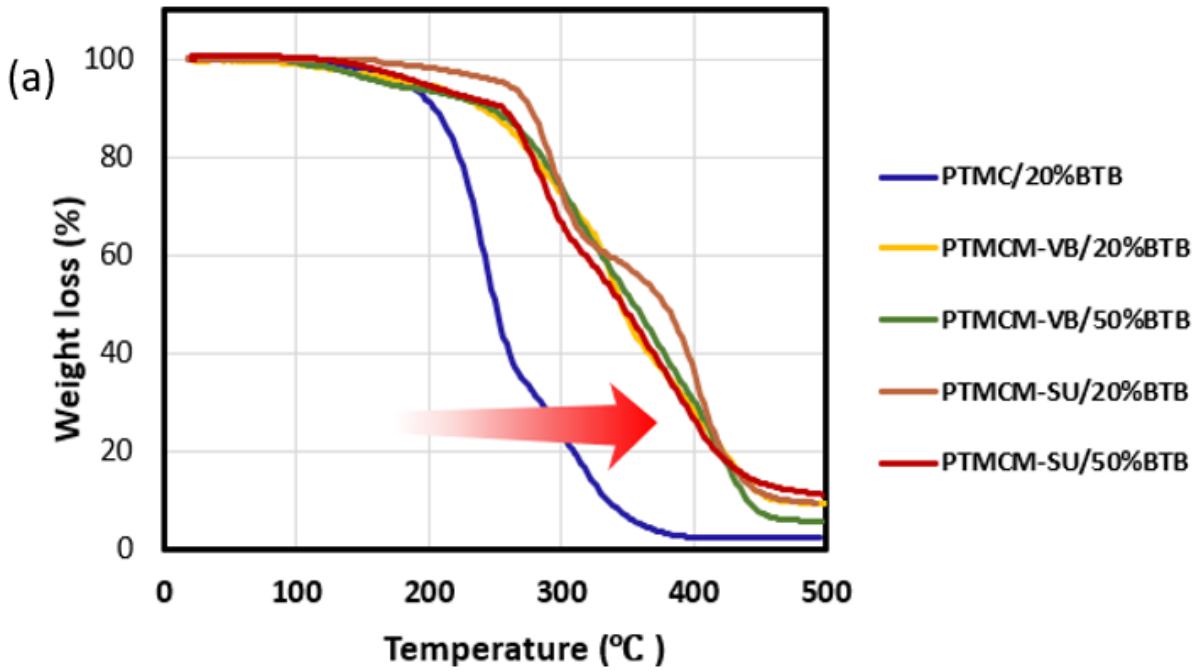

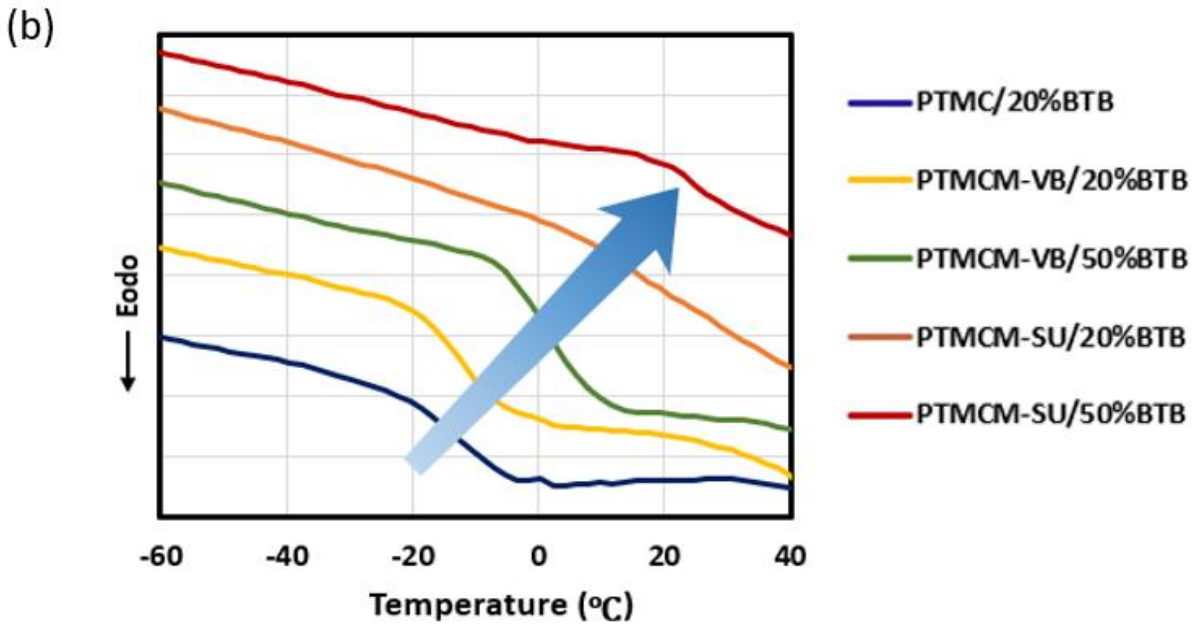

Figure 1-5. Thermal stability profile of the synthetic films by TGA measurement (a) and DSC analysis (b).

1.3.4 Mechanical properties

It is worth discussing these interesting PTMC films revealed by the results of tensile strength as shown in **Figure 1-6 and Table 1-5**. Based on the result, PTMCM-VB/20%BTB and PTMC/20%BTB had elongation at break as 26.8±2.86% and 10.7±1.20%. It implied that introduction of aromatic pendant group in PTMC found increased ductility as compared with unmodified PTMC films. Whereas, increasing of BTB content from 20% to 50% could boost the tensile strength of PTMCM-VB/50%BTB from 0.85 MPa ± 0.02 to 2.21 MPa ± 0.91. The Young's modulus of PTMCM-VB/20%BTB, PTMCM-VB/50%BTB, PTMCM-SU/20%BTB and PTMCM-SU/50%BTB were 3.17 ± 0.36 MPa, 9.88 ± 0.97 MPa, 179.58 ± 130.28 MPa, and 474.72 ± 142.95 MPa, respectively (**Figure 1-7**). The correlation between the tensile strength and Young's modulus of the film associated with the crosslinking network and intermolecular interaction of

urea group, could convey non-slippage film as the beneficial stiffness. Moreover, the flexibility and stiffness of polymer films could be influenced by their glass transition temperature. PTMC/20%BTB, PTMCM-VB/20%BTB and PTMCM-VB/50%BTB possessed T_g below room temperature, experienced flexible and ductile behavior whereas PTMCM-SU/20%BTB and PTMCM-SU/50%BTB turned to be rigid and glassy as its T_g closed to the room temperature

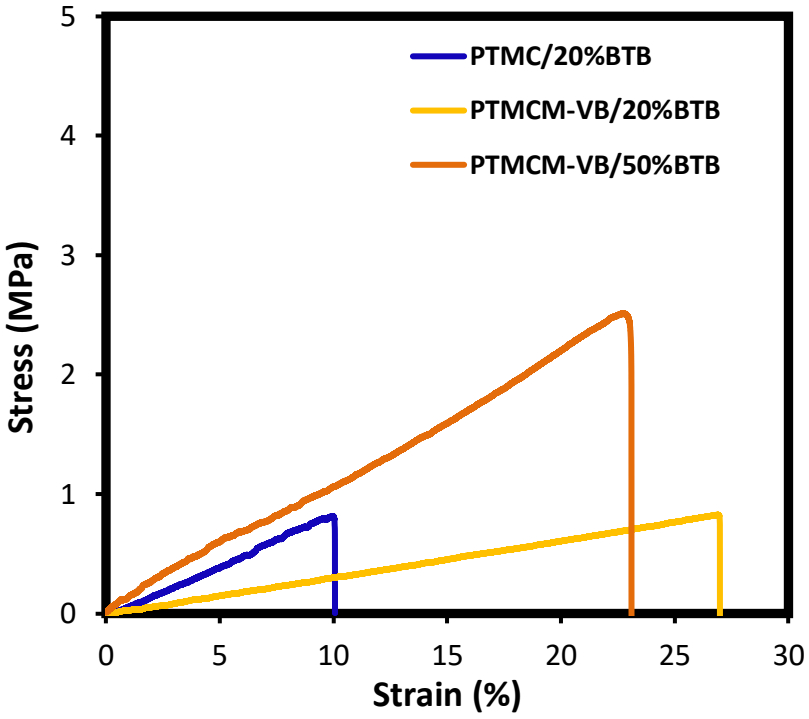

Figure 1-6. Stress-strain curves of polymeric films.

Table 1-5. Mechanical properties of the films.

Entry	Sample	σ [MPa]	ε [%]	E [MPa]
1	PTMC/20%BTB	0.89 ± 0.11	10.66 ± 1.20	8.72 ± 1.58
2	PTMCM-VB/20%BTB	0.85 ± 0.02	26.81 ± 2.86	3.17 ± 0.36
3	PTMCM-VB/50%BTB	2.21 ± 0.91	21.03 ± 7.20	9.88 ± 0.97

4	PTMCM-SU/20%BTB[a]	3.91 ± 1.50	5.06 ± 2.01	179.58 ± 130.28
5	PTMCM-SU/50%BTB[b]	9.94 ± 3.91	4.21 ± 2.31	474.72 ± 142.95

[a, b] 2 replicates were tested.

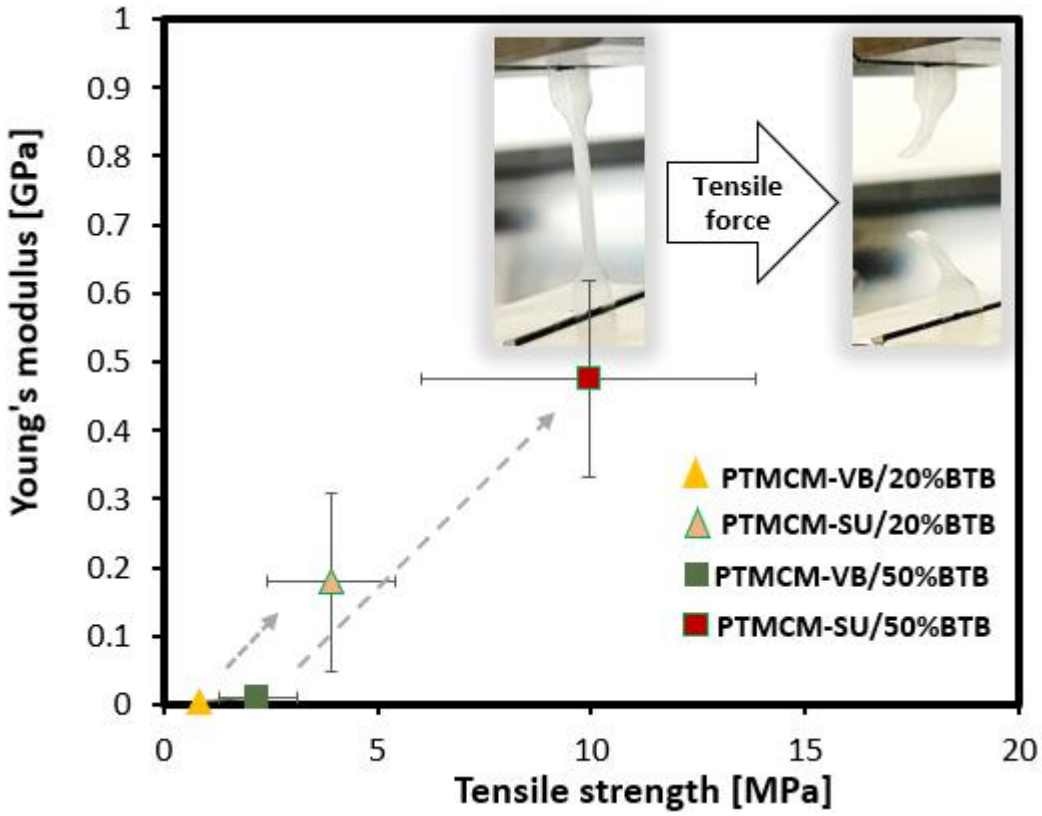

Figure 1-7. Young's Modulus of polymeric films.

1.3.5 Swelling degree of films

The water swelling of polymeric materials plays an important role in evaluation of bioresorbable films. The swelling degree of the films, PTMCM-VB/20%BTB, PTMCM-VB/50%BTB, PTMCM-SU/20%BTB, and PTMCM-SU/50%BTB were summarized in **Figure 1-8**. To stimulate biological circumstance, the swollen state was measured after soaking in PBS solution for 24 hours. Their degrees of swelling ratio were 6.47 % ± 0.14 for PTMCM-VB/20%BTB, 6.44 % ±

0.56 for PTMCM-VB/50%BTB, 11.15% ± 1.57 for PTMCM-SU/20%BTB, and 7.70% ± 0.44 for PTMCM-SU/50%BTB. Based on the results, the hydrophobic film (PTMCM-VB/BTB) had significantly lower retaining ability compared to PTMCM-SU/BTB due to the hydrophilic urea enhancement. It was found that PTMCM-SU/20%BTB was the most swollen film, considered to the network density and urea containing.

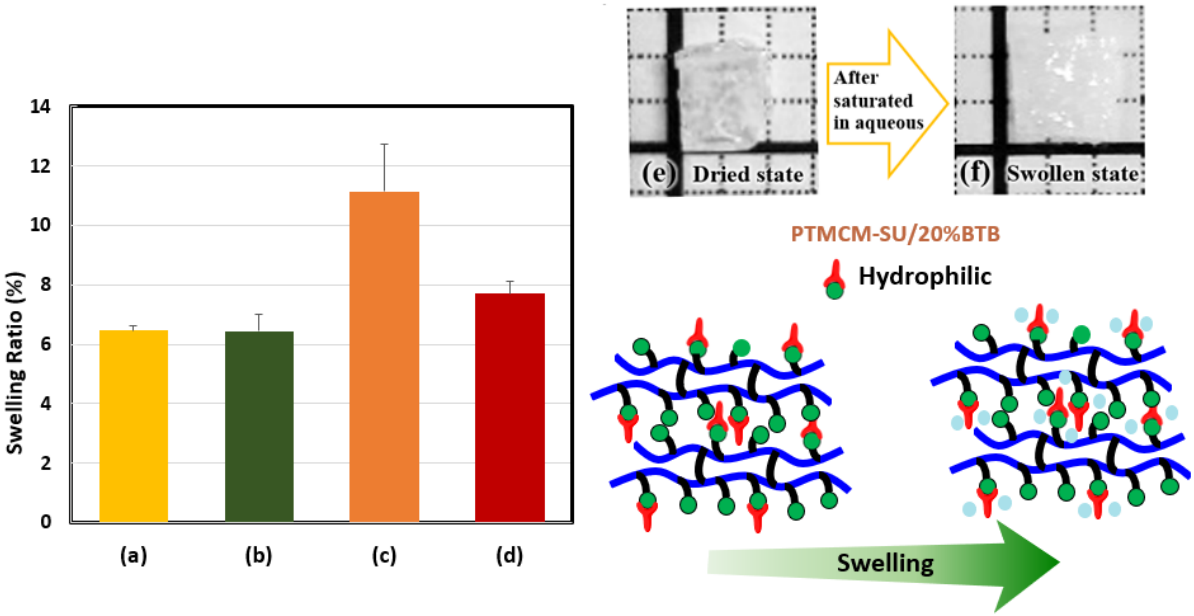

Figure 1-8. Swelling degree of PTMCM-VB/20%BTB (a), PTMCM-VB/50%BTB (b), PTMCM-SU/20%BTB (c) and PTMCM-SU/50%BTB (d).

1.4 Conclusions

In this work we demonstrate that the design and preparation of the crosslinked PTMC films containing aromatic vinyl and urea-moiety can be fabricated with ester-free structures. The degradation study of PTMCM-VB/20%BTB showed promising stability in lipase condition. It is shown that, all the polymeric films had high thermally resistance above 200°C. The functional PTMCM-VB/20%BTB, PTMCM-VB/50%BTB, PTMCM-SU/20%BTB, and PTMCM-SU/50%BTB films had improved thermal stabilities in terms of T_{10} and T_g compared with reference PTMC/20%BTB film. The incorporation of aromatic functionality and crosslink significantly enhanced the mechanical properties as PTMCM-VB/20%BTB and PTMCM-VB/50%BTB. The stiffness of post-modified films as PTMCM-SU/20%BTB and PTMCM-SU/50%BTB were induced with incorporation of urea as well as crosslinker ratio. The swelling ratio showed urea-functionalized film displayed higher swollen ability due to its hydrophilicity. Finally, these results suggested the improvement of PTMC performance with desire functions and meaningful materials to approach in clinical applications.

1.5 Supplementary Materials

^{1}H NMR spectrum of BTB crosslinker

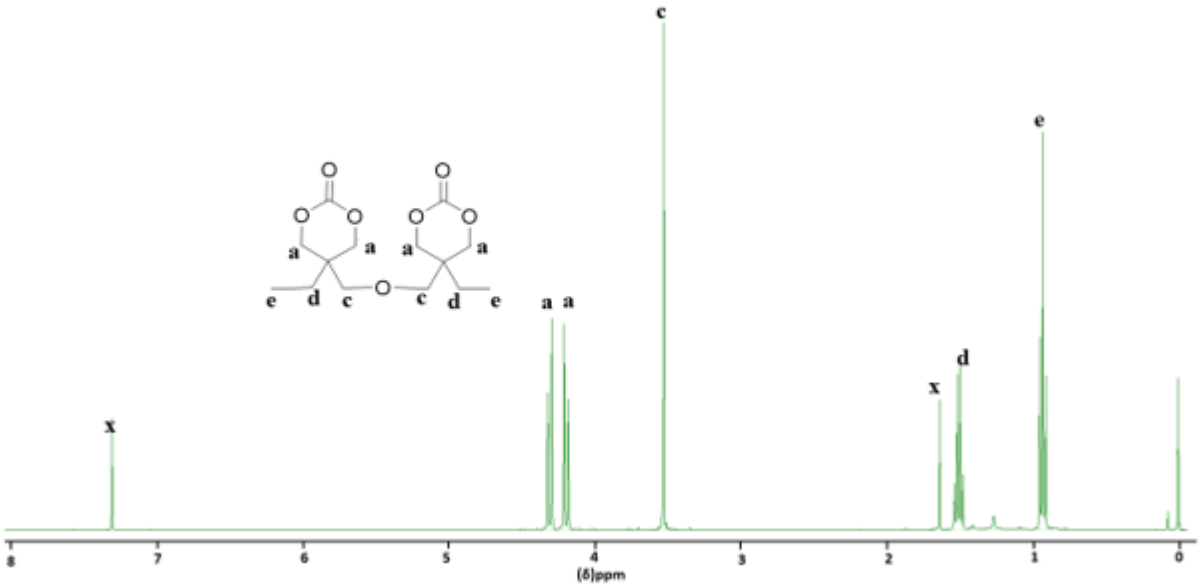

Figure S1-1. ^{1}H NMR spectrum of BTB in $CDCl_3$.

^{1}H NMR spectrum of SU precursor

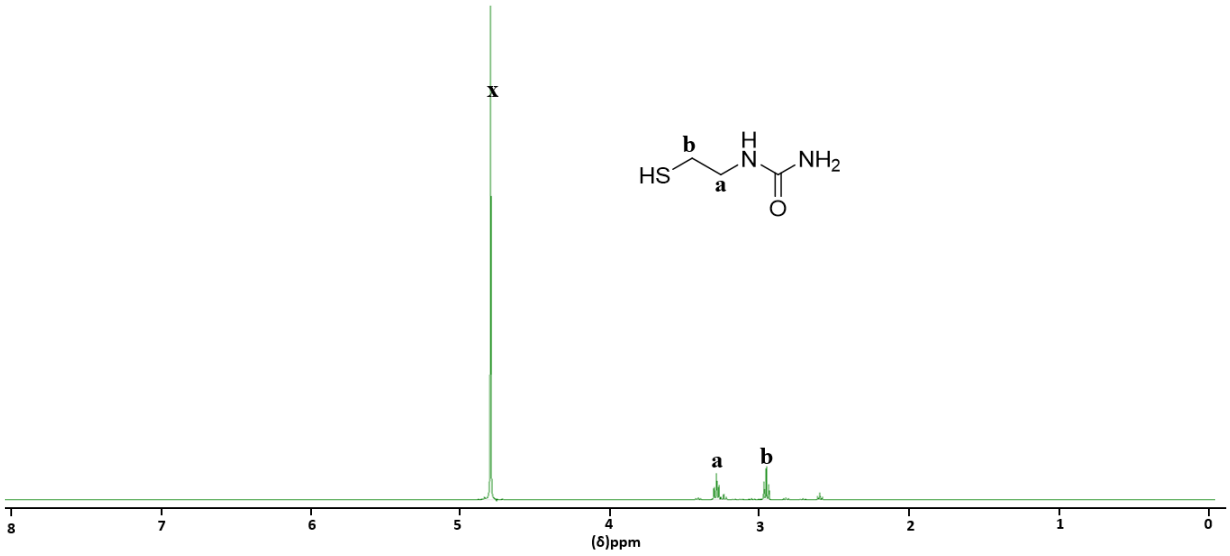

Figure S1-2. ^{1}H NMR spectrum of SU in $CDCl_3$.

Stress-strain curves of polymeric films.

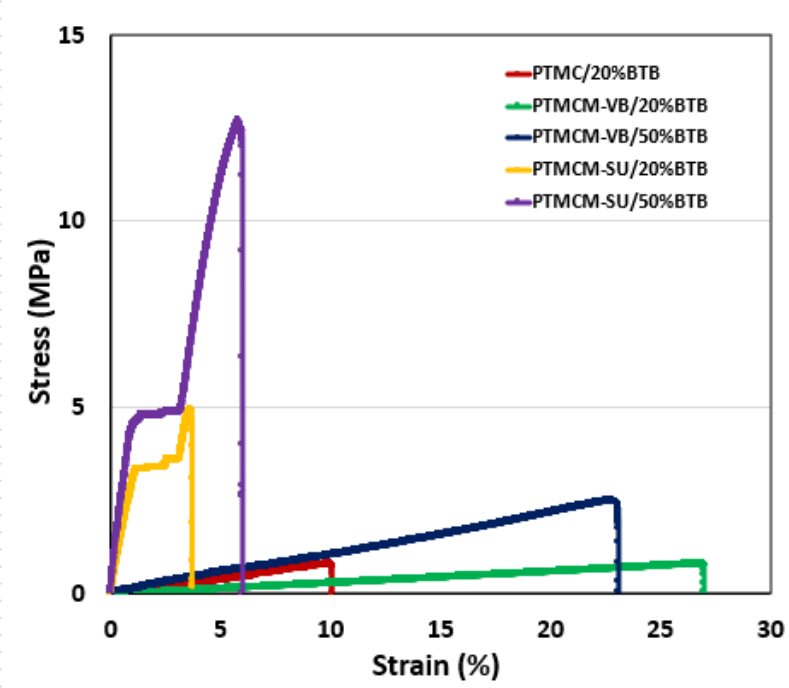

Figure S1-3. Stress-strain curves of PTMC/20%BTB, PTMCM-VB/20%BTB, PTMCM-VB/50%BTB, PTMCM-SU/20%BTB, PTMCM-SU/50%BT

1.6 References

1 A. W. Lloyd. *Med Device Technol*. **2002,** 13, 18-21.

2 J. W. Lee. *Biomater. Res.*. **2018,** 22.

3 X. Zhang, MA. Geven, X. Wang, L. Qin, DW. Grijpma, T. Peijs, D. Eglin, O. Guillaume, JE. Gautrot. *Int J Nanomedicine*. **2018**, 13, 5701-5718.

4 P. B. Maurus and C. C. Kaeding, *Oper. Tech. Sports Med.*, **2004,** 12, 158–160.

5 J. Middleton, A.J Tipton. *Biomaterials*, **2000**, 21, 2335-2346.

6 K. Fukushima. *Biomater. Sci.*, **2016**, 4, 9.

7 Z. Zhang, R. Kuijer, S. K.Bulstra, D. W. Grijpma, J. Feijen. *Biomaterials*, **2006**, 27, 1741-1748.

8 J. Jaworska, K. Jelonek, M. Sobota, J. Kasperczyk, P. Dobrzynski, M. Musial-Kulik, A. Smola-Dmochowska, H. Janeczek and B. Jarzabek, *J. Appl. Polym. Sci.* **2015,** 132, 41902.

9 A. D. Messias, K. F. Martins,A.C. Motta, E.A.R.Duek. *Int J. Biomater*. **2014**.

10 A. Pêgo, D. W. Grijpma, J. Feijen. *Polymer*, **2003**, 44, 6496-6504.

11 S. Tempelaar, L. Mespouille, O. Coulembier, P. Dubois, A. P. Dove. *Chem. Soc. Rev*. **2013**, 42, 1312-1336.

12 N. Chanthaset and H. Ajiro, *Materialia*, **2019**, 5, 100178.

13 P. Y. W. Dankers, Z. Zhang, E. Wisse, D. W. Grijpma, R. P. Sijbesma, J. Feijen and E. W. Meijer, *Macromolecules*, **2006**, 39, 8763–8771.

14 H. Nobuoka and H. Ajiro, *Tetrahedron Lett.* **2019**, 60, 164–170.

15 H. Ajiro, Y. Takahashi and M. Akashi, *Macromolecules* **2012**, 45, 2668–2674.

16 S. Edizer, B. Veronesi, O. Karahan, V. Aviyente, I. Değirmenci, A. Galbiati and D. Pasini,

Macromolecules, **2009**, 42, 1860–1866.

17 E. Lizundia, V. A. Makwana, A. Larrañaga, J. L. Vilas and M. P. Shaver, *Polym. Chem.*, **2017**, 8, 3530–3538.

18 S. Do, S. Stepp and G. Youssef, *Materials Today Commun.* **2020**, 25, 101464.

19 P. G. Parzuchowski, M. Jaroch, M. Tryznowski and G. Rokicki, *Macromolecules*, **2008**, 41, 3859–3865.

20 A. B. Lowe, C. E. Hoyle and C. N. Bowman, *J. Mater. Chem.* **2010**, 20, 4745–4750.

21 F. Faghihi and P. Hazendonk, *Polymer*, **2017**, 128, 31–39.

22 V. Truong, I. Blakey and A. K. Whittaker, *Biomacromolecules*, **2012**, 13, 4012–4021.

23 D. Xing, L. Ma and C. Gao, *Macromol. Biosci.*, **2014,** 14, 1429–1436.

24 R. J. Williams, I. A. Barker, R. K. OReilly and A. P. Dove, *ACS Macro Lett.*, **2012**, 1, 1285–1290.

25 D. M. Stevens, S. Tempelaar, A. P. Dove and E. Harth, *ACS Macro Lett.*, **2012**, 1, 915–918.

26 J. C. Grim, T. E. Brown, B. A. Aguado, D. A. Chapnick, A. L. Viert, X. Liu and K. S. Anseth, *ACS Central Sci.*, **2018**, 4, 909–916.

27 L. Yang, B. He, S. Meng, J. Zhang, M. Li, J. Guo, Y. Guan, J. Li, Z. Gu. *Polymer* **2013**, 54, 2668-2675.

28 L. Tiwari, V. Kumar, B. Kumar and D. Mahajan, *RSC Adv.* **2018,** 8, 21585–21595.

29 T. Miyagawa, M. Shimizu, F. Sanda and T. Endo, *Macromolecules* **2005,** 38, 7944–7949.

30 Z. Zhang, R. Kuijer, SK. Bulstra, DW. Grijpma, J. Feijen, *Biomaterials* **2006**, 27, 1741.

31 X. Li, N. Mignard, M. Taha, C. Fernández-de-Alba, J. Chen, S. Zhang, L. Fort and F. Becquart, *Macromol. Chem. Phys.*, **2020**, 221, 1900367.

32 K. Bandzierz, L. Reuvekamp, J. Dryzek, W. Dierkes, A. Blume and D. Bielinski, *Materials* **2016,** Vol. 9, Page 607, 2016, 9, 607.

Chapter 2

Surface Coating and Characteristics of Ester-free Poly(trimethylene carbonate) Bearing an Aromatic Urea Moiety for Biomaterials Use

2.1 Introduction

With the advent of biotechnology, biodegradable polymeric coating materials have attracted attention in clinical applications due to their flexible modification to meet specific requirements and diverse applicability. Modification biomaterial surface is vital to obtain biocompatibility and bifunctionality. The surface properties such as wettability, bioactivity, adherence, scratch and abrasion resistance can be tailored to be used in cell proliferation[1], tissue growth and repair[2], delivery of biomolecules such as drugs[3], growth factors[4], and antimicrobial agents[5]. For instances, Xu et.al. fabricated reduced-lysozyme and polyphosphate multifunctional coating on the surface of Ti-based biomaterials to enhance the implantation performance, exhibit certain antiadhesive and bactericidal activity by effectively restricting the growth of Gram-negative bacteria, which cannot be killed by most present antibiotics due to the hindrance of their outer membrane[6]. In order to increase bioactivity and greater osseointegration of titanium-based orthopedic implants, Barão and co-workers have applied plasma electrolytic oxidation treatment to coat bioactive glass to enhance Ti mechanical and tribological properties with higher

corrosion resistance[7]. Moreover, the biomaterial coating can increase the ability of osteoblast-like cell adhesion, proliferation, and differentiation behaviors. Liu et al. used poly(2- methyl-2-oxazoline) (PMOXA) as a pseudopeptide polymer to produce a non-brush bionic polymer coating by electrochemical assembly on a 316L SS surface **(Figure 2-1)**. Bioactivity and anti-fouling properties were observed for PMOXA with a modest degree of hydrolysis and molecular weight[8]. Furthermore, they found that cell migration and proliferation were enhanced by these coatings. It was claimed that the coating could successfully modify the surface of the complex 3D vascular stent, which could have potential applicability in the prevention of late stent thrombosis and in-stent restenosis. The well-known biodegradable polymer has been applied on the biomaterial coating are polylactide acid (PLA)[9], polyglycolide acid (PGA)[10], polycaprolactone (PCL)[11], chitosan[12], polymethyl methacrylate (PMMA)[13], polydimethylsiloxane (PDMS)[14], etc **(Figure 2-2)**.

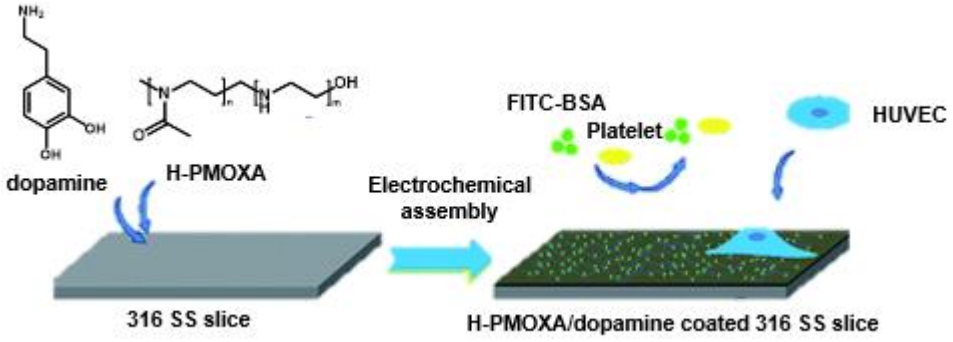

Figure 2-1. schematic illustration of the electrochemical assembly process of DA and H-PMOXA on 316L SS surfaces, and the anti-fouling and HUVEC adhesive properties of H-PMOXA/dopamine modified surface[8].

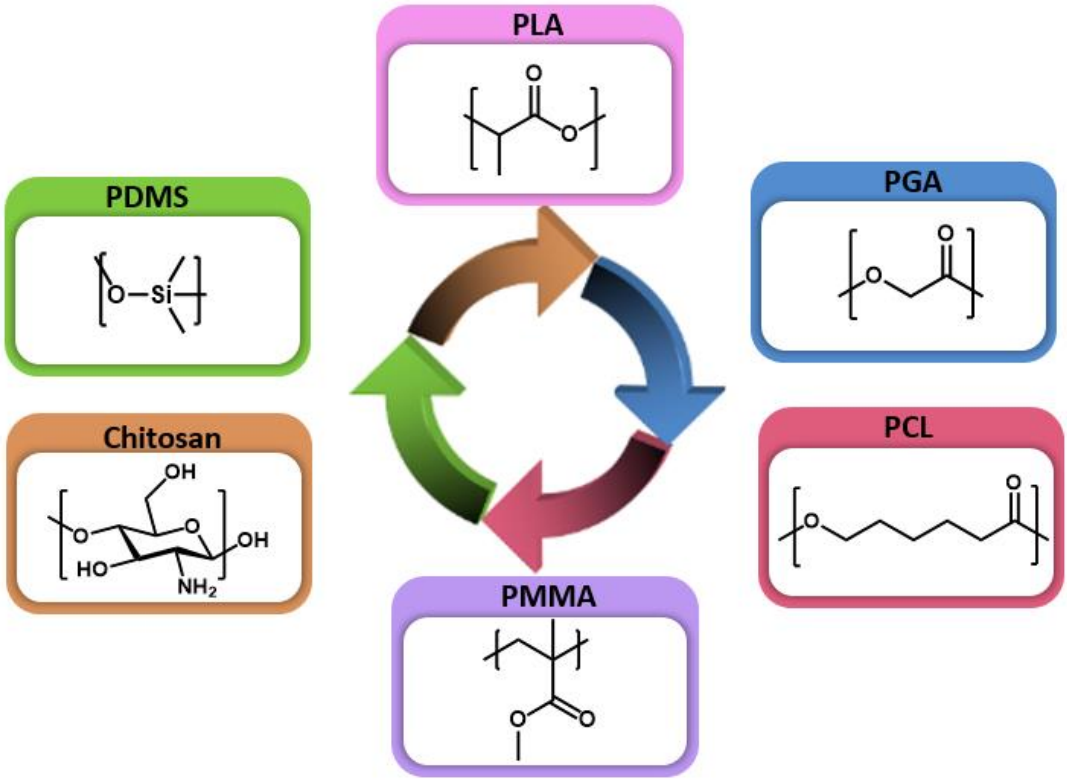

Figure 2-2. Well-known biodegradable polymer in biomaterial coating.

Poly(trimethylene carbonate) (PTMC) is another potential biodegradable polymer to be developed for biomaterial coating. The degradation mechanism of PTMC undergone surface-eroding model from exterior to interior of coating, remained uniformly thickness compared to bulk eroding characteristics. In surface erosion, PTMC degrades from exterior surface while interior of coating does not degrade till the surrounding material around it has been eroded. Whereas, polyester such as PLA undergone bulk erosion which the degradation occurred throughout the whole material equally. Thus, surface erosion is beneficial for obtaining homogeneous surface properties after implanted in human body[15]. The degradation by-product from the trimethylene carbonate moiety in PTMC is carbon dioxide and 1,3-propanediol, which is low toxicity and neutral condition that neither accelerates the corrosion of metallic implant nor

triggers inflammation on the surrounding tissue in comparison with acidic byproducts of associated with commonly used aliphatic polyester biodegradable polymers[16]. To be use in biomaterial application such as drug delivery and tissue engineering, it is beneficial to be able to tune the PTMC structure to enable specific interactions with cells or organs. It can be done by copolymerization and blending with other biodegradable polymers (i.e. poly(lactide), poly(glycolide), poly(caprolactone)) and the introduction of functional end-groups[17]. Addition of bioactive molecules or the precise control over the physical performances onto the PTMC structure however, is optimal to functionalize via post-modification of desired functionalities in the polymer backbone. Such pendant functionalities may be introduced via the ROP of cyclic carbonate monomers bearing the desired functionality however, not all functional groups are compatible with the ring-opening polymerisation process and in some cases the added functionality limits the polymerisation efficiency[18]. As a result, further modification of the polymer backbone following polymerisation is often required.

Current development of PTMC biomaterial coating involved homopolymerization and introduction of functionality into PTMC structure. For instances, Tang et al. studied the PTMC and PGA coating for magnesium based cardiovascular stents, showed PTMC coating provided stable drug release and improved corrosion resistance[19] **(Figure 2-3)**. Rongen et al. developed lubricious layer by grafting methacrylated poly(ethylene glycol) and methoxy-poly(ethylene

glycol) were grafted onto poly(trimethylene carbonate) networks by photo-crosslinking for artificial joints application[20] **(Figure 2-4)**. Furthermore, our group previously studied a block copolymer comprised of hydrophobicity of PTMC and hydrophilicity of PTMC bearing ethylene glycol chains with performances such as contact angle, thermal properties, protein adsorption and platelet adhesion for designing stent coating material[21] **(Figure 2-5)**. It is obvious that the desired properties of the biomaterial coating would be vary depending on the clinical use or indication. Furthermore, some application required material should be actively interact with tissue, while in some cases the material should be inhibit for unnecessary attachment with biological molecules.

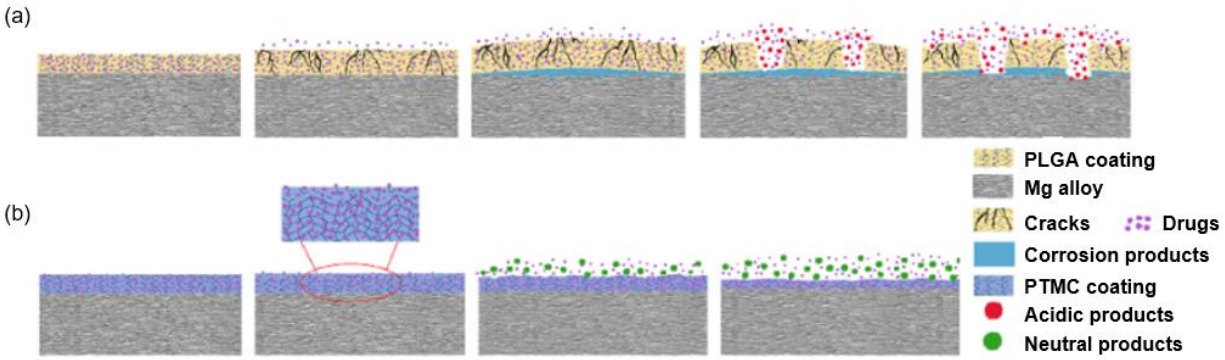

Figure 2-3. Schematic illustration of the erosion models and drug release for (a) PLGA coated and (b) PTMC coated samples[19].

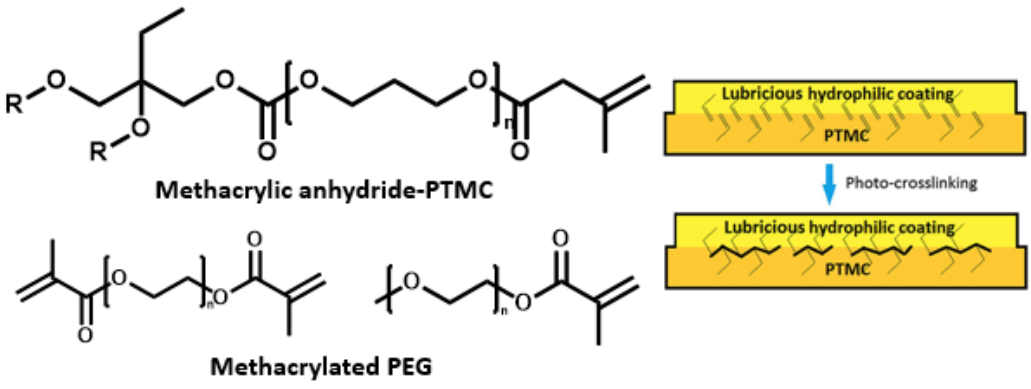

Figure 2-4. Schematic representation of the grafting of a lubricious hydrophilic coating onto a partly crosslinked PTMC network by photo-crosslinking[20].

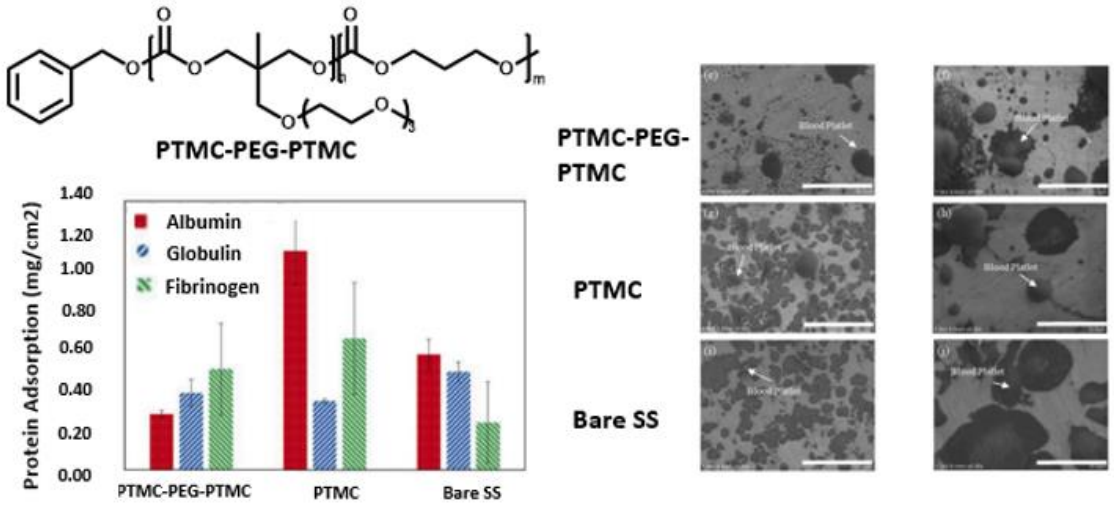

Figure 2-5. Protein adsorption and adherent platelets of block copolymer of poly(trimethylene carbonate) with oligo(ethylene glycol) (PTMC-PEG-PTMC, PTMC coated on stainless steel[21].

It is important to study the biological response of different biomaterial coating. Surface with different functional group have different chemically and physically properties in term of wettability, roughness, rigidity, and these could correlate to blood and tissue-interaction and compatibility. Lee and co-workers studied different functional groups (-COOH), -CH_2OH, -$CONH_2$ and -CH_2NH_2) on the cell adhesion effect[22]. The results showed amine group-grafted surface is the most compatible with the cells among the functional groups used. Influence of wettability of various polymer surfaces has been investigated on the interactions of the different types of biological species[23]. The cells tend to be adhered more on the sections with moderate hydrophilicity. Ying et al. explored the hindered urea bond, a urea structure with a bulky substituent on one of the nitrogen atoms. The hydrolysis kinetics were tuned by manipulating

the substituent's bulkiness, which has potential in tissue engineering applications for controlling the release kinetics of cells or proteins to wound sites[24].

In our previous study, we successfully synthesized cross-linked PTMC bearing an aromatic pendant and 1-(2-mercaptoethyl)urea (SU). The PTMCM-SU in the form of a film incorporating a 50% crosslinker of 2,2'- bis(trimethylene carbonate-5-ly)-butyl ether (BTB) showed a greater tensile strength of 9.94 MPa than non-functionalized PTMC (0.89 MPa)[25]. However, the polymer materials could not be coated on any substrates, and the post-modification behavior was unclear due to the crosslinked gel material. So, I motivated to apply the polymer materials for the surface coating of biomaterials using soluble PTMC derivatives without crosslinking. For specific use in the medical field, the study of biological responses is essential to understand the behavior and interaction with the surrounding biological microenvironment. The requirements for biological interaction or effects of the biomaterials differ depending on the therapeutic application[26]. This study aimed to evaluate the bioactivity of SU for potential use in biomaterials using linear polymers of PTMC derivatives, for tissue engineering, and drug release.

In this study as shown in **Figure 2-6**, an aromatic bearing vinyl moiety was introduced into a PTMC side chain followed by post-modification of PTMC with a thiol bearing a urea group through UV irradiation. The polymers were coated on stainless steel (SS) to study their

characteristics. For use as a polymeric coating material in clinical applications, the thermal properties, contact angles, roughness, protein adsorption and cell adhesion were discussed in order to study the influence of surface properties after introduction functional group onto the PTMC.

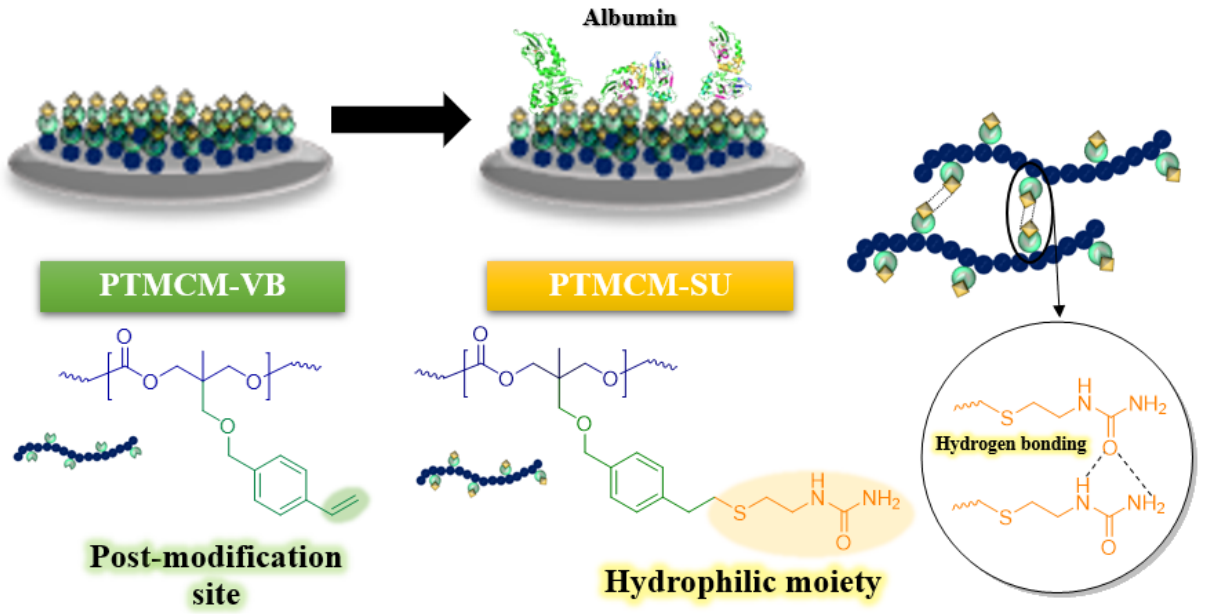

Figure 2-6. Ester-free PTMC bearing with aromatic urea-functional group for biomaterial coating.

2.2 Experimental Section

2.2.1 Materials

Trimethylolethane, ethyl chloroformate, hexafluoro-2-propanol, 1,8-diazabicyclo[5.4.0]-7-undecene (DBU) and 2,2-dimethyl-1-propanol were purchased from Tokyo Chemical Industry (TCI), Japan. Potassium hydroxide pellet (KOH), potassium cyanate (KOCN) and 1M

hydrochloric acid (HCl) were purchased from Nacalai Tesque. 2,2-Dimethoxy-2-phenylacetophenone (DMPA) and 4-vinylbenzyl chloride was purchased from Sigma-Aldrich. Trimethylamine was purchased from Fujifilm Wako Pure Chemical (WAKO), Japan. Anhydrous dimethyl sulfoxide (DMSO), dimethylformamide (DMF), tetrahydrofuran (THF), ethyl acetate, hexane, isopropanol, sodium chloride, dichloromethane (DCM) were used further purification.

2.2.2 Synthesis of 2-methyl-2-[{(4-vinylbenzyl)methoxy}methyl]-1,3-propanediol (diol-styrene) and 5-methyl-5-[{(4-vinylbenzyl)methoxy}methyl]-1,3-dioxanone (TMCM-VB)

Synthesis of 2-methyl-2-[{(4-vinylbenzyl)methoxy}methyl]-1,3-propanediol (diol-styrene) and 5-methyl-5-[{(4-vinylbenzyl)methoxy}methyl]-1,3-dioxanone (TMCM-VB) and (SU) were synthesized according to the same procedure as reported from our previous paper[27].

2.2.3 Synthesis of PTMCM-VB and PTMC

Under N_2 atmosphere, TMCM-VB (1.0 g, 3.81 mmol) was dissolved in anhydrous DCM solution with MS4A and stirred for 6 hr. The solution was then transferred to another flask and the solvent was removed by vacuum evaporated at room temperature overnight. The polymerization was carried out by using 2,2-dimethyl-1-propanol and DBU as initiator and catalyst. Briefly, the dried monomer was dissolved in anhydrous DCM (1.91 ml) with 2M concentration. Subsequently, DBU (56.9 µl, 0.381 mmol) and 1M 2,2-dimethyl-1-propanol (38.1 µl, 0.0381 mmol) were added. The polymerization was carried out for 24 hr under room temperature. The polymerization was stopped

by dissolving small amount of DCM. After precipitation with mixture against large excess of cold methanol, the polymer was recovered by decantation and centrifugation and finally dried vacuo under room temperature (88% yield). PTMC was polymerized from monomer 1,3-dioxane-2-one with same procedure as described above (91% yield).

2.2.4 Post modification of Thiol-ene of PTMCM-VB with (SU)

Post-modification was performed under nitrogen atmosphere. The PTMCM-VB (0.8g, 3 mmol, ~25 vinyl aromatic units per chain) was dissolved in 31 ml of DMF until homogenous solution. SU (3.67g, 31mmol) and DMPA as photo-initiator (0.16g, 0.62 mmol) were added into the mixture. The mixture was stirred at room temperature under UV light (365 nm). The reaction was monitored at specific time interval by NMR. After 4h, the UV light was turned off and the mixture was vacuum evaporated to remove solvent. The obtained compound was re-dissolved in HFIP/H_2O (1:10) and then placed into dialysis bag (cut off Mn 2 kDa) and dialyzed against water for 1 day to remove unreactive thiol-urea. The solution outside the mixture of dialysis bag was replaced with fresh water every 12 h. After that, the mixture in the dialysis bag was vacuum dried at 50°C for overnight to obtain post-modified polymer (PTMCM-SU) (22% yield).

2.2.5 Coating procedure

Spin coating of synthetic polymers were applied on the stainless steel (SS). The solution of synthetic polymer in HFIP/DCM (1:1) at 10 mg/ml and dropped 40 µl of polymeric solution to the

spinning substrate under 1000 rpm for 30s for two time-repeated coating. (Spincoater 1H-D7, Mikasa Co., Ltd.). The coated substrates were then dried under vacuum before testing.

2.2.6 Characterization

^{1}H NMR (400MHz) spectra was recorded on a JEOL JNM-ECX400 instrument with tetramethylsilane (TMS) as an internal standard. Chemical shifts were measured in $CDCl_3$ or DMSO-d_6 at 25°C depend on the polymer solubility. PTMCM-VB was measured using $CDCl_3$ while PTMCM-SU was measured using DMSO-d_6. Fourier transform infrared spectrometer (FT-IR) spectra were obtained with an IR Affinity-1S Shimadzu. Size Exclusion Chromatography (SEC) measurement were conducted for average molecular weight (M_n) and dispersity distribution (PDI) of synthetic polymers. The system equipped of RI-2031 Plus Intelligent RI detector, PU-2080 Plus Intelligent HPLC pump, AS-2055 Plus Intelligent Sampler, CO-2065 Plus Intelligent Column oven (JASCO), commercial columns (TSKgel SuperH3000 and TSKgel GMHXL) were connected in series. Polystyrene standard (Shodex) (1mg/ml, 0.6 ml/min) were employed and tetrahydrofuran for PTMCM-VB while dimethylformamide for PTMCM-SU were used as an eluent at 40 °C.

2.2.7 Contact angles

The static water contact angle of coated substrates was measured by Flow Design CAM-004 (Tokai Hit TPX-S). Image were taken after DI water 40 µl was dropped on film surface with

three replicates at different locations to obtain mean value of the contact angle.

2.2.8 Laser scanning microscope.

Morphology and roughness of coated substrates were measured using Olympus LEXT OLS4100 3D laser scanning microscope. (Horizontal:X-Y direction resolution of 0.12 μm; light source: 405 nm semiconductor laser; detector: photomultiplier).

2.2.9 Protein Adsorption

Protein adsorption of coated samples were examined using bovine serum albumin (BSA) (Sigma, St. Louis, U.S.A.) with concentration of 4.5 mg/ ml. The samples were soaked in 900 μm protein solution and incubated for 4 h at 37 °C. After rinsing with PBS, adsorbed protein was detached by 1 wt% of n-sodium dodecyl sulfate (SDS) for 4 h. Bicinchoninic acid (BCA) protein assay reagent was used as indicator for protein adsorption on the samples. UV measurement at 562 nm for protein on sample surface was interpreted by absorbance microplate reader (MTP-310lab, Corona Electric) based on standard control and calibration curve of the protein.

2.2.10 Thermal resistance.

The thermal stability of the polymer was determined by a thermo-gravimetric analyser TGA-50 (Shimadzu) under nitrogen atmosphere with 10°C/min flow rate to 500°C. Differential scanning calorimetry (DSC) spectra were also analysed by a Hitachi DSC6200 in the atmosphere with

temperature ramp rate 10°C/min in range 70°C — 200°C.

2.2.11 Cell adhesion

The in vitro cell adhesion behavior of polymeric coating was examined using L929 fibroblast. PTMC, PTMCM-VB and PTMCM-SU were chosen to study the cell adhesion behavior. The coated sample was described in section 2.2.5. The coated samples were prior soaked in PBS under UV lamp to fully adapt to the water environment before cell adhesion test. The cell culture was stained with green fluorescent tracker to facilitate the quantitative counting. 100 µl of 4000 cells/cm^2 cell solution was seeded on the coated sample and incubated at 37 ºC under 5% CO_2 for 7 h and 7 days. The cell morphology was observed using fluorescence microscope and the number of cells was counted.

2.3 Results and Discussion

2.3.1 Polymerization and post-modification

The synthetic route for vinyl aromatic TMC monomers is depicted in **Scheme 2-1** and the functionalized ester-free design was conducted as previously reported[28]. SU comprising a urea moiety was selected for introduction into the PTMCM-VB side chain to enhance the intermolecular interaction and bioactive properties. In this study, post-modification by UV light (365 nm) was used for irradiation with the aid of a DMPA photo-initiator. The reaction was performed at room temperature, thus preventing any side reaction.

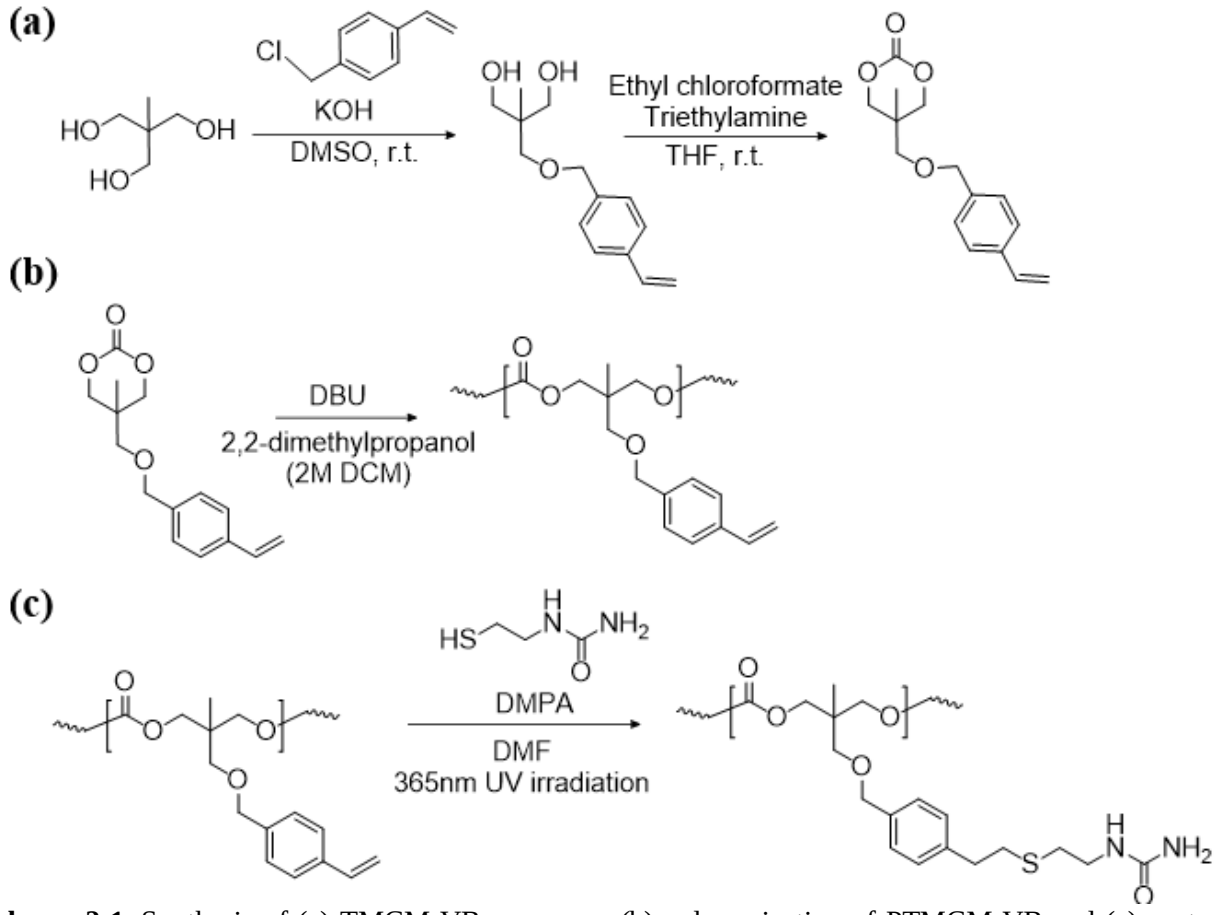

Scheme 2-1. Synthesis of (a) TMCM-VB monomer, (b) polymerization of PTMCM-VB and (c) post-polymerization modification of PTMCM-SU.

The reaction was monitored by ^{1}H NMR at time intervals of 30, 60, 120, and 240 min as shown in **Figures 2-7a, 2-7b, 2-7c, and 2-7d**, respectively. Resonance signals at 5.18 ─ 5.22, 5.75 ─ 5.80, and 6.65 ppm (**Figure 2-7**) were attributed to the vinyl group and slightly decreased in intensity upon reaction time. Also, after SU modification, the aromatic proton signal at 7.17 ─ 7.22 ppm, and 7.35 ─ 7.40 ppm in **Figure 2-8c** shifted to 7.17 ppm in **Figure 2-8b,** indicating successful modification of PTMCM-SU. Appearance resonances at 2.53 ppm, 2.73 ppm, 3.12 ppm, 3.26 ppm, 5.52 ppm, and 6.02 ppm which corresponded to the SU group are also shown in **Figure 2-8b**. To complete the conversion of the vinyl double bond of PTMCM-VB and prevent consumption of active thiols as a possible side reaction, thiol-ene molar ratio of 10:1 was proceeded[29]. A modification percentage of almost 100% was achieved according to the ^{1}H NMR spectra. Excess of SU at resonances of 2.53 ppm, 2.73 ppm, 3.12 ppm, 3.26 ppm, 5.52 ppm, and 6.02 ppm were removed by dialysis after reaction as shown in **Figure 2-8**. The polymers PTMC, PTMCM-VB and PTMCM-SU were synthesized for comparison of their properties. The molecular weights of PTMC, PTMCM-VB and PTMCM-SU are detailed in **Table 2-1 and Figure S2-1.** The molecular weight of non-functionalized PTMC was 6,400 g/mol with a PDI of 1.5 (**Table 2-1**, **entry 1).** The molecular weights and PDI of PTMCM-VB (**Table 1, entry 2**) and after urea post-modification with SU (**Table 2-1, entry 3)** were 5,100 g/mol and 1.2, and 7,900 g/mol and 2.1, respectively. The increase in molecular weight of the post-modified polymer demonstrates that the SU had been incorporated into the side chain of

PTMC whereas the broadening of polydispersity was possibly due to either a side reaction for attachment of SU at different positions on the vinyl or chain scission that occurred during UV irradiation.

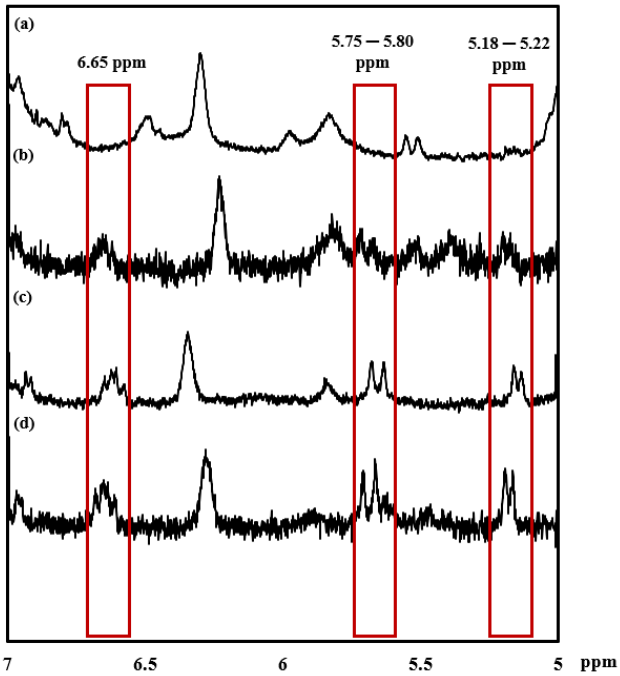

Figure 2-7. [1]H NMR spectra of PTMCM-VB modified with SU at specific time points. (a) 240 min. (b) 120 min. (c) 60 min. (d) 30 min.

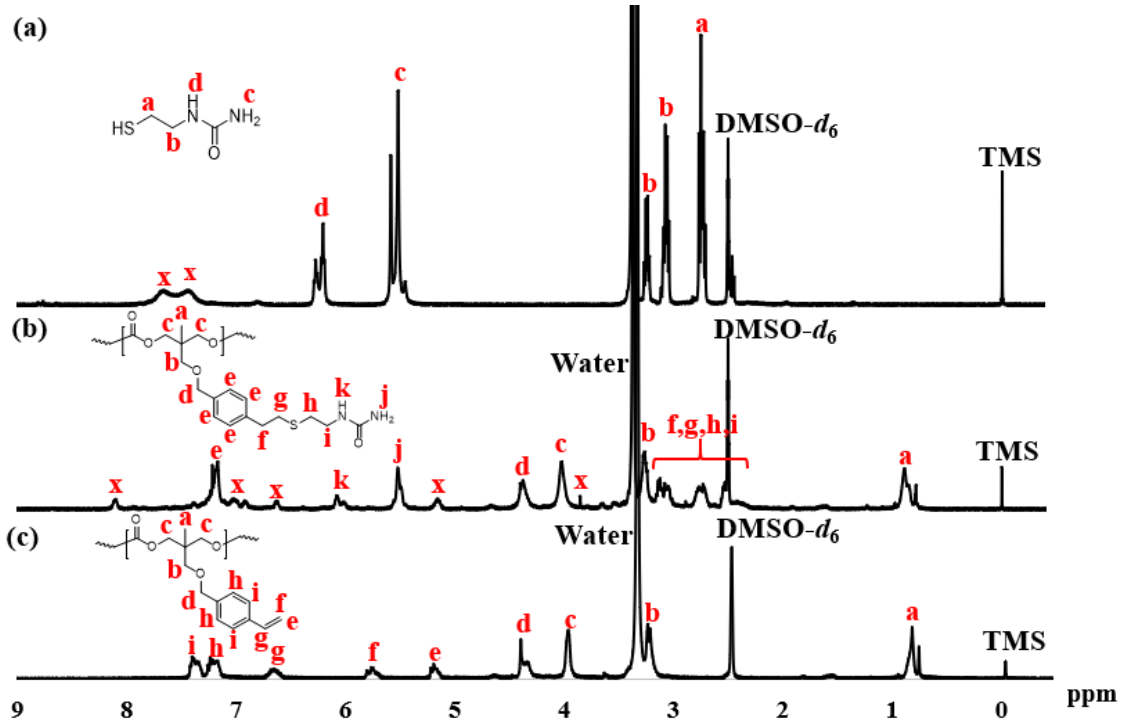

Figure 2-8. [1]H NMR spectra of SU (a), PTMCM-SU (b), PTMCM-VB (c).

Table 2-1. Summary of polymer PTMC, PTMCM-VB, and PTMCM-SU properties.

Entry	Polymer	Yield (%)	M_n	PDI[c]	T_g (°C)
1	PTMC[a]	91	6400	1.5	-29
2	PTMCM-VB[a]	88	5100	1.2	-11
3	PTMCM-SU[b]	22	7900	2.1	-2

[a] Polymerization condition as [Monomer] : [Catalyst] : [Initiator] = 100 : 10 : 1. Initiator = 2,2-Dimethyl-1-propanol. Catalyst = DBU. Solvent = THF. Purification polymer in methanol. M_n determined by SEC in THF with PS standards.
[b] Purification polymer in water by dialysis. M_n determined by SEC in DMF with PS standards.
[c] PDI was defined as M_w/M_n.

The chemical structures of PTMC, PTMCM-VB and PTMCM-SU were also determined by FT-IR (**Figure 2-9a, 2-9b, and 2-9c**), respectively. The significant wavenumbers for PTMC were at 2,970 cm^{-1}, 1,744 cm^{-1} and 1,233 cm^{-1} which were attributed to the C-H, C=O and C-O stretching at the polymer backbone. After introduction of the vinyl aromatic as PTMCM-VB, there was a new peak at 1,645 cm^{-1} represented as a C=C double bond stretching vibration of the vinyl aromatic group. Whereas, after modification of PTMCM-VB with the thiol-urea, a new peak appeared at 3,337 cm^{-1} showing the frequencies of N-H stretching. Also, the C=O of the urea group appeared at 1,651 cm^{-1} while the C-N stretching frequency was seen at 1,557 cm^{-1}. These observations lead to the conclusion that the vinyl aromatic and thiol-urea groups were successfully introduced. To investigate the presence of hydrogen bonding, a thiol-urea precursor was used to measure ^1H NMR (**Figure 2-8**). Splitting peaks were observed between 5.52 ─ 5.58 and 6.21 ─ 6.27 ppm which could be due to the hydrogen bonding between the amide and carbonyl groups of SU. In the case of the modified polymer, although the peaks were displayed in a broad range making it difficult to observe clear splitting, they still showed an analogous pattern.

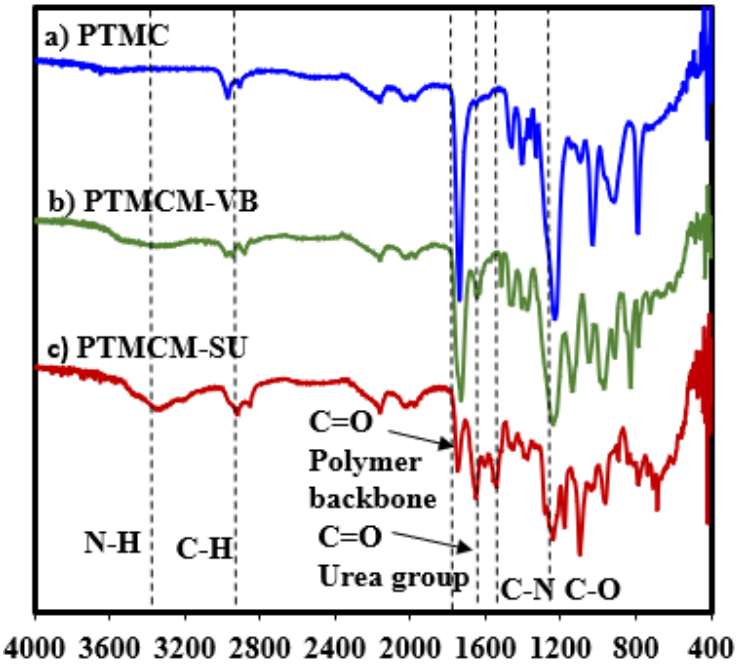

Figure 2-9. FT-IR spectra of PTMC (a), PTMCM-VB (b), and PTMCM-SU (c).

2.3.2 Thermal stability

The thermal stability of non-functionalized PTMC usually has a lower T_g so its performance has been restricted even though it has good biodegradability. For this reason, introduction of a rigid functional group or using intermolecular bonding allows us to overcome these limitations. **Table 2-1** and **Figure S2-2** show a comparison of T_g for PTMC, PTMCM-VB and PTMCM-SU which were -29 °C, -11 °C and -2 °C, respectively. Lizundia et al. reported that ring-opening polymerization of a novel monomer, 2,3-dihydro-5H-1,4-benzodioxepin-5-one (2,3- DHB), yielded a biodegradable aliphatic polyester and that introducing an aromatic into the polymer backbone resulted in exceptional thermal properties with a T_g of nearly 27 °C[30]. The results were similar to those of Nobuoka et al. where the introduction of aromatic

derivatives into the side chain of PTMC yielded a T_g of up to 1°C[31]. The presence of an SU group in the side chain of PTMC further improved T_g, suggesting the presence of self-association hydrogen bonding of the polymer chains. This is supported by the findings of Shieh et al. who incorporated acrylic acid units into poly(N-isopropylacrylamide) (PNIPAAm) tended to increase T_g due to strong hydrogen bonding between the amide groups presence in the PNIPAAm[32]. Based on the result, presence of aromatic as well as thiol-urea were asserted to form π-π interaction and hydrogen bonding that restricted the polymer chain, thus increase T_g.

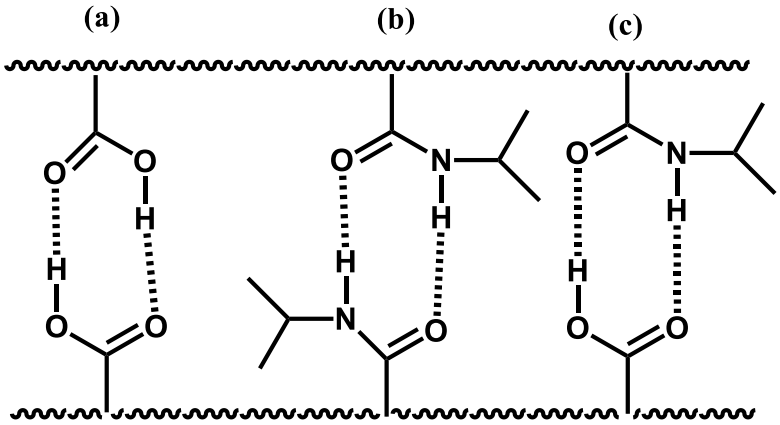

Figure 2-10. Noncovalent interactions of PNIPAm-*co*-PAA copolymers: (a) self-association of PAA units; (b) self-association of PNIPAAm units; and (c) inter-association of PNIPAAm-*co*-PAA[32].

2.3.3 Surface morphology

The synthetic polymers PTMC, PTMCM-VB and PTMCM-SU were spin-coated on a SS (8mm diameter, 0.1 mm thickness) substrate to assess their suitability as coating materials. All the polymers were dissolved in HFIP/DCM at a 1:1 ratio. The roughness and surface morphologies were investigated by laser scanning microscope as shown in **Figure 2-11**. Based on the surface morphologies, the PTMC-coated surface on the substrate would not be fully

covered by the polymer, showed droplet form. This could possibly be due to sticky liquid of PTMC polymer solutions behaving as viscous solutions that are more resistant to deformation from the shear forces of the spin coating process. Thus, coverage area could be one of the influences for its coating performance. PTMCM-VB showed rough, solidified coating surface due to rigidity nature of aromatic presented on polymer chain. Whereas, PTMCM-SU had a slight agglomeration on the substrate surface. This could be due to the solvent evaporation driving the concentration above the solubility limit, leading to interaction of SU within the polymer chains.

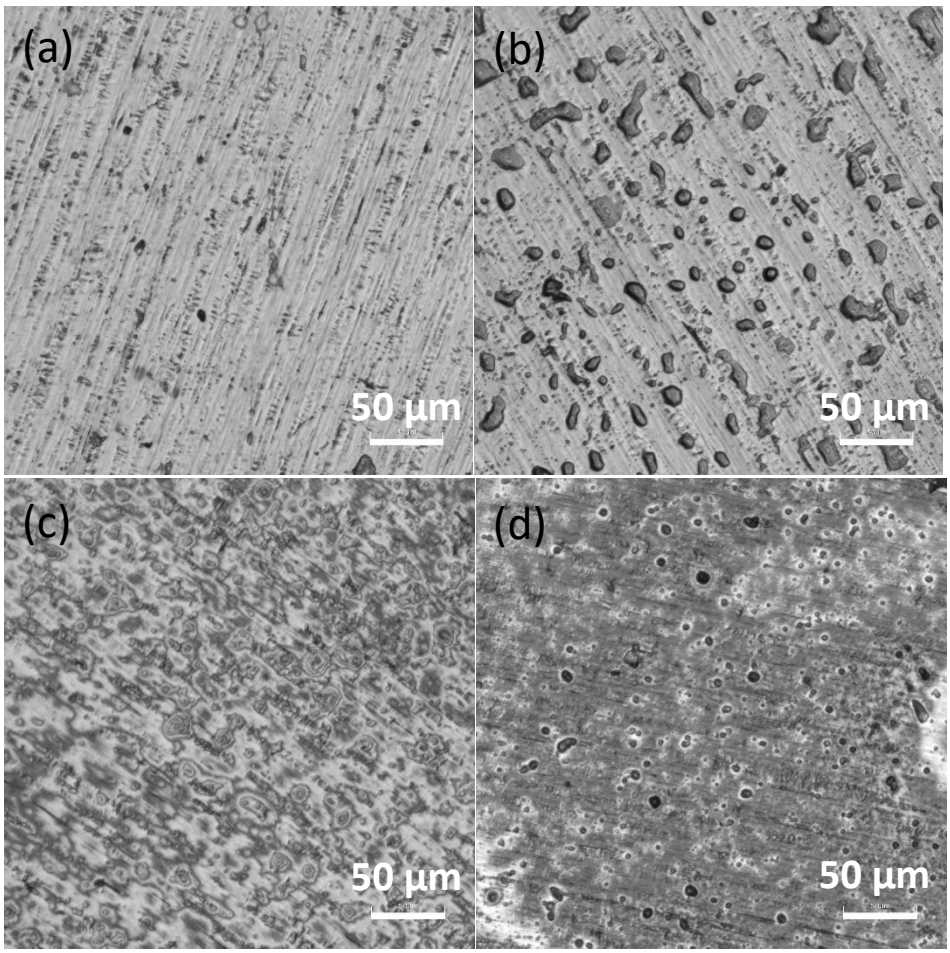

Figure 2-11. Surface morphologies of SS (a), PTMC/SS (b), PTMCM-VB/SS (c), PTMCM-SU/SS (d).

2.3.4 Contact angle

Surface hydrophilicity may play an important role in the material behavior with biological molecules in physiological environment. The water contact angle of spin-coated polymers on the SS were determined as shown in **Figure 2-12**. The contact angles were 87 ° ± 1.06, 65° ± 1.00, 73° ± 0.86 and 53° ± 0.54 for bare SS, PTMC, PTMCM-VB and PTMCM-SU respectively. Compared to bare SS, the PTMC coating was slightly hydrophilic. This could possibly be attributed to the presence of a hydroxyl group in the end chain of the polymer. Whereas the contact angle of the aromatic PTMCM-VB coating was hydrophobic compared to PTMC due to the presence of the aromatic group. Conversely, after introducing the SU coating, PTMCM-SU coating was hydrophilic. Amino groups could have improved the hydrophilicity by interacting with water molecules through hydrogen bond. Contact angles coating on glass and PE were performed and shown in **Figure S2-3**.

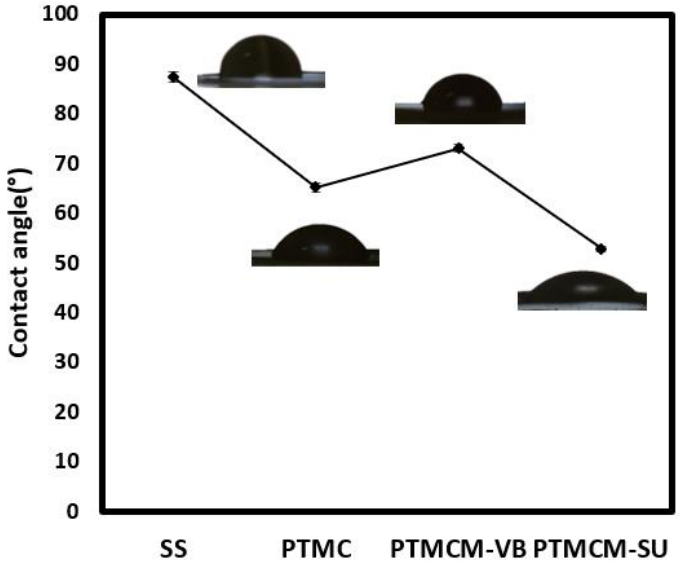

Figure 2-12. Contact angles of SS, PTMC/SS, PTMCM-VB/SS, PTMCM-SU/SS.

2.3.5 Protein adsorption

Protein adsorption of a coating biomaterial is important for determining its biocompatibility when exposed to the physiological environment. It is believed that interaction between the proteins and biomaterials may mediate cellular adhesion that affect the long-term performance of the medical device. Thus, investigating the surface modification of a coating is a matter of concern. **Figure 2-13** shows the protein behaviors in response to PTMC, PTMCM-VB and PTMCM-SU on SS substrate. Albumin, the major protein of human blood plasma, was used in this study. The protein adsorption of non-coated substrates of SS was 4.61 $\mu g/cm^2$ ± 0.002. After coating with PTMC, PTMCM-VB and PTMCM-SU, the protein adsorption was 4.39 $\mu g/cm^2$ ± 1.20, 7.13 $\mu g/cm^2$ ± 1.63, 9.14 $\mu g/cm^2$ ± 0.46. Based on this result, there is a marked difference in protein adsorption for PTMCM-SU which is attributed to its high affinity to adsorb protein compared to non-functionalized and other PTMC derivatives used in this study. According to Arima et al., the effects of surface functional groups such as amines showed higher protein adsorption compared to CH_3, OH and COOH[33]. The aggregation on the substrate could be a factor to consider in a large, adsorbed amount of protein due to more of the surface area of PTMCM-SU being accessible. Furthermore, the effect of wettability could contribute to inducing favorable conditions for protein adsorbed on the surface. Cells effectively adhere onto a polymer surface with moderate wettability with water contact angles of 40─70 °. This is in line with our result as the contact angles of PTMCM-SU were 53 ° ─ 59 °, thus greater protein

interaction with the polymer surface is expected as there is a correlation between cell adherence and protein adsorption. Protein adsorption coating on glass and PE were performed and shown in **Figure S2-4**.

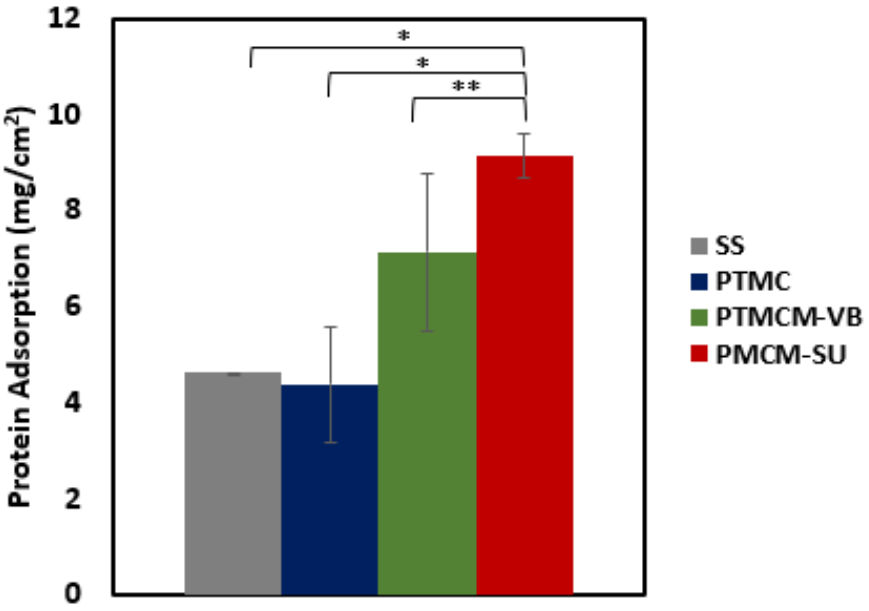

Figure 2-13. Albumin (BSA) protein adsorption on SS (a), PTMC/SS (b), PTMCM-VB/SS (c), PTMCM-SU/SS (d). (n=4, ****p*<0.5, ***p*<0.1, **p*<001).

2.3.6 Cell adhesion

As shown in **Figures 2-14** and **2-15**, the attachment and proliferation of L929 fibroblast cells were investigated after culture for 7 h. The cell attachment of cell at 7 h was quantitative through counting the fluorescence images observed from microscope. For the effect of polymer type on the cell adhesion behavior was observed on the bare SS, PTMC, PTMCM-VB and PTMCM-SU 812 ± 106, 738 ± 85, 1320 ± 181, 1450 ± 138 cells per cm^2 respectively. The cell more adherent on the functionalized PTMC-coated compared to non-functionalized PTMC and

bare SS. There was significant effect on cell adherence after coating with PTMCM-VB and PTMCM-SU. The possible dominant factors could be due to rigidity of aromatic ring, specific hydrogen bonding between the urea group of the polymer and the polar groups of the cell surfaces.

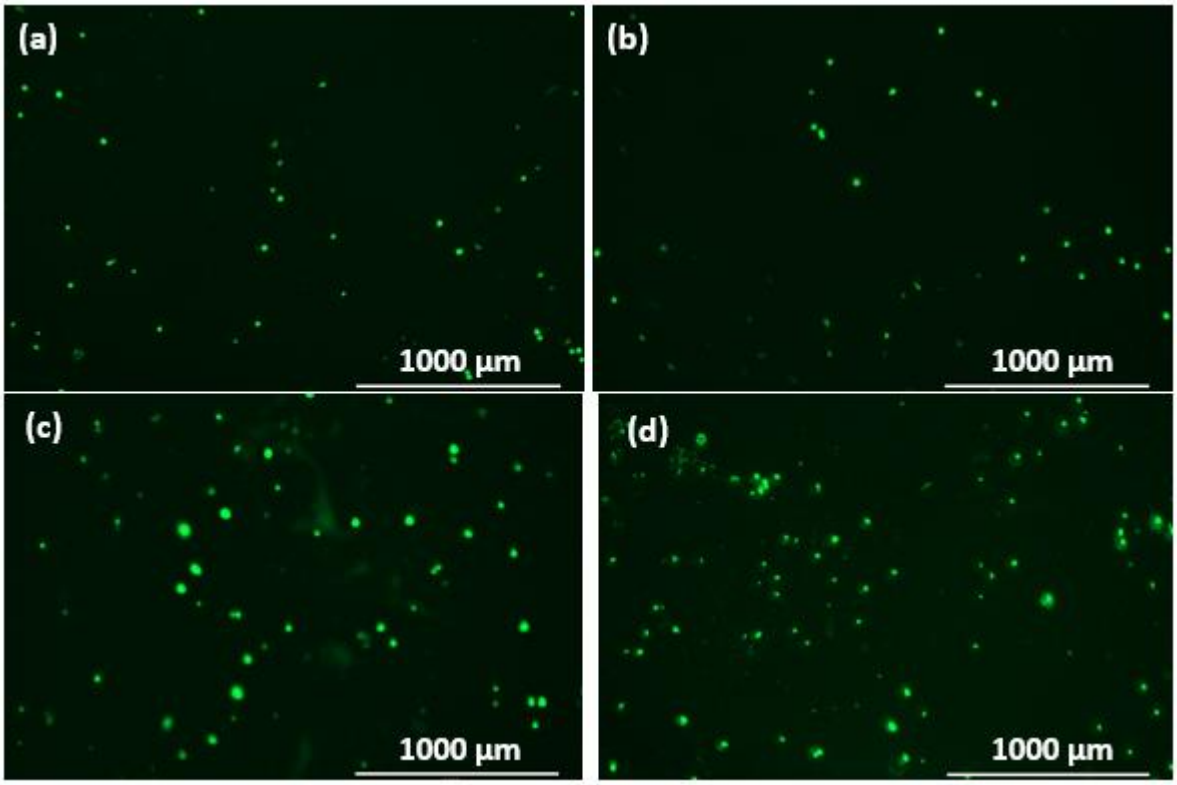

Figure 2-14. Images of L929 cell adhesion on bare stainless steel (SS) (a), PTMC/SS (b), PTMCM-VB/SS (c), PTMCM-SU/SS.

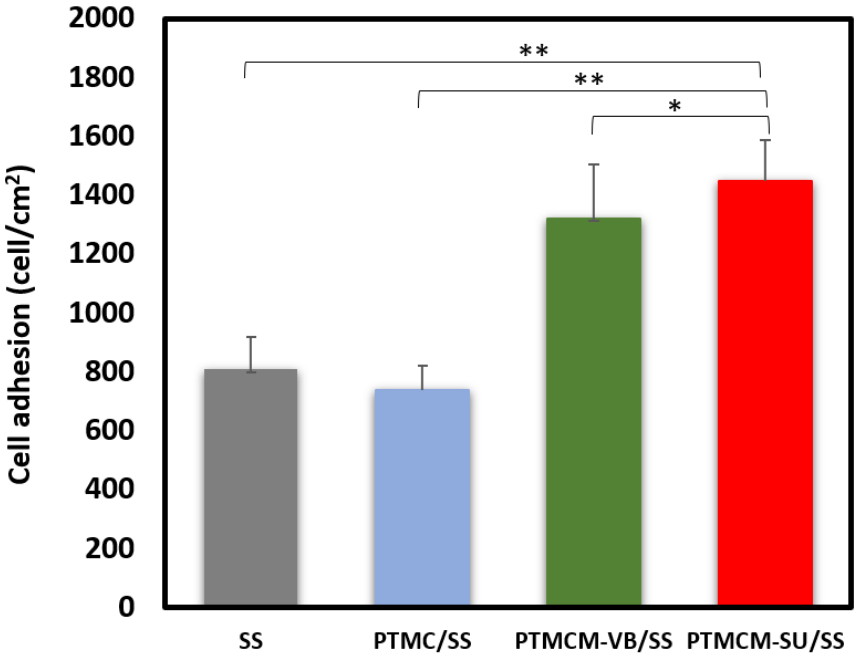

Figure 2-15. Cell adhesion of L929 cell adhesion on bare stainless steel (SS), PTMC/SS, PTMCM-VB/SS, PTMCM-SU/SS (n=5, * p<0.5, ** p<0.1).

2.4 Conclusions

In this study we have successfully been in a design of ester-free PTMC derivatives with aromatic urea moiety, PTMCM-SU for biomaterials coating and its performance. PTMCM-SU has proficiently synthesized via post-modification of vinyl aromatic under UV irradiation method. An induction of hydrogen bonding between polymer chains was investigated as well as its effect on the thermal properties' improvement with T_g = -2 °C. The presence of amine on urea pendant tended to increase hydrophilicity with contact angle between 48 ° to 59 ° of the modified polymer. Besides, the protein adsorption of PTMCM-SU showed high affinity to the albumin on the surface in the range between 5.38 µg/cm^2 to 9.14 µg/cm^2. The cell adherence of PTMCM-SU showed better cell adhesion compared to non-functionalized PTMC. As a result, the synthetic polymer showed promise for use as a biomaterial in tissue engineering and scaffold applications by promoting the bioactivity of the material.

2.5 Supplementary Materials

Molecular weight distribution for PTMC, PTMCM-VB and PTMCM-SU

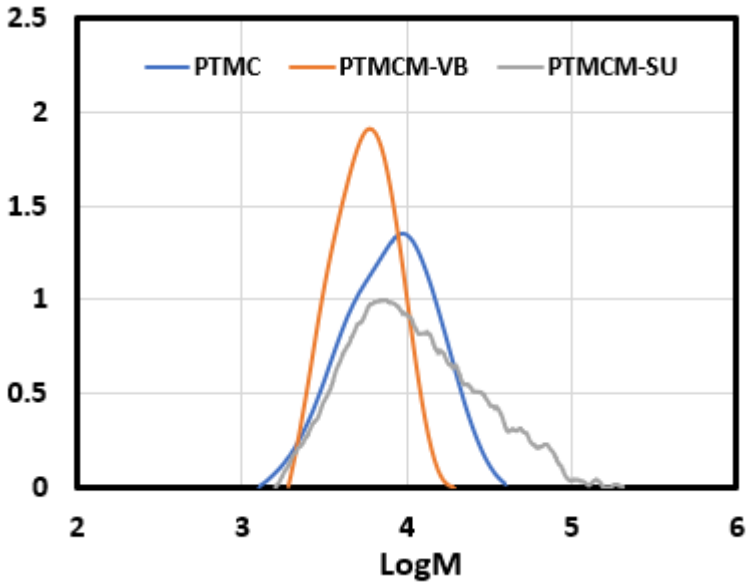

Figure S2-1. Molecular weight distribution for PTMC, PTMCM-VB and PTMCM-SU.

Glass transition temperature (T_g) for PTMC, PTMCM-VB and PTMCM-SU

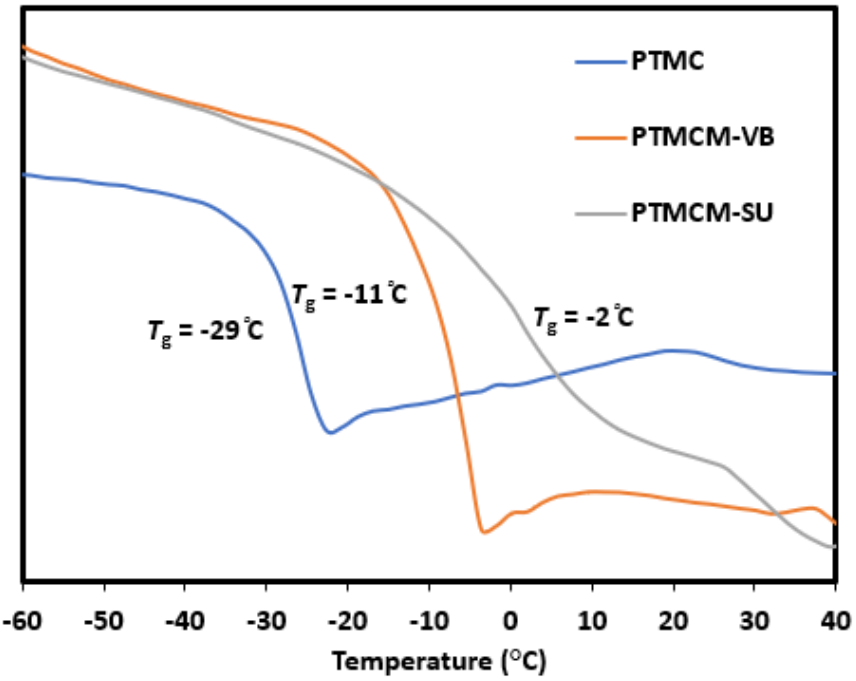

Figure S2-2. Expanded spectra for glass transition temperature (T_g) for PTMC, PTMCM-VB and PTMCM-SU.

Contact angles of polymers on glass, stainless steel (SS) and PE

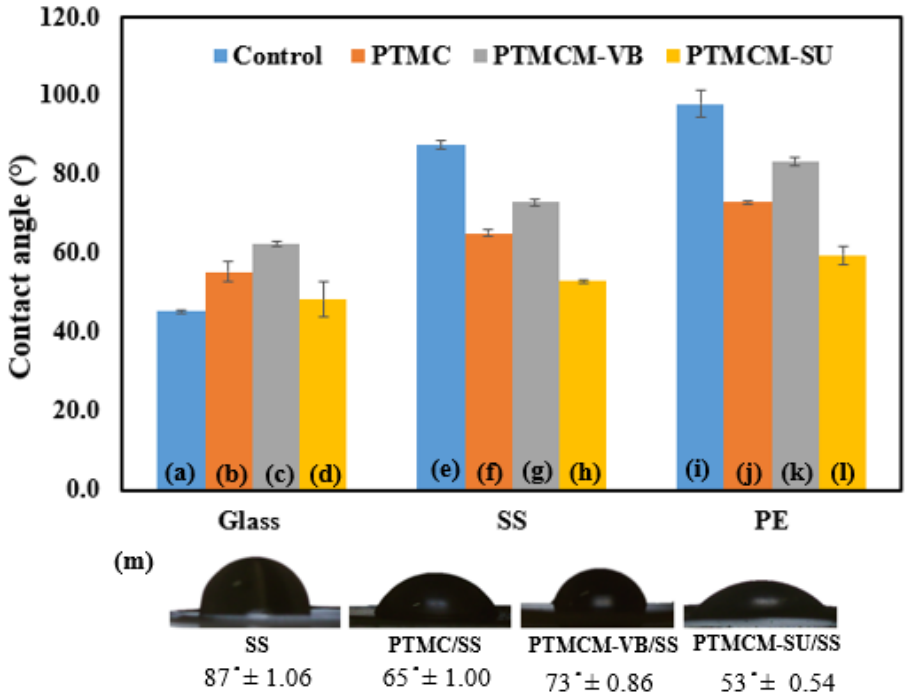

Figure S2-3 Contact angles of (a) glass (b) PTMC/glass (c) PTMCM-VB/glass (d) PTMCM-SU/glass (e) SS (f) PTMC/SS (g) PTMCM-VB/SS (h) PTMCM-SU/SS (i) PE (j) PTMC/PE (j) PTMCM-VB/PE (k) PTMCM-SU/PE (m) Image of SS, PTMC/SS, PTMCM-VB/SS, PTMCM-SU/SS.

Albumin protein adsorption of polymers on glass, stainless steel (SS) and PE

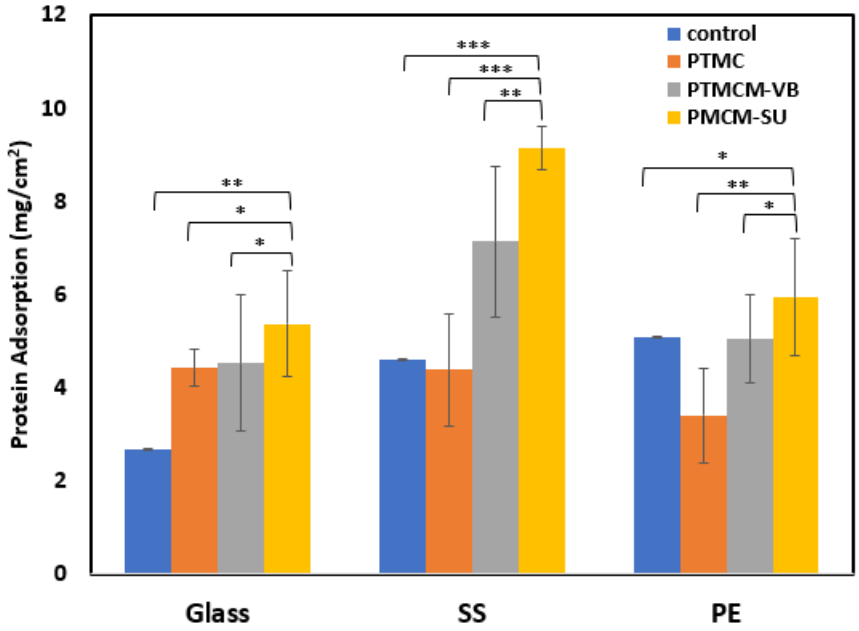

Figure S2-4. Albumin (BSA) protein adsorption of (a) glass (b) PTMC/glass (c) PTMCM-VB/glass (d) PTMCM-SU/glass (e) SS (f) PTMC/SS (g) PTMCM-VB/SS (h) PTMCM-SU/SS (i) PE (j) PTMC/PE (j) PTMCM-VB/PE (k) PTMCM-SU/PE (m) Image of SS, PTMC/SS, PTMCM-VB/SS, PTMCM-SU/SS.(n=4, ***p<0.5, **p<0.1, *p<0.01

2.6 References

1 A. Joy, D. M. Cohen, A. Luk, E. Anim-Danso, C. Chen and J. Kohn, *Langmuir* **2011**, 27, 1891–1899.

2 M. Tallawi, E. Rosellini, N. Barbani, M. Grazia Cascone, R. Rai, G. Saint-Pierre and A. R. Boccaccini, *J. R. Soc. Interface*, **2015**, 12.

3 S. Kim, J. Tan, F. Nederberg, K. Fukushima, J. Colson, C. Yang, A. Nelson, Y. Yang, J. Hedrick, *Biomaterials* **2010**, 8063-8071.

4 Z. Wang, Z. Wang, W. Lu, W. Zhen, D. Yang, S. Peng, *NPG Asia Mater.*, **2017**, 9.

5 Y. Qin, J. Yang and J. Xue, *J. of Mater. Sci.* **2015**, 50, 1150–1158.

6 X. Xu, D. Zhang, S. Gao, T. Shiba, Q. Yuan, K. Cheng, H. Tan and J. Li, *Biomacromolecules*, **2018,** 19, 1979–1989.

7 R. C. Costa, J. G. S. Souza, J. M. Cordeiro, M. Bertolini, E. D. de Avila, R. Landers, E. C. Rangel, C. A. Fortulan, B. Retamal-Valdes, N. C. da Cruz, M. Feres and V. A. R. Barão, *J. Colloid and Interface Sci.* **2020**, 579, 680–698.

8 S. Liu, C. Chen, L. Chen, H. Zhu, C. Zhang, Y. Wang, *RSC. Adv*. **2015**, 5, 98456-98466.

9 H. M. Mousa, A. Abdal-Hay, M. Bartnikowski, I. M. A. Mohamed, A. S. Yasin, S. Ivanovski, C. H. Park and C. S. Kim, *ACS Biomater. Sci. Eng.* **2018**, 4, 2169–2180.

10 A. J. Nathanael and T. H. Oh, *Polymers* **2020**, 12, 3061.

11 Y. K. Kim, K. B. Lee, S. Y. Kim, Y. S. Jang, J. H. Kim and M. H. Lee, *Sci. Rep.* **2018,** 8, 1–11.

12 M. Farrokhi-Rad, T. Shahrabi, S. Mahmoodi and S. Khanmohammadi, *Ceram. Int.*, **2017**, 43, 4663–4669.

13 M. Reggente, P. Masson, C. Dollinger, H. Palkowski, S. Zafeiratos, L. Jacomine, D. Passeri, M. Rossi, ¶ Nihal, E. Vrana, □ Geneviè Ve Pourroy and A. Carradò, *ACS Appl. Mater. Interfaces*, **2018**, 10, 5967–5977.

14 D. B. Gehlen, L. C. de Lencastre Novaes, W. Long, A. Joelle Ruff, F. Jakob, Y. Chandorkar, L. Yang, P. van Rijn, U. Schwaneberg and L. de Laporte, *ACS Appl. Mater. Interfaces*, **2019,** 11, 41091–41099.

15 J. Wang, Y. He, M. F. Maitz, B. Collins, K. Xiong, L. Guo, Y. Yun, G. Wan and N. Huang, Acta *Biomaterialia*, **2013**, 9, 8678–8689.

16 D. Pappalardo, T. Mathisen and A. Finne-Wistrand, *Biomacromolecules*, **2019**, 20, 1465–1477.

17 K. Odelius and A. C. Albertsson, *J. Polym. Sci., Part A-1: Polym. Chem.*, **2008**, 46, 1249–1264.

18 F. Nederberg, V. Trang, R. C. Pratt, A. F. Mason, C. W. Frank, R. M. Waymouth and J. L. Hedrick, *Biomacromolecules*, **2007**, 8, 3294–3297.

19 H. Tang, S. Li, Y. Zhao, C. Liu, X. Gu and Y. Fan, *Bioact. Mater.*, **2022**, 7, 144–153.

20 B. van Bochove, J. J. Rongen, G. Hannink, T. G. van Tienen, P. Buma and D. W. Grijpma, *Polym. Adv. Technol.*, **2015**, 26, 1428–1432.

21 Y. Haramiishi, R. Kawatani, N. Chanthaset and H. Ajiro, *Polym. Test*, **2020**, 86, 106484.

22 J. H. Lee, H. W. Jung, I. K. Kang and H. B. Lee, *Biomaterials*, **1994**, 15, 705–711.

23 J. H. Lee, H. B. Lee and J. Ho, *J. Biomater. Sci. Polymer Edn*, **1993**, 4, 467-481.

24 H. Ying, J. Yen, R. Wang, Y. Lai, J.-L.-A. Hsu, Y. Hu and J. Cheng, *Biomater. Sci.*, **2017**, 5, 2398-2402.

25 L. Y. Tan, N. Chanthaset, S. Nanto, R. Soba, M. Nagasawa, H. Ohno and H. Ajiro,

Macromolecules, **2021**, 54, 5518–5525.

26 H. Y. Ang, Y. Y. Huang, S. T. Lim, P. Wong, M. Joner and N. Foin, *J. Thorac. Dis.*, **2017**, 9, S923.

27 S. Kim, J. Tan, F. Nederberg, K. Fukushima, J. Calson, C. Yang, A. Nelson, Y.Yang J. Hedrick, *Biomaterials*, **2010**, 31, 8063-8071.

28 L. Y. Tan, N. Chanthaset, S. Nanto, R. Soba, M. Nagasawa, H. Ohno and H. Ajiro, *Macromolecules*, **2021**, 54, 5518–5525.

29 J. Yue, X. Li, G. Mo, R. Wang, Y. Huang and X. Jing, *Macromolecules*, **2010**, 43, 9645–9654.

30 E. Lizundia, V. Makwana, A. Larrañaga, J. Vilas, M. Shaver, *Polym. Chem.***, 2017**,8, 3530-3538.

31 H. Nobuoka and H. Ajiro, *Macromol. Chem. Phys.* **2019**, 220, 1900051.

32 Y. T. Shieh, P. Y. Lin, T. Chen and S. W. Kuo, *Polymers*, **2016,** 8, 434.

33 Y. Arima and H. Iwata, *J. Mater. Chem.*, **2007**, 17, 4079–4087.

Chapter 3

Synthesis of New Ester-free Poly(trimethylene carbonate) Bearing Cinnamyl Moiety for Biomaterials Applications

3.1 Introduction

Biomedical implant is becoming vital in human healthcare realm. Over the decades, diverse medical implant such as drug delivery [1], scaffold[2], medical adhesive[3], etc have been widely applied to save lives for many people. Recently, there is a concern about the risk associated with bacterial attaching and proliferating on surfaces of medical implant and causes development of hospital-acquired infections. The mostly types of high-risk infections from *Staphylococci, Pseudomonads* and *Escherichia coli* still remains[4]. It could be posing a substantial treat to patients' health and might lead to death. It is difficult to treat when there are no analogous early warning symptoms, and often diagnosis occurred when full-blown infection has already caused damage to tissue and host organism.

Nature resources extracted from plant such as cinnamyl derivatives and essential oil exhibit antibacterial properties with different level of antibacterial extent. Cinnamyl derivatives

cinnamaldehyde, cinnamate, cinnamic acid has been reported to be able to perform bactericidal activity[5]. There were reported to exert antibiofilm effects on methicillin-resistant *Staphylococcus aureus* and *Staphylococcus epidermidis*[6], *Strepto-coccus pyogenes*[7], *Burkholderia spp.*[8], *E. coli, Pseudomonas sp*.[9], *Listeria sp.*[10], *Salmonella sp.*[11], and *Vibrio spp*.[12]. Whereas essential oil such as thymol, carvacrol were found expressed strong antioxidant and antibacterial potential. These compounds have potential applications in food packaging, cosmetic, pharmaceutical etc, and that their biological activity varies depending on the chemical composition of the compound[13].

Herein, I motivated to introduce these compounds into biodegradable polymer particularly PTMC as antibacterial medical application. Currently, ester-based cinnamyl derivatives have been developed in corporation with PTMC. Jing and co-workers have reported TMC with cinnamate moiety with multiple synthetic routes and further photodimerization of the cinnamate moiety through [2+2] cycloaddition[14]. Julian et al. have synthesized cinnamoyl copolymer of PTMC with molecular weight M_n 3700 g/mol with T_g at -7 °C[15]. Also, the effect of cinnamaldehyde in the PLA/PTMC packaging film was investigated in term of physical, mechanical and antimicrobial properties. The study showed that films comprising 9% cinnamaldehyde or higher displayed a good antimicrobial activity against *E.coli* and *S.aureus*[16].

[2+2]-Cycloadditions of cinnamyl derivatives particular with electron-rich alkenes afford

cyclobutanes, which proposed to be improved physical state of products. Previous study had capable to used cinnamoyl moieties that having methacrylate to photo-crosslinked and de-crosslinked using different wavelength of UV light[17]. Methoxy-cinnamyl having electron-donating group at -para-position is proposed able to activate the aromatic ring toward the cycloaddition. According to Takahiro et al., recent developed initiators such as chemical oxidant, electrochemical method and photoredox catalyst are used for cycloaddition[18]. With this reference, methoxy-cinnamyl was proposed to introduce into side chain of PTMC and further cycloaddition for improving physical state of the polymer.

In this study as demonstrated in **Figure 3-1**, I functionalize cinnamyl derivatives to introduce antibacterial properties and improving physical state of PTMC. The cinnamyl group is an attractive functionality for its aromatic ring structure that could expected to induce π-π interaction. Also, there is possibility to utilize the double bond as crosslinking site for cycloaddition. This approach creates a new planform for the preparation of complex multifunctional materials where combination of reactive functionalities and essential oil for introducing biological properties such as antibacterial performances could be achieved. Hence, in this study, I synthesize cinnamyl PTMC derivatives with simple steps in the homo and copolymer forms and its physical properties have been studied as well, in order to create more sophisticated PTMC with both physically-improvement with promising functionality needed for cutting edge of

medical field.

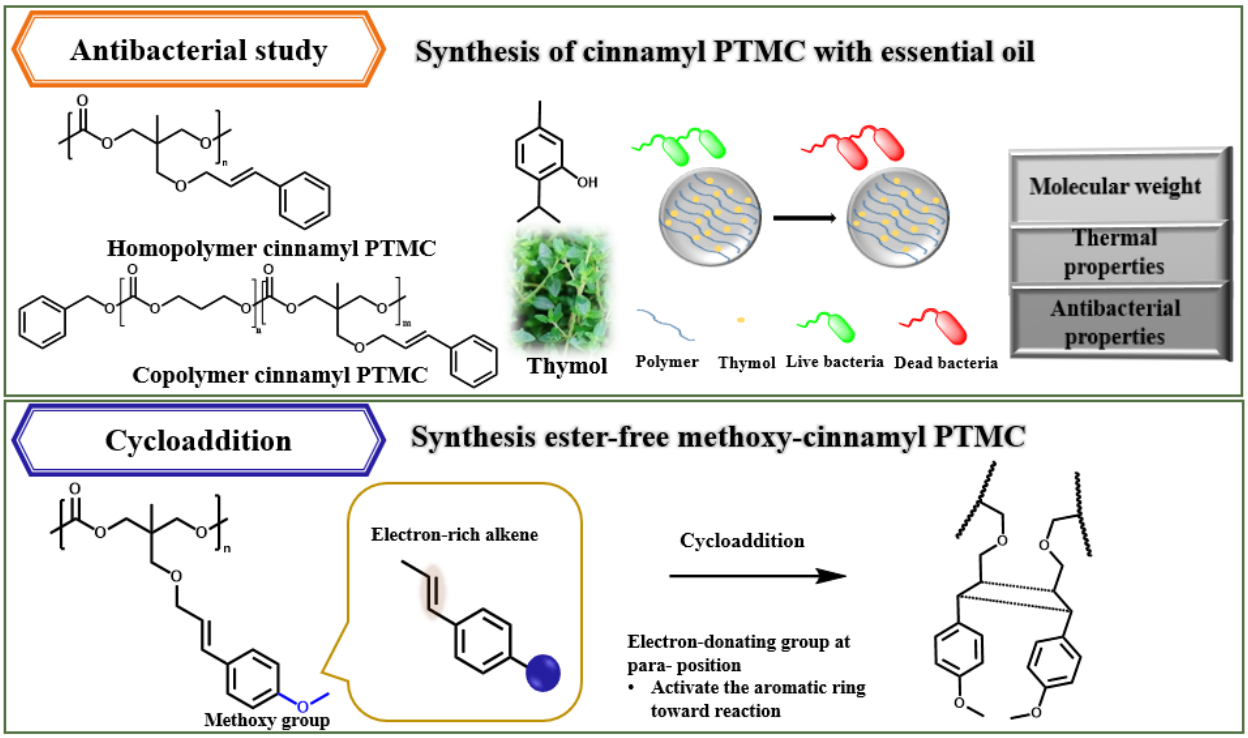

Figure 3-1. Cinnamyl derivative of ester-free PTMC with antibacterial performance and cycloaddition possibility.

3.2 Experimental Section

3.2.1 Materials

Trimethylolethane, ethyl chloroformate, di(trimethylopropane), cinnamyl chloride, 1,8-diazabicyclo [5.4.0]-7-undecene (DBU) and benzyl alcohol (BnOH), 4-methoxycinnamaldehyde, hexafluoro-2-propanol (HFIP), (diacetoxyiodo)benzene (PIDA) were purchased from Tokyo Chemical Industry (TCI), Japan. Potassium hydroxide pellet (KOH) and 1M hydrochloric acid (HCl) were purchased from Nacalai Tesque. Trimethylamine was purchased from Fujifilm Wako Pure Chemical (WAKO), Japan. Anhydrous dimethyl sulfoxide (DMSO), dimethylformamide

(DMF), tetrahydrofuran (THF), ethyl acetate, hexane, isopropanol, sodium chloride, dichloromethane (DCM) for monomer and polymer synthesis as well as purification were used.

3.2.2 Synthesis of 2-((cinnamyloxy)methyl)-2-methylpropane-1,3-diol (diol-cinnamyl)

Diol-cinnamyl was synthesized as follow. To a solution of 25.6 g (0.21 mol) trimethylolethane in 85 ml of anhydrous DMSO, 11.9 g (0.21 mol) of KOH pellet were added under nitrogen atmosphere. The mixture was kept at 0 ℃ and 15 ml (0.11 mol) of cinnamyl chloride was added dropwise. The reaction mixture was allowed to stir at room temperature for 4 h. The mixture was then quenched with 5M HCl under ice bath followed by extraction with ethyl acetate and brine. The organic phase was retained, dried over $MgSO_4$ and evaporated in vacuo. The crude was purified by column chromatography through ethyl acetate/ hexane (5:1) system. The product fraction was dried to give a white solid yield 13.0 g (45 %) of white solid. ^{1}H NMR (400Hz, $CDCl_3$): δ 7.26 (multiple, J = 2H, -C_6H_5-), 6.57 (d, J =16 Hz 2H, -CH(C_6H_5)=CH), 6.28 (dt, J = H, -CH=CH C_6H_5), 4.15 (d, J = 6.4 Hz 2H, -OCH_2CH=CH-), 3.71 (d, J = 2H, CH_2OH), 3.64 (d, J = 2H, CH_2OH), 3.50 (s, 2H, -CH_2OC-), 0.82 (s, 3H, -CH_3). IR: v (cm^{-1}) 3256 (-OH); 2935-2889 (-CH stretch); 1597-1576 (C=C). ESI MS: m/z: calcd for $C_{14}H_{20}O_3Na$, 259.1310 $[M+Na]^+$; found: 259.1301.

3.2.3 Synthesis of 5-((cinnamyloxy)methyl)-5-methyl-1,3-dioxan-2-one (TMCM-MC)

TMCM-MC was synthesized by charging the solution of diol-cinnamyl (6.38 g, 0.027 mol) in anhydrous THF (27ml) and ethyl chloroformate (7.71 ml, 0.09 mol) under nitrogen atmosphere. Next, the mixture was kept at 0 °C and trimethylamine (11.17 ml, 0.09 mol) was added dropwise. The mixture was stirred for 4 h. The mixture was quenched with 1M HCl and extraction with DCM and water. The organic phase was then dried with $MgSO_4$ and the solvent was evaporated. The crude product was recrystallized from hexane/isopropanol to obtain 5.00 g (0.02 mol) of white crystals of TMCM-MC (yield: 71 %).^{1}H NMR (400Hz, CDCl3): δ 7.26 (d, 2H, -C_6H_5-), 6.57 (d, 2H, -CH(C_6H_5)=CH), 6.25 (dt, H, -CH=CH C_6H_5), 4.36 (d, 2H, CH_2OC=O), 4.16 (d, 2H, -OCH_2CH=CH-) 4.11 (d, 2H, CH_2OC=O), 3.43 (s, 2H, -CH2OC-), 1.12 (s, 3H, -CH_3). IR: v (cm^{-1}) 2970-2855 (-CH stretch); 1726 (C=O); 1575 (C=C); 1111 (C-O). ESI MS: m/z: calcd for $C_{15}H_{18}O_4Na$, 285.1103 $[M+Na]^+$; found: 285.1088.

3.2.4 5-Methyl-5-hydroxymethyl-2-(p-methoxystyryl)-[1,3]dioxane

10.0 g (83.2 mmol) trimethylolethane with 0.43 g (2.49 mmol) *p*-toluenesulfonic acid (TsOH) dissolved in 145 ml of anhydrous THF until homogeneous solution. A solution of 13.5 g (83.2 mmol) of 4-methoxycinnamaldehyde in 50 ml of THF was dropwise under nitrogen atmosphere at 0 °C. The reaction mixture was allowed to stir at room temperature for overnight. The mixture was extracted with dichloromethane and water. The organic phase was retained, dried over $MgSO_4$ and evaporated in vacuo. The crude was purified by recrystallization through ethyl acetate. The product fraction was dried to give a white solid yield 12.0 g (56 %) of white solid. ^{1}H NMR (400Hz, $CDCl_3$) δ 7.33 (d, J = 8.8 Hz, 2H, -C_5H_4(CH=CH)-), 6.84 (d, J =8.4 Hz 2H, -(C_5H_4)-OCH_3), 6.72 (d, J =

16 Hz, CH C_5H_4), 6.06 (dd, J = 10.8 Hz 1H, -CH=CH C_5H_4-), 5.06 (d, J = 4.8 Hz 1H, -OCH(O), 3.99 (d, J = 11.6 Hz 2H, -CH_2OC-), 3.86 (d, J = 6 Hz, 2H, -CH_2OH-), 3.80 (s, 3H, -OCH_3), 3.56 (d, J = 12 Hz 2H, -CH_2OC-), 0.78 (s, 3H, -C(CH_3)(CH_2)$_2$).

3.2.5 5-Methyl-5-hydroxymethyl-2-(p-methoxystyryl)-[1,3]diol

5-methyl-5-hydroxymethyl-2-(p-methoxystyryl)-[1,3]dioxane (8.6 g, 32.5 mmol) was dissolved in 65 ml THF and made anhydrous solution using MS4A was added to two-neck round-bottom flask under N_2 atmosphere. The solution was cooled to 0 ℃ using ice bath, DIBAL (97.5 ml) was added very slowly, and the mixture was stirred at room temperature for overnight. The mixture was cooled to 0 ℃ using ice bath and methanol (68 ml) was slowly added dropwise with vigorous stirring. After confirming that the solution became cloudy and turned into viscous solution, a saturated potassium sodium tartrate solution was added, and the mixture was stirred at room temperature until separation into two layers. The mixture was extracted with dichloromethane and H_2O. The organic layer was dried over $MgSO_4$ and evaporated. The crude was purified by silica gel column chromatography using ethylacetate/hexane (1:6) to give white powder (3.13 g, 11.8 mmol, 36 %). ^{1}H NMR (400 MHz, $CDCl_3$): δ (ppm) = δ 7.32 (d, J = 8.4 Hz, 2H, -C_5H_4(CH=CH)-), 6.86 (d, J =8.8 Hz 2H, -(C_5H_4)-OCH_3), 6.52 (d, J = 15.6 Hz, CH C_5H_4), 6.11 (dt, J = 16 Hz 1H, -CH=CH C_5H_4-), 4.12 (dd, J = 6.4 Hz 2H, -OCH_2C=C), 3.81 (s, 3H, -OCH_3), 3.72 (d, J = 10.4 Hz, 2H, -CH_2OH-), 3.60 (d, J = 8 Hz 2H, -CH_2OH-), 3.47 (s, 1H, -CH_2OCH_2-), 0.83 (s, 3H, -C(CH_3)(CH_2)$_2$).

3.2.6 (E)-5-(((3-(4-methoxyphenyl)allyl)oxy)methyl)-5-methyl-1,3-dioxan-2-one (methoxy-cinnamyl) TMC

5-Methyl-5-hydroxymethyl-2-(*p*-methoxystyryl)-[1,3]diol (3.13 g, 12.4 mmol) was dissolved in 12 ml THF and made anhydrous solution using MS4A was added to two-neck round-bottom flask under N_2 atmosphere. Ethylchroloformate (3.5 mL, 37.2 mmol) was added to the solution and cooled to 0 ℃ using ice bath. Then, triethylamine (5.12 ml, 37.2 mmol) was slowly added dropwise and the mixture was stirred for 4 hours. The reaction was quenched by the addition of 1.0 M HCl. The mixture was extracted with dichloromethane and H_2O. The organic layer was dried over $MgSO_4$ and evaporated. The crude was purified by recrystallization by dissolving in good solvent dichloromethane and mixed with hexane:isopropanol (9:1) to give white solid (2.84 g, 9.71 mmol, 78 %).^{1}H NMR (400 MHz, $CDCl_3$): δ (ppm) = δ 7.33 (d, J = 11.6 Hz, 2H, -C_5H_4(CH=CH)-), 6.86 (d, J =8.8 Hz 2H, -(C_5H_4)-OCH_3), 6.53 (d, J = 15.6 Hz, CH(C_5H_4)), 6.09 (dt, J = 16 Hz 1H, -CH=CHC_5H_4-), 4.37 (d, J = 11.2 Hz, 2H, -CH_2O(C=O)-), 4.13 (dd, J = 6.4 Hz 2H, -OCH_2C=C), 3.81 (s, 3H, -OCH_3), 4.09 (d, J = 11.2 Hz, 2H, -CH_2O(C=O)-), 3.42 (s, 2H, CH_2OCH_2-), 3.47 (s, 1H, -CH_2OCH_2-), 1.11 (s, 3H, -C(CH_3)(CH_2)$_2$). ESI MS: m/z: calcd for $C_{16}H_{20}O_5$, 315.12 $[M+Na]^+$; found: 315.14.

3.2.7 Homopolymerization of PTMCM-MC

In the two-neck flask, the homopolymer of PTMCM-MC was prepared by dissolving TMCM-MC (0.50 g, 1.91 mmol) in anhydrous DCM solution with MS4A and stirred for 6 hr under N_2

atmosphere. The solution was then transferred into another flask and the solvent was removed by vacuum evaporation overnight. Briefly, the dried monomer was polymerized via organocatalyst, DBU and initiators, benzyl alcohol and 2,2-dimethyl-1-propanol, 4-(2-hydroxyethoxy)benzaldehyde and 2-(p-tolyloxy)ethan-1-ol respectively. To start the polymerization, monomer concentration was adjusted to 2 M by dissolving monomer with 0.95 ml of anhydrous DCM. Subsequently, DBU (28 µl, 0.191 mmol) and 1 M benzyl alcohol (19.1 µl, 0.0191 mmol) were added. The polymerization proceeded for 23 hr under room temperature. The reaction was stopped by dissolving small amount of DCM and precipitated into poor solvent methanol. The product was recovered by decantation and centrifuged under vacuum (99 % yield). The polymerization initiated by 2,2-dimethyl-1-propanol, 4-(2-hydroxyethoxy)benzaldehyde and 2-(p-tolyloxy)ethan-1-ol were carried out same procedure as described above. The initiators 4-(2-hydroxyethoxy)benzaldehyde and 2-(p-tolyloxy)ethan-1-ol were synthesized and confirmed by ^{1}H NMR (**Figure S3-3 and Figure S3-4**).

3.2.8 Polymerization of benzyl-PTMC

Under N_2 atmosphere, 1,3-dioxan-2-one (TMC) (1 g, 9.8 mmol) of was dissolved in anhydrous DCM solution with MS4A and stirred for 6 hr under N_2 atmosphere. The solution was then transferred into another flask and the solvent was removed by vacuum evaporation overnight. The dried TMC was then dissolved in 4.90 ml anhydrous DCM. Next, DBU (146 µl, 0.98 mmol) and 1 M benzyl alcohol (98 µl, 0.098mmol) were introduced respectively. The polymerization

was carried out for 23 hr under room temperature. The reaction was stopped by dissolving small amount of DCM and precipitated into poor solvent of hexane/2-propanol (9/1, v/v). The product was recovered by decantation and centrifuged under vacuum (90 % yield).

3.2.9 Polymerization of PTMC-OH

Under N_2 atmosphere, 1,3-dioxan-2-one (TMC) (0.8 g, 7.8 mmol) of was dissolved in anhydrous DCM solution with MS4A and stirred for 6 hr under N_2 atmosphere. The solution was then transferred into another flask and the solvent was removed by vacuum evaporation overnight. The dried TMC was then dissolved in 3.5 ml anhydrous DCM. Next, DBU (123 µl, 0.83 mmol) and water (1.49 µl, 0.083 mmol) were introduced respectively. The polymerization was carried out for 26 hr under room temperature. The reaction was stopped by dissolving small amount of DCM and precipitated into poor solvent of hexane/2-propanol (9/1, v/v). The product was recovered by decantation and centrifuged under vacuum (99 % yield).

3.2.10 Copolymerization of PTMCM-MC (PTMCM-MC-*b*-PTMC)

The prepared benzyl-PTMC and PTMC-OH were used as macroinitiator to synthesize block copolymer of PTMCM-MC-*b*-PTMC1, PTMCM-MC-*b*-PTMC2, PTMCM-MC-*b*-PTMC3 as shown in **Table 1 (Entry 5, 6 and 7)**. The monomer concentration and [DBU]/[macroinitiator] ratio was manipulated as shown in **Table 1**. In short, macroinitiator was dissolved in anhydrous DCM solution with MS4A and stirred for 6 hr under N_2 atmosphere. The solution was then

transferred into another flask and the solvent was removed by vacuum evaporation overnight. The specific amount of TMCM-MC, DCM and DBU were introduced under N_2 atmosphere. The reaction was allowed to stand for 22 hr at room temperature. After that, small amount of DCM was diluted with reaction crude and precipitated into poor solvent methanol. The product was recovered by decantation and centrifuged under vacuum. The yield was summarized in **Table 3-1**.

3.2.11 Polymerization of methoxy-cinnamyl PTMC

Under N_2 atmosphere, (E)-5-(((3-(4-methoxyphenyl)allyl)oxy)methyl)-5-methyl-1,3-dioxan-2-one (0.5 g, 1.71 mmol) of was dissolved in anhydrous DCM solution with MS4A and stirred for 6 hr under N_2 atmosphere. The solution was then transferred into another flask and the solvent was removed by vacuum evaporation overnight. The dried TMC was then dissolved in 0.85 ml anhydrous DCM. Next, DBU (25.5 µl, 0.17 mmol) and 1 M benzyl alcohol (17.1 µl, 0.017 mmol) were introduced respectively. The polymerization was carried out for 24 hr under room temperature. The reaction was stopped by dissolving small amount of DCM and precipitated into poor solvent methanol. The product was recovered by decantation and centrifuged under vacuum.

3.2.12 Cycloaddition of methoxy-cinnamyl PTMC

To a cold (0 °C) solution of methoxy-cinnamyl PTMC (0.3 g, 1.03 mmol) in 5.14 ml HFIP under nitrogen atmosphere. 5 % PIDA was added and was stirred at that temperature for 2h and then

warmed up to room temperature for overnight. The solvent was evaporated under reduced pressure and purified in cold methanol.

3.2.13 Characteristics

^{1}H NMR spectra were recorded using a JEOL JNM-ECX400 instrument at 400 MHz with tetramethylsilane (TMS) as an internal standard. Elemental analyses were measured with a Perkin Elmer 2400 II CHNS/O. Fourier transform infrared spectrometer (FT-IR) spectra were obtained with an IR Affinity-1S Shimadzu. Average molecular weight (M_n) and dispersity distribution (PDI) of synthetic polymers were determined by Size Exclusion Chromatography (SEC) the system consists of RI-2031 Plus Intelligent RI detector, PU-2080 Plus Intelligent HPLC pump, AS-2055 Plus Intelligent Sampler, CO-2065 Plus Intelligent Column oven (JASCO), commercial columns (TSKgel SuperH3000 and TSKgel GMHXL) were connected in series. Polystyrene standard (Shodex) (1mg/ml, 0.6 ml/min) were employed and tetrahydrofuran was used as an eluent at 40℃.

3.2.14 Thermal properties

The thermal stability of the polymeric film was determined by thermo-gravimetric analyser TGA-50 (Shimadzu) under nitrogen atmosphere with 10°C/min flow rate to 500°C. Differential scanning calorimetry (DSC) spectra were also analyzed by Shimadzu DSC-60 Plus in the atmosphere with temperature ramp rate 10°C/min in range 70°C-200°C.

3.2.15 Antibacterial Test

The antimicrobial activity of PTMC-MC with thymol 1, 3, 6% was evaluated by way of liquid culture test against *Escherichia coli*. A 0.1 mL of an overnight culture of *E. coli* in Mueller Hinton Broth (MHB) was added to a glass vial containing samples (0.18-0.20 g each) and 10 mL of MHB. The concentration of cultures was adjusted to 10^6 CFU/mL and the cultures were incubated at 30°C. After 0, 2, 18, and 24 h of incubation, the cultures were serially diluted with sterile phosphate buffer (pH 7.4) and then pour plated onto nutrient agar (NA). All plates were incubated at 30°C for 24 h and the colony of bacteria (CFU) was counted by total plate count (TPC).

3.3 Results and Discussion

3.3.1 Synthesis cinnamyl TMC and polymerization

The ester-free TMC (TMCM-MC) derivative bearing cinnamyl group was successfully synthesized with two steps of nucleophilic substitution and cyclization (**Figure S3-1**). This study obtained the functionalized monomer with less reaction steps by direct attachment of cinnamyl chloride into trimethylolethane through S_N2, Williamson ether reaction (**Scheme 3-1a**). After cyclization process, the structure was confirmed by the ^{1}H NMR spectrum (**Figure 3-2a**). The peaks at 7.26, 6.57 and 6.25 ppm were attributed from benzyl and double bond of cinnamyl structure, had appeared on the side chain of TMC. The polymerization was performed through ring-opening polymerization via DBU as catalyst and either benzyl alcohol, 2,2-dimethyl-2-

propanol, 4-(2-hydroxyethoxy)benzaldehyde and 2-(p-tolyloxy)ethan-1-ol (**Scheme 3-1b**) and macroinitiators, benzyl-PTMC and PTMC-OH (**Scheme 3-1c**). From the ^{1}H NMR, the peaks presented at 4.36, 4.16 and 4.11 of the monomer spectra combined into single peak at 4.08 on the polymer spectrum, indicated polymerization had occurred (**Figure 3-2b, c**). For copolymerization of TMCM-MC, there were additional peaks at 4.24 and 2.05 ppm attributed structure of initiator PTMC (**Figure 3-2c**). **Figure S3-2** showed the FTIR spectra of TMCM-MC, PTMCM-MC and PTMCM-MC-*b*-PTMC. The conversion kinetic of monomer initiated by benzyl alcohol was determined from the integration peak area of 4.36 and 4.08 ppm in the ^{1}H NMR **(Figure 3-3).** At 8 hr, almost all the monomer was completely polymerized**.**

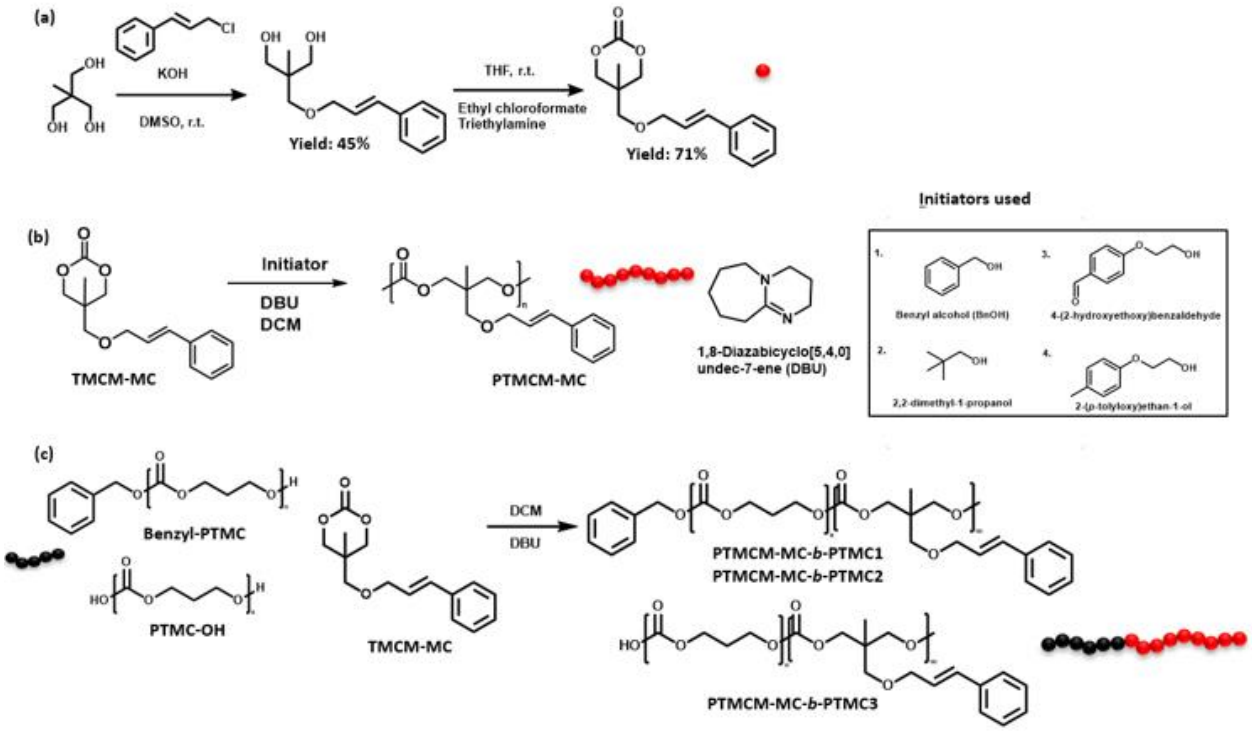

Scheme 3-1. Synthesis of TMCM-MC pathway (a), homopolymerization of TMCM-MC (b), copolymerization of TMCM-MC (c).

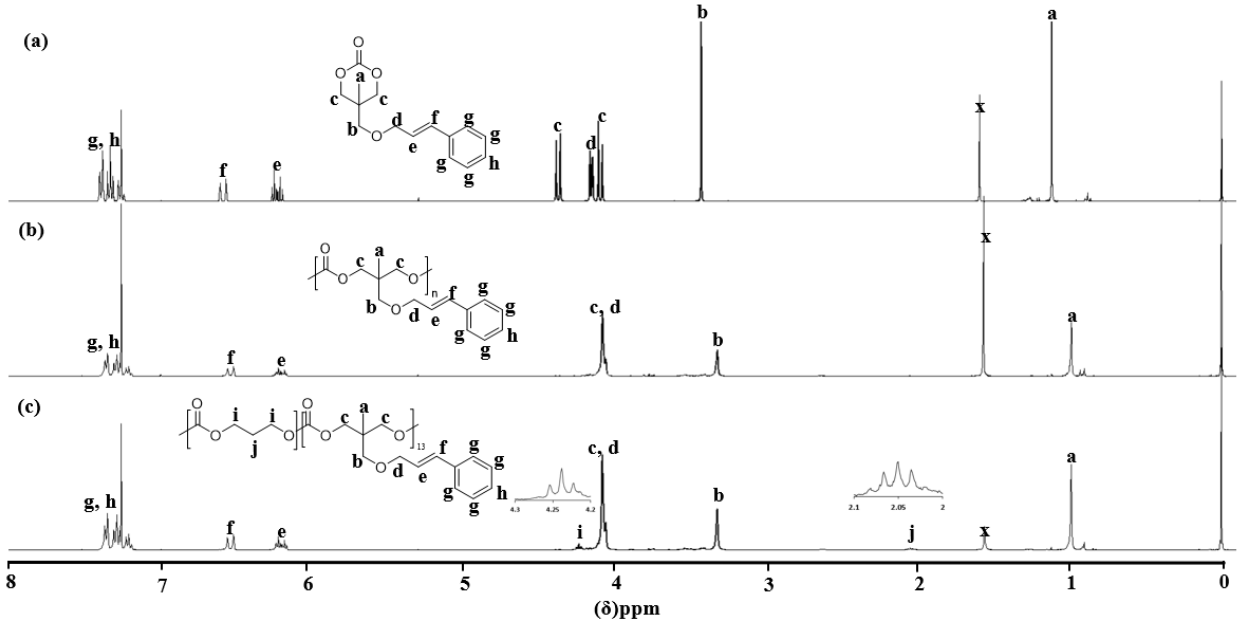

Figure 3-2. ^{1}H NMR spectra of TMCM-MC (a), PTMCM-MC and PTMCM-MC-*b*-PTMC (c) ($CDCl_3$, 400 MHZ, r.t).

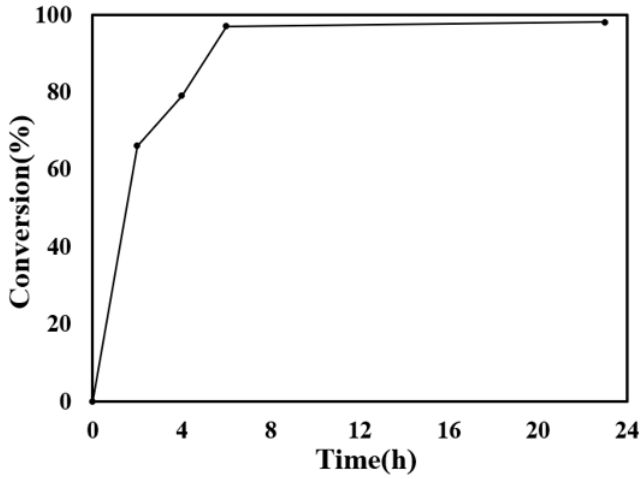

Figure 3-3. The conversion kinetic of TMCM-MC.

3.2.2 Polymer properties

Table 3-1 showed the polymer properties in term of molecular weight and thermal properties. By using the initiator of benzyl alcohol and 2,2-dimethyl-1-propanol, the molecular weight can be achieved at 7000 g/mol whereas the polymers initiated by 4-(2-hydroxyethoxy)benzaldehyde and

2-(p-tolyloxy)ethan-1-ol were 1400g/mol and 4300 g/mol respectively. In order to increase the molecular weight of polymer, copolymerization with PTMC possessed end group of -OH, which is benzyl-PTMC and PTMC-OH were performed. Based on the result, by adjusting catalyst/ initiator ratio and molecular weight of macroinitiator, the molecular weight of cinnamyl PTMC copolymer can be up to 12,000 g/mol. The molecular weight effect can be observed by the physical state of polymer whereby the homopolymer tend to be sticky liquid (**Figure 3-4a**) while copolymer behave as amorphous solid (**Figure 3-4b and Figure 3-4c)**. Thermal properties in T_{10} and T_g were studied in **Table 3-1**. All the polymers had T_{10} above 200 °C and T_g ranged approximately at around 7 ─ 8°C.

Table 3-1: Analysis data of PTMCM-MC and PTMCM-MC-*b*-PTMC.

Entry	Sample	[Initiator]	Initiator	Yield (%)	M_n (× 10^3)[a]	PDI	T_{10} (°C)	T_g (°C)
1	PTMCM-MC	0.01	Benzyl alcohol	99	7.41	1.47	253	-
2	PTMCM-MC	0.01	2,2-dimethyl-1-propanol	64	7.36	1.35	264	8
3	PTMCM-MC	0.01	4-(2-hydroxyethoxy)benzaldehyde	100	1.40	1.11	210	-6
4	PTMCM-MC	0.01	2-(p-tolyloxy)ethan-1-ol	100	4.30	1.80	240	0
5	PTMCM-MC-*b*-PTMC1	0.017	Benzyl-PTMC (*M*n = 5300)	81	5.41	1.17	221	-
6	PTMCM-MC-*b*-PTMC2	0.001	Benzyl-PTMC (*M*n = 5300)	90	9.72	1.37	268	7
7	PTMCM-MC-*b*-PTMC3	0.001	PTMC-OH (*M*n = 9032)	92	12.27	1.26	259	8

[a] Determined by SEC by polystyrene (PS) standard in THF, 40 °C.
[b] [Catalyst]/[Initiator] ratio was 0.1/0.01 except entry 6 and entry 7.
Concentration of polymerization were performed in 2M DCM except entry 6 with 1M DCM.

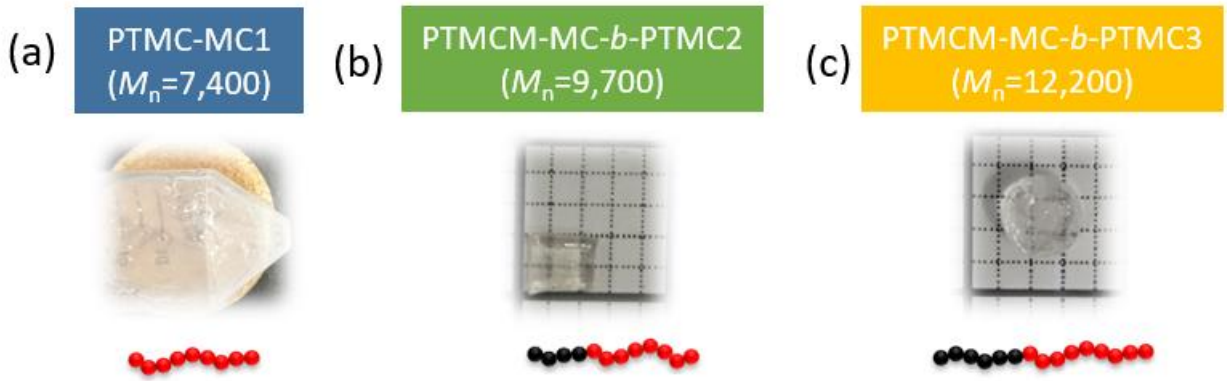

Figure 3-4. The physical state of homopolymer, PTMC-MC1 (a), PTMCM-MC-*b*-PTMC2 (b) PTMCM-

MC-*b*-PTMC3 (c).

3.2.3 Antibacterial Test

Figure 3-5 showed the results of the antimicrobial test of cinnamyl PTMC coated at PE substrate against *E.coli.* As based on the **Figure 3-5** bare substrate of PE itself did not show any antimicrobial activity which remained $\log_{10}$ 5.2 × 10^6 CFU/ml after 24 h. Cinnamyl PTMC (PTMCM-MC) and PTMCM-MC with 1% and 3% thymol revealed similar trend of antibacterial efficiency. After 24 h of incubation, the samples for PTMCM-MC, PTMCM-MC/1% thymol and PTMCM-MC/3% thymol were 4.8× 10^6 CFU/ml, 4.6× 10^6 CFU/ml, and 4.7 × 10^6 CFU/ml respectively. PTMCM-MC with 6% thymol was significant effective against *E.coli* when compared with other samples. At 2, 18, and 24 h incubation, the E. coli reduced from 6.0 × 10^6 CFU/ml to 2.3 × 10^6 CFU/ml, 3.3× 10^6 CFU/ml and 3.6× 10^6 CFU/ml respectively. At first 2 h, the number of bacteria decreased could be attributed by the experienced stress due to the cell exposure to new environment. Approximately 55 % reduction of *E.coli* growth has been suppressed by formulation of PTMC-MC with 6% thymol. In this study, PTMCM-MC with 6% thymol showed effective antimicrobial activity against *E.coli* compared to other formulations

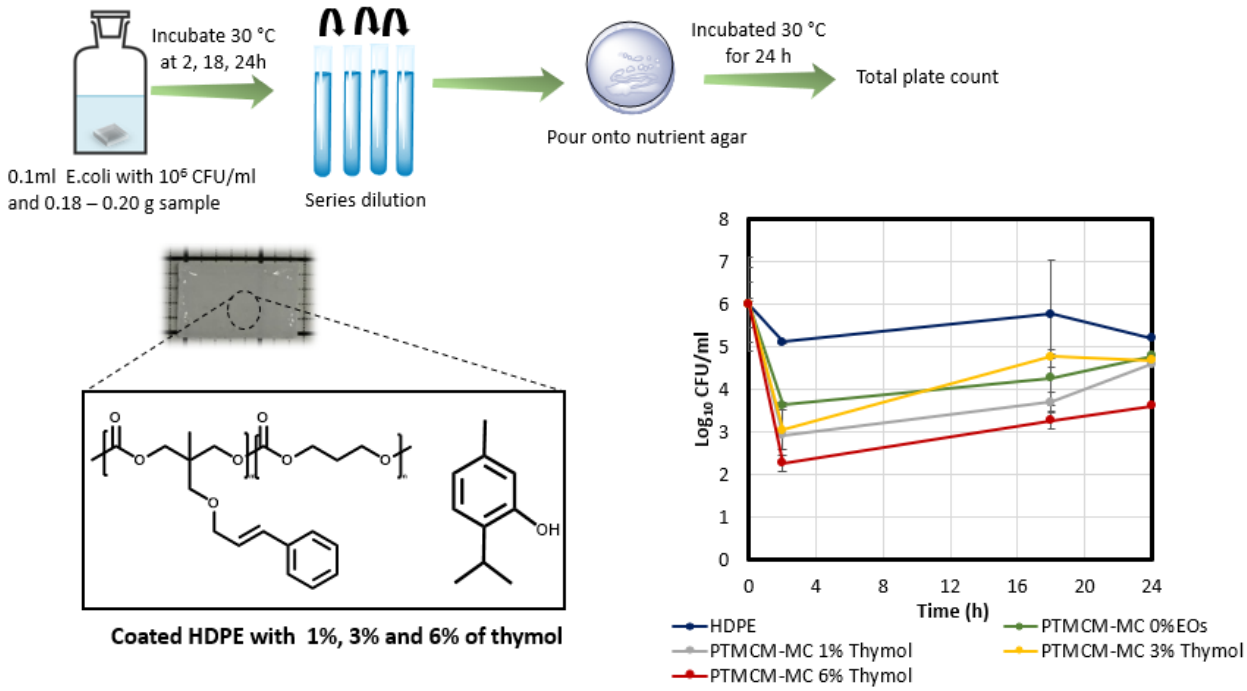

Figure 3-5. Antimicrobial test of against *E.coli*.

3.2.4 Synthesis of methoxy-cinnamyl PTMC

To extend the effort to improve physical state of PTMC and further utilize cinnamyl derivatives, methoxy-cinnamyl moiety has targeted to introduce into side chain of PTMC. Methoxy-cinnamyl group has successfully functionalized into TMC through 3 steps: introduction of methoxy-cinnamyl aldehyde, selective deprotection by diisobutylaluminium hydride (DIBAL) and cyclization **(Scheme 3-2(a)).** The reaction was confirmed with ^{1}H NMR and mass spectrometry, ESI. Due to the presence of methoxy group induced electron-rich alkene in the cinnamyl structure, prompt to activate the cycloaddition reaction **(Scheme 3-2(b)).** By using diacetoxyiodo)benzene (PIDA) as catalyst and hexafluoro-2-propanol (HFIP) as solvent, cycloaddition was performed by adjusting reaction concentration, catalyst ratio and reaction time as shown in **Table 3-2**. The

reaction was determined by ^{1}H NMR as shown in **Figure 3-6** whereby the integral of double bond was reduced along the reaction. **Table 3-2** and **Figure 3-7** showed the results of the cycloaddition condition and molecular weight distribution. For reaction proceed at 24h with 0.2 M concentration and 5% catalyst, the cycloaddition yield was 59% with molecular weight increased from 2400 g/mol **(Figure 3-7 (a))** to 2900 g/mol **(Figure 3-7 (b)).** This is proposed the cycloaddition was carried out within the intra-molecular polymer chain. On the other hand, with increased reaction to 48h with concentration of 1 M and 10% catalyst, cycloaddition yield was 61% with the molecular weight has significantly increased from 3300 g/mol **(Figure 3-7 (c))** to 5900 g/mol **(Figure 3-7 (d)).** With the 2M reaction concentration, the polymer has highly crosslinked that it cannot be dissolved for measuring molecular weight. This phenomenon attributed to intermolecular polymer chain was achieved as we expected.

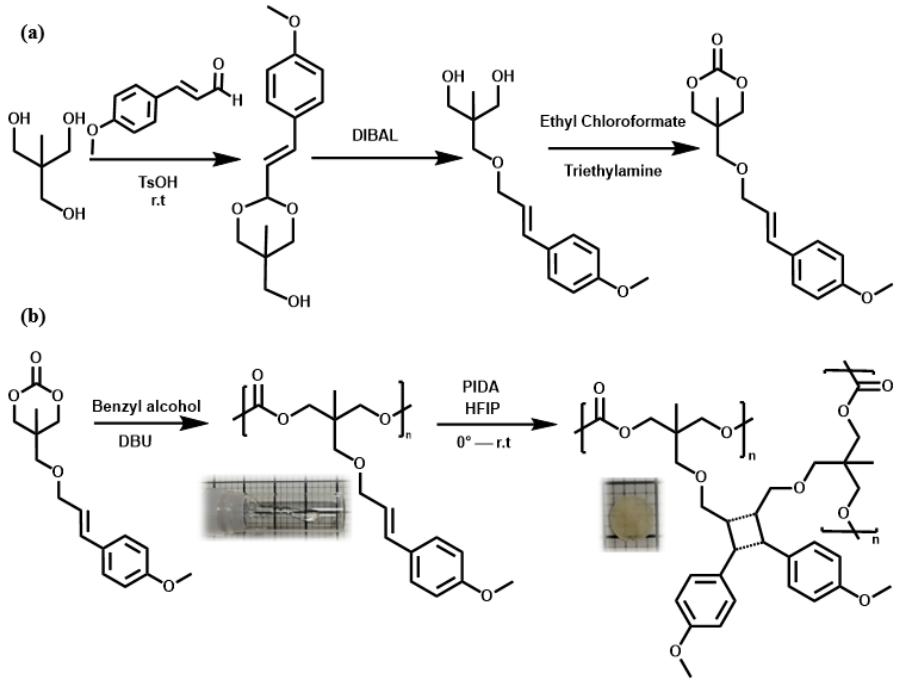

Scheme 3-2. Synthesis of methoxy-cinnamyl TMC pathway (a), polymerization of TMCM-MC and cycloaddition (b).

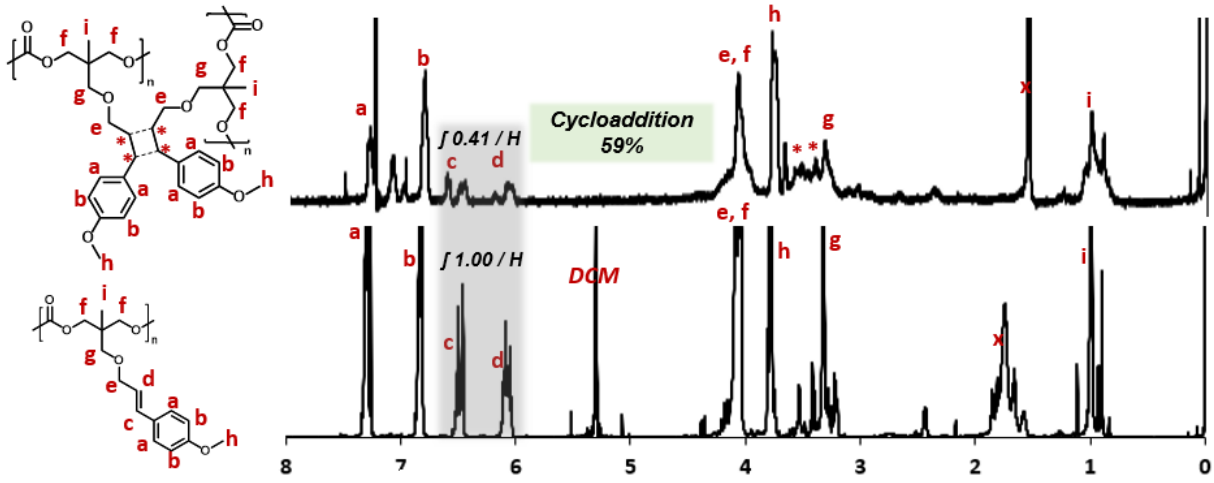

Figure 3-6. ^{1}H NMR spectra for cycloaddition reaction in $CDCl_3$.

Table 3-2: Analysis data of PTMCM-MC and PTMCM-MC-*b*-PTMC.

Entry	Concentration (M)	Catalyst ratio	Time (h)	Cycloaddition %	Mn (PDI)	
					Before	After
1	0.2	0.05	24	59	2400 (1.36)	2900 (1.80)
2	1	0.10	48	61	3300 (1.40)	5900 (3.50)
3	2	0.15	48	85	3300 (1.40)	- [a]

[a] Cannot be determined.

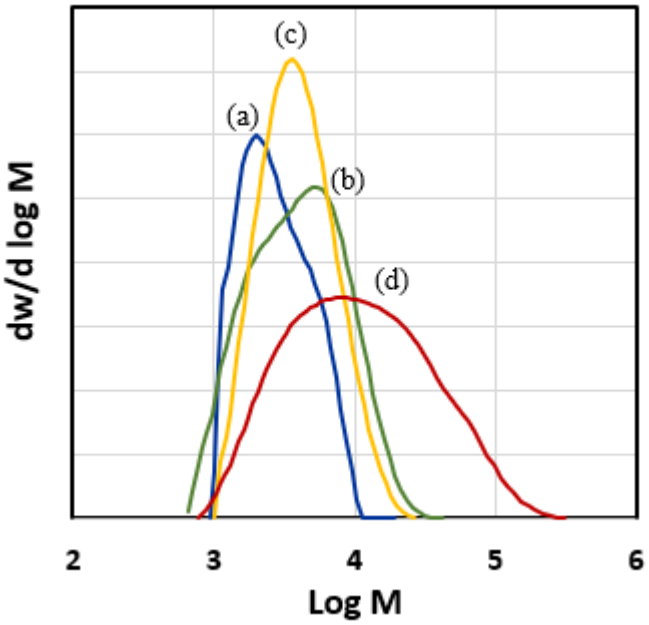

Figure 3-7. Molecular weight dispersity of the polymer before and after cycloaddition.

3.4 Conclusions

Ester-free PTMC with cinnamyl derivatives has been successfully synthesized with facile synthetic pathway. The physical and thermal properties can be improved through copolymerization with macroinitiator with optimal [C]/[I] 0.1/0.001. The resulted polymer can be afforded amorphous solid with molecular weight M_n of 12,000 g/mol and thermal properties T_{10} = 259 ℃ and T_g = 8 ℃. Cinnamyl derivative PTMC with 6% thymol coating displayed considerably antibacterial efficiency against *E.coli*. Also, methoxy-cinnamyl PTMC derivative was able to perform cycloaddition to improve physical properties of PTMC.

3.5 Supplementary materials

^{1}H NMR spectra of TMCM-MC and diol cinnamyl

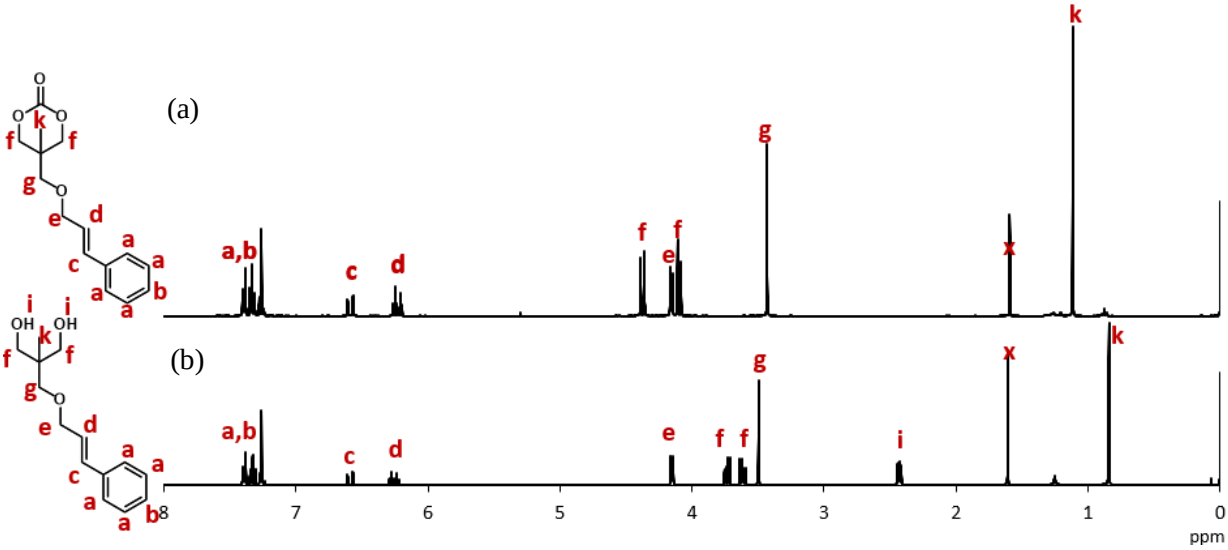

Figure S3-1. ^{1}H NMR spectra ($CDCl_3$, 400 MHz, r.t) of TMCM-MC (a) 2 (diol-cinnamyl) (b).

FTIR spectra of cinnamyl monomer of TMCM-MC, homopolymer of PTMCM-MC and copolymer of PTMCM-MC-*b*-PTMC

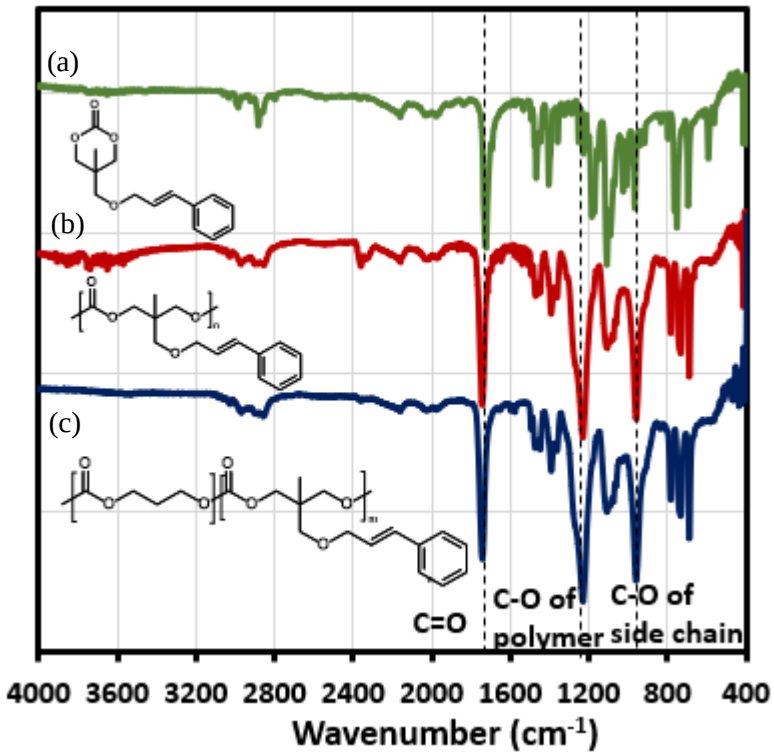

Figure S3-2. FTIR spectra of TMCM-MC (a) PTMCM-MC (b) and PTMCM-MC-*b*-PTMC (c).

^{1}H NMR spectra of initiator 2-(p-tolyloxy)ethan-1-ol for TMCM-MC

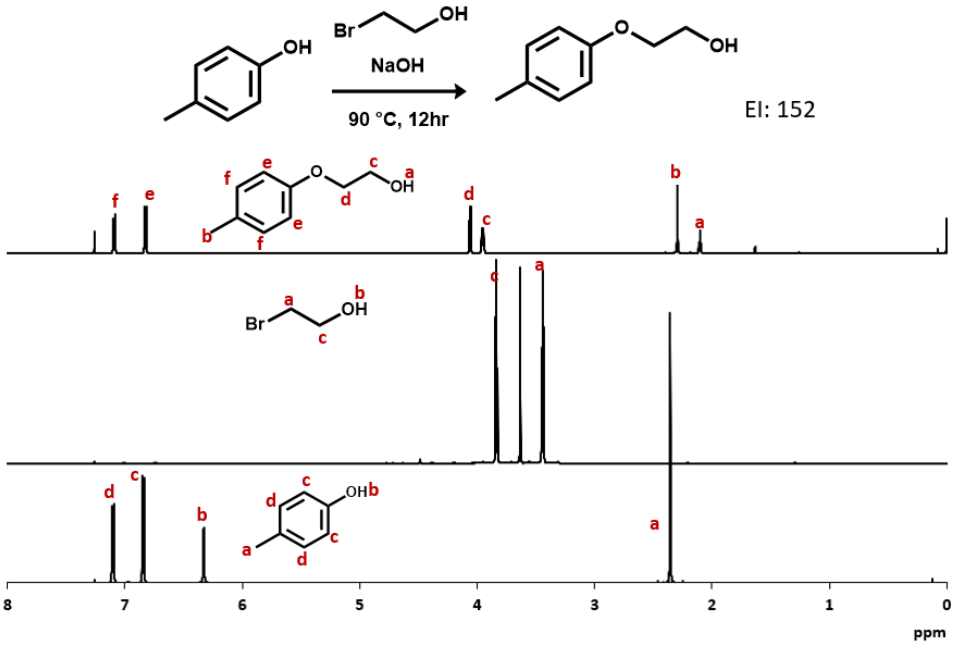

Figure S3-3. ^{1}H NMR spectra ($CDCl_3$, 400 MHz, r.t) of initiator 2-(p-tolyloxy)ethan-1-ol.

^{1}H NMR spectra of initiator 4-(2-hydroxyethoxy)benzaldehyde for TMCM-MC

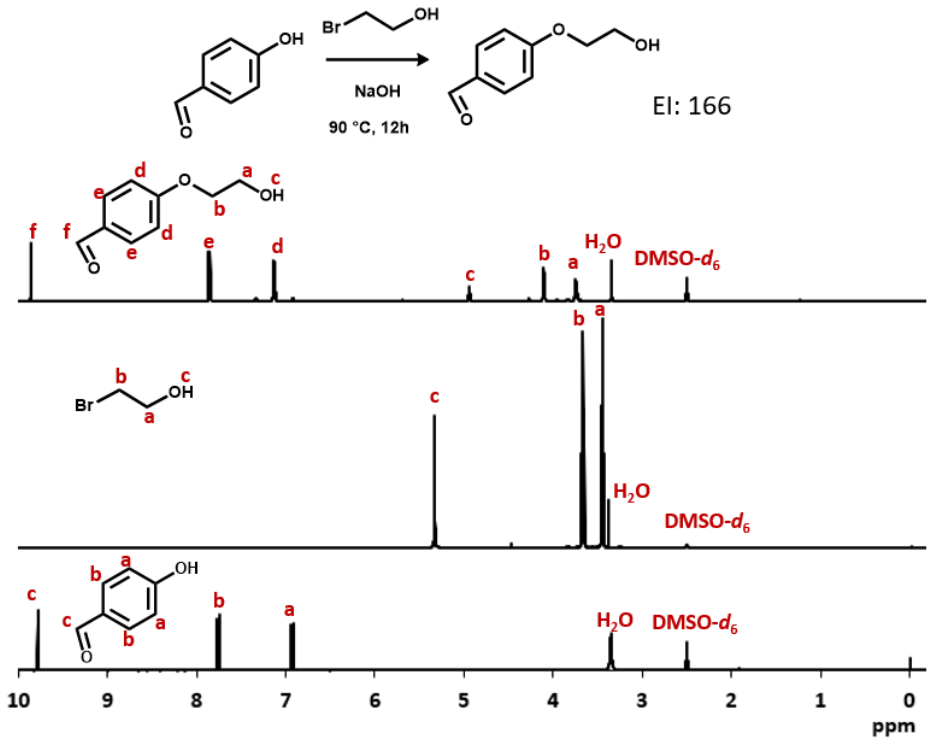

Figure S3-4. ^{1}H NMR spectra ($CDCl_3$, 400 MHz, r.t) of initiator 4-(2-hydroxyethoxy)benzaldehyde

3.6 References

1 Z. Zhang, D. Grijpma, J. Feijen, *J. Control. Release*, **2006,** 111, 263-270.

2 S. Theiler, P. Mela, S. E. Diamantouros, S. Jockenhoevel, H. Keul and M. Mö Ller, *Biotechnol Bioeng*, **2011**, 108, 694–703.

3 S. Zhang, H. Li, M. Yuan, M. Yuan, M. Yuan, H. Chen, *Int. J. Mol. Sci*. **2017**, 18(10), 2041

4 A. Singh and A. K. Dubey, *ACS Appl. Bio Mater*. **2018**, 1, 1, 3–20

5 N. G. Vasconcelos, J. Croda and S. Simionatto, *Microb. Pathog.*, **2018**, 120, 198–203.

6 P. Jia, Y. Xue, X. Duan, S. Shao. *Lett Appl Microbiol,* **2011**, 53, 409–416.

7 R. Mohmed, B. Shafreen, C. Selvaraj, S. K. Singh and S. Karutha Pandian, *J. Mol. Recognit.*, **2014**, 27, 106–116.

8 G. Brackman, U. Hillaert, S. Calenbergh, H. Nelis, T. Coenye, *Res Microbiol,* **2009**, 160, 144-151..

9 C. Niu, E. Gilbert, *Appl Environ Microbiol*, **2004**, 70, 6951–6956.

10 A. Upadhyay, I. Upadhyaya, A. Johny, K. Venkitanarayanan, *Food Microbiol*, **2013**, 36, 79-89.

11 H. Zhang, W. Zhou, W. Zhang, A. Yang, Y. Liu, Y. Jiang, S. Huang, J.Su, *J. Food Prot,* **2014**, 77, 927-933.

12 G. Brackman, S. Celen, U. Hillaert, S. van Calenbergh, P. Cos, L. Maes, H. J. Nelis and T. Coenye, *PLoS ONE*, **2011**, 6, 16084.

13 A. Escobar, M. Perez, G. Romanelli, G. Blustein, *Arab. J. Chem.*, **2020**, 13, 9243-9269..

14 X. Hu, X. Chen, H. Cheng and X. Jing, *J. Polym. Sci., Part A-1: Polym. Chem.*, **2009**, 47, 161–169.

15 J. P. Chesterman, T. C. Hughes and B. G. Amsden, *Eur. Polym. J.*, **2018**, 105, 186–193.

16 Y. Qin, J. Yang and J. Xue, *J. Mater. Sci.*, **2015**, 50, 1150–1158.

17 J. P. Chesterman, F. Chen, A. J. Brissenden and B. G. Amsden, *Polym. Chem*., **2017**, 8, 7515–7528.

18 T. Horibe and K. Ishihara, *Chem. Lett***. 2020**, 49, 107–113.

Chapter 4

PTMC Derivatives Bearing Aromatic Moieties and Urea Groups for Drug-Release Control Application

4.1 Introduction

Coronary heart disease are major heart disease and leading cause of death in the worldwide. It occurs when the coronary arteries are narrowed or blocked caused by the buildup of fatty material known plaque. Percutaneous coronary intervention (PCI) or known as angioplasty with stent is one of effective treatment of this disease and has been introduced since in the late 1970s[1]. It is a non-surgical treatment that implant a stent by using catheter to open the blood vessels in the heart, and series of processes will be take place in sequence, with an order of thrombosis, smooth muscle cell (SMC) proliferation, and endothelization, respectively[2]. In the early invention bare metal stents (BMS) are applied yet problem encountered such as re-narrowing of the treated artery due to in-stent restenosis (ISR) whereby diameter stenosis of more than 50% in the stented region of the blood vessel primarily due to excessive neointimal

proliferation within the stented segment. Bare metal stent restenosis in high-risk patient such as diabetes, small vessel and long segments of diffusely diseased arteries still unacceptably high (30-60%)[3].

With intense improvements in PCI, design stent coating material and incorporation with drug to prevent ISR formation or neointima growth associated with stent implantation in PCI. Therefore, drug combination therapy is an effective in curb the ISR formation problem. Incorporation of antiplatelet and vasodilator agent into stent coating have effectively inhibit the ISR formation. This formation is analogous to the benign tissue growth process, which had led to the discovery of anti-tumor drugs such as sirolimus and paclitaxel as promising agent for the treatment of ISR[3]. In order to provide the platform for drug delivery, bioresorbable polymer is considered an excellent candidate for coating with the drug on the stent.

Poly(L-lactide) (PLLA) and poly(glycolide acid) (PGA) have been developed as polymer coating with the drug for DES. Roger Laham and co-workers have studied the release profile of both paclitaxel and sirolimus combination from a poly (D, L-lactide-*co*-glycolide)/amorphous calcium, phosphate, PLGA/ACP coated stent. The result showed both drugs had similar drug release kinetics and the burst release was occurred at the early stage[3]**.** Ni and co-workers investigated release profile of sirolimus in poly(L-lactide) (PLLA) stents under

various conditions. The release percentage of sirolimus can be controlled by bi-layer coating and drug/ polymer ratio[4]. However, there is some issues in term of serious bulk erosion problems, like high local acidity and poor mechanical properties.

With the concern of more long-term safety and efficacy of DES, the releasing drug in a control manner to achieve a therapeutic goal for the effective treatment of coronary heart disease and prevent any side effect of sudden burst release of drug in a short period is still inspiringly ongoing researched and developed. A controlled release formulation over an extended period offers prolonged efficacy, decreased toxicity, and more compliance to patient. The role of intermolecular bonding could be pronounced factor to prevent burst release of drug at the initial stage. Ouazib and co-workers developed polymeric drug delivery system of polyvinylpyrrolidone/acebutolol that physically interact each other that have a large effect on the rate of release drugs from a polymer matrix[5].

Notably, urea is associated with hydrogen bonding as a strategy for improving physical properties and desired intermolecular interaction such as drug release control[6]. Kim and co-workers have studied that introducing a urea-bearing functional group into a copolymer for forming stable micelle for drug delivery. Presence of urea-functional group lowered critical micelle concentration, enhanced kinetic stability of the micelles. With the non-covalent interaction with

doxorubicin (a model anticancer drug). The increase of urea content led to a slight decrease in doxorubicin release rate.

Inspired by these findings, it is proposed that the addition of a urea group into the side chain of PTMC with an ester free design would be potential polymeric drug delivery system (**Figure 4-1**). PTMC, PTMCM-VB and PTMCM-SU incorporated with sirolimus, and paclitaxel drugs coated on stainless steel to study the influence of different functional group on the drug release control behaviour. Also, PTMCM-SU/sirolimus coating was used to study the influence of polymer and drug effect on the cell adhesion behaviour.

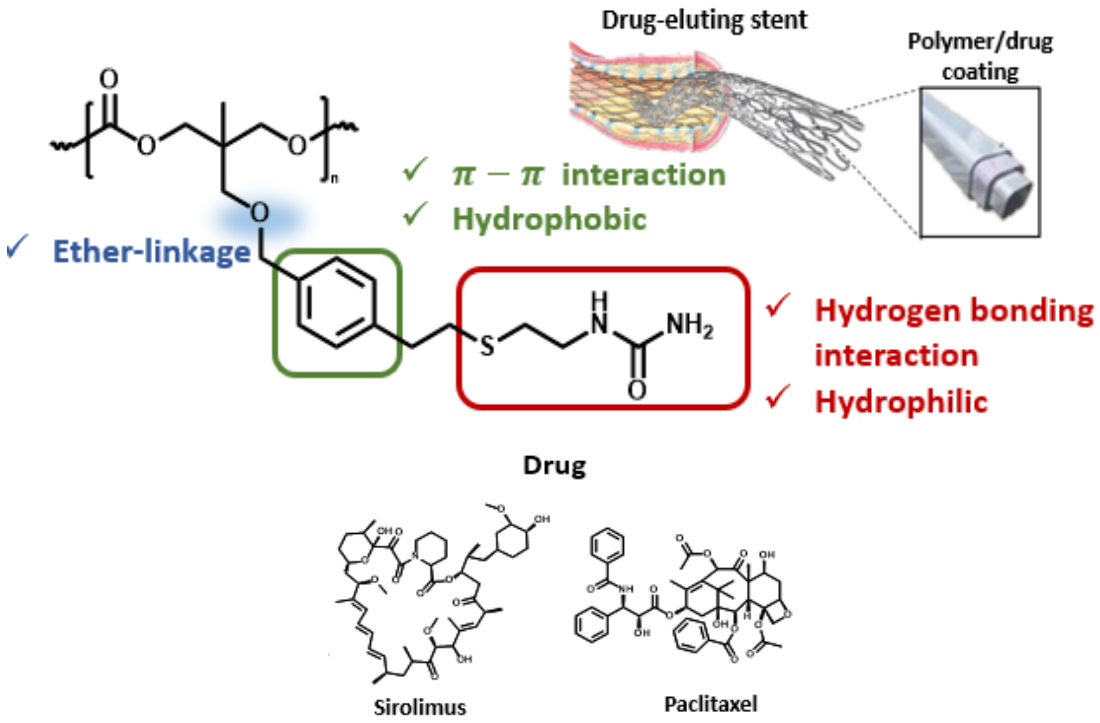

Figure 4-1. Ester-free PTMC bearing with urea-functional group and potential drug incorporation for biomaterial coating[7,8].

4.2 Experimental Section

4.2.1 In vitro drug release test

Polymers of PTMC, PTMCM-VB and PTMCM-SU that synthesized in Chapter 2 were applied for incorporation with sirolimus and paclitaxel drugs. In vitro drug release measurements were carried out by 316L stainless steel with dimension of 5 mm x 5 mm size. Before coating, all the bare samples were pre-treated with ethanol for cleaning the surface. The drug loaded polymers were prepared by solubilizing drug (50 wt% to polymer) in HFIP/DCM (1:1) with the concentration of 2% (w/v). The drug-polymeric solution was sonicated for homogenous solution prior to the dip coating. The pre-treated stainless steel was dip for a few seconds, the substrate was withdrawn at a constant speed and purged with N_2 for drying. The coated samples were immersed in PBS (pH 7.4) as release medium and incubated at 37°C. At predetermined time points, the samples were taken out from the solution. Methanol, good solvent for dissolving the drug was added into the solution with the ratio of PBS/methanol (1:1)[9]. The solution was sonicated to dissolve drug completely. The detector wavelength was set to 277 nm and 230 nm using UV spectrophotometry to obtain sirolimus and paclitaxel response respectively. Three separate samples were measured for each formulation and immersion period. The drug releasing intensities were shown in **Figure S4-1** to **Figure S4-6**.

4.2.2 Cell adhesion and proliferation

The in vitro cell adhesion behavior of polymeric coating was examined using L929 fibroblast. PTMCM-SU with sirolimus coated sample was made with the drug concentration of 10 mg/ml to study the effect of incorporation of drug on the cell adhesion. The coated sample was described in section 2.2.5. The coated samples were prior soaked in PBS under UV lamp to fully adapt to the water environment before cell adhesion test. The cell culture was stained with green fluorescent tracker to facilitate the quantitative counting. 100 µl of 4000 cells/cm^2 cell solution was seeded on the coated sample and incubated at 37 ºC under 5% CO_2 for 7 h and 7 days. The cell morphology was observed using fluorescence microscope and the number of cells was counted.

4.3 Results and Discussion

4.3.1 In vitro drug release test

In this study, the influence of urea-functional group on the drug sirolimus and paclitaxel release profiles were studied using PBS as releasing medium and mixture of PBS/ methanol for measuring UV intensities. The releasing curve in **Figure 4-2** and **Figure 4-3** illustrated both sirolimus and paclitaxel release rates from all polymer types. For sirolimus releasing profile was measured at maximum absorption wavelength 277 nm. Based on the result in **Figure 4-2**, the sirolimus drug releasing from the PTMCM-SU were slower as compared to that of PTMC. The dominant factor was proposed from the presence of urea functional group, forming hydrogen bonding between sirolimus molecules and urea group presented in PTMC polymeric

chain. **Figure S4-7** and **Figure S4-8** displayed the investigation of possible interaction between sirolimus and polymer by the FTIR spetra shift. On the other hand, the release of paclitaxel from polymeric coating was measured at maximum absorption wavelength 230 nm. As compared with the sirolimus releasing rate, the significance of urea group on slower the paclitaxel releasing is much smaller (**Figure 4-3**). This is in line with Ma and his coworkers' study which have similar trend[10]. The release rate of paclitaxel was a little faster than that of sirolimus in vitro. The phenomena are still under investigated. This could be likely due to the extent of hydrogen bonding formation probably influenced by the bulkiness of the drug, entrapment of sirolimus structure with polymer lead to more interaction between sirolimus with polymer chain. **Figure S4-9** and **Figure S4-10** displayed the investigation of possible interaction between sirolimus and polymer by the FTIR spetra shift.

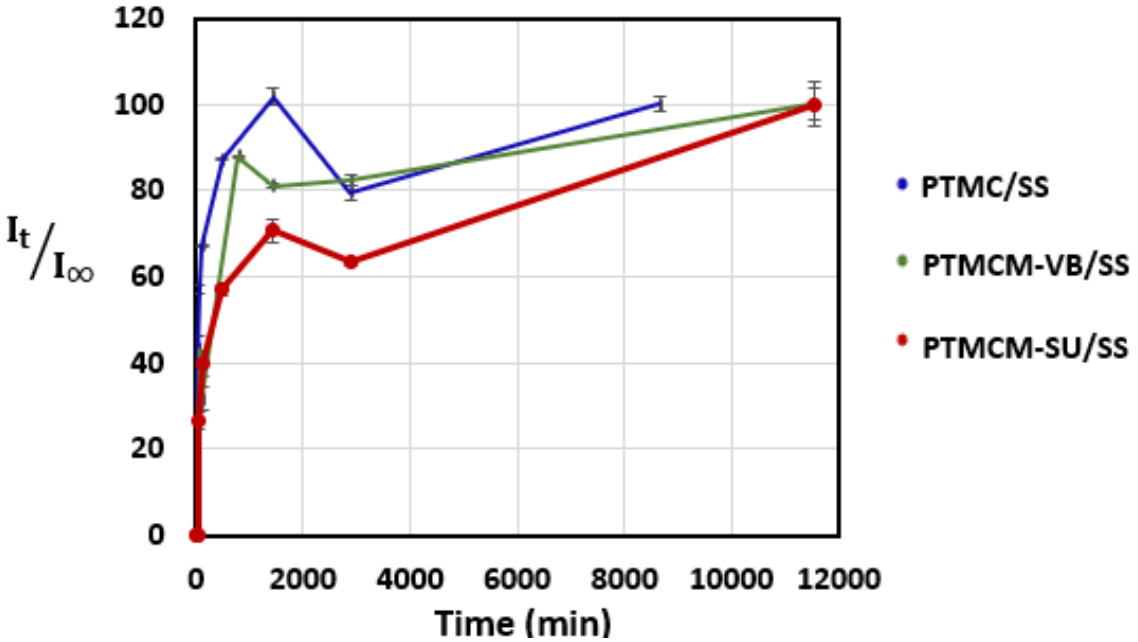

Figure 4-2. Sirolimus drug release profile for PTMC, PTMCM-VB and PTMCM-SU coated on SS substrate.

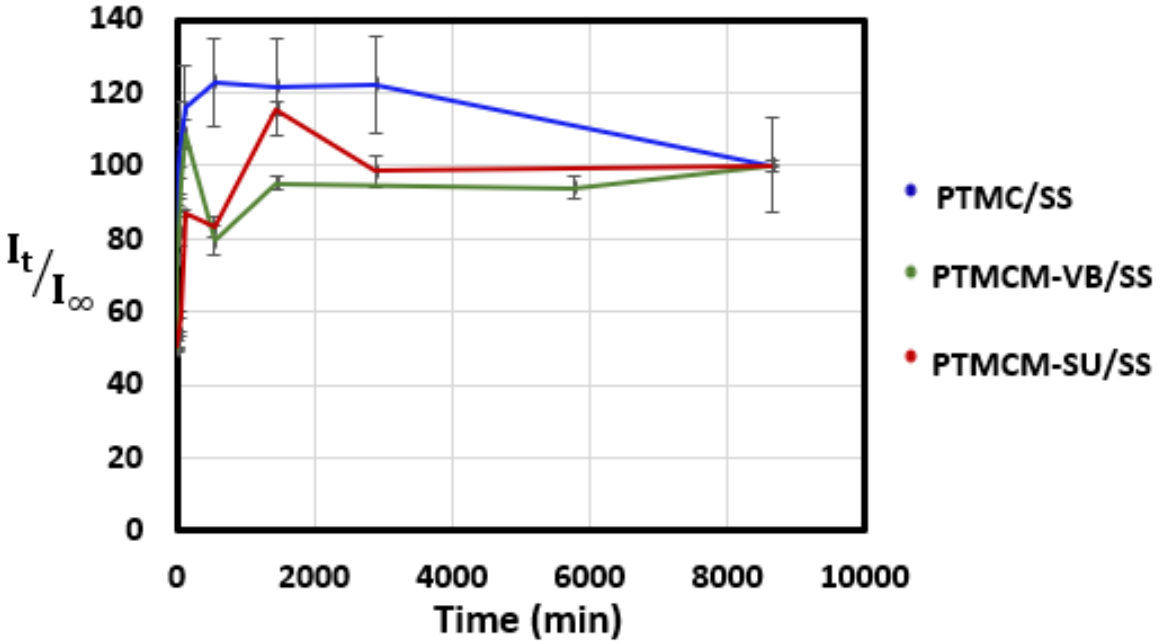

Figure 4-3. Paclitaxel drug release profile for PTMC, PTMCM-VB and PTMCM-SU coated on SS substrate.

4.3.2 Cell adhesion and proliferation

As shown in **Figure 4-4**, the attachment and proliferation of L929 fibroblast cells were investigated after culture for 7 h for 7 days. The cell attachment of cell at 7 h was quantitative through counting the fluorescence images observed from microscope (**Figure 4-4 (a-b)).** The cell adhesion of PTMCM-SU and PTMCM/sirolimus were 1448 ± 235 cells per cm^2 and 596 ± 117 cells per cm^2 respectively (**Figure 4-5).** After incorporation with sirolimus drug, PTMCM-SU/sirolimus coated sample showed fewer cells attached on the sample. There is a comparative study of introduction of sirolimus with PTMC in inhibits the human muscle cells and endothelial cells by Hou and his coworkers[8]. After coating with sirolimus, these materials could not inhibit the adhesion and proliferation of smooth muscle cells. The presence of sirolimus with PTMCM-SU can suppressed

the cell adhesion for the application required unnecessary cell adherent on the biomaterial surface such as drug-eluting stent application. The cell proliferation was studied after 7 days as shown in (**Figure 4-4 (c-f)).** The cell with solely PTMCM-SU tend to in spindle-shaped that spread over the coated substrate while sample with sirolimus was observed almost no cell on the surface. As similar trend as cell adhesion, cell after incorporation of sirolimus drug into polymer PTMCM-SU could inhibited the cell proliferation.

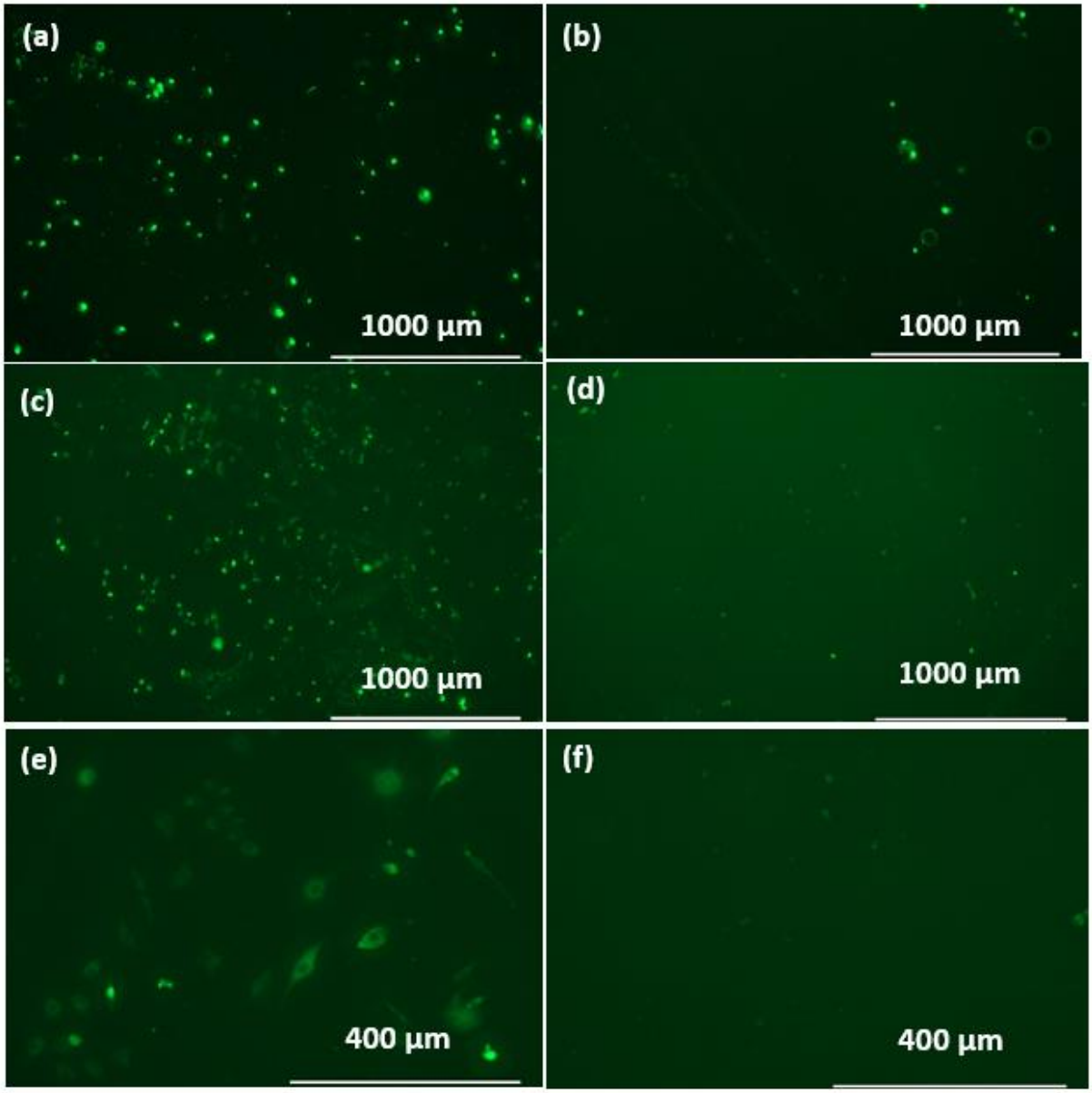

Figure 4-4. Images of L929 cell adhesion on PTMCM-SU/SS (a), PTMCM-SU/sirolimus/SS (b) for 7 h,

PTMCM-SU/SS (c), PTMCM-SU/sirolimus/SS (d) for 7 days with x 1000 µm magnification, PTMCM-SU/SS (e), PTMCM-SU/sirolimus/SS (f) for 7 days with x 400 µm.

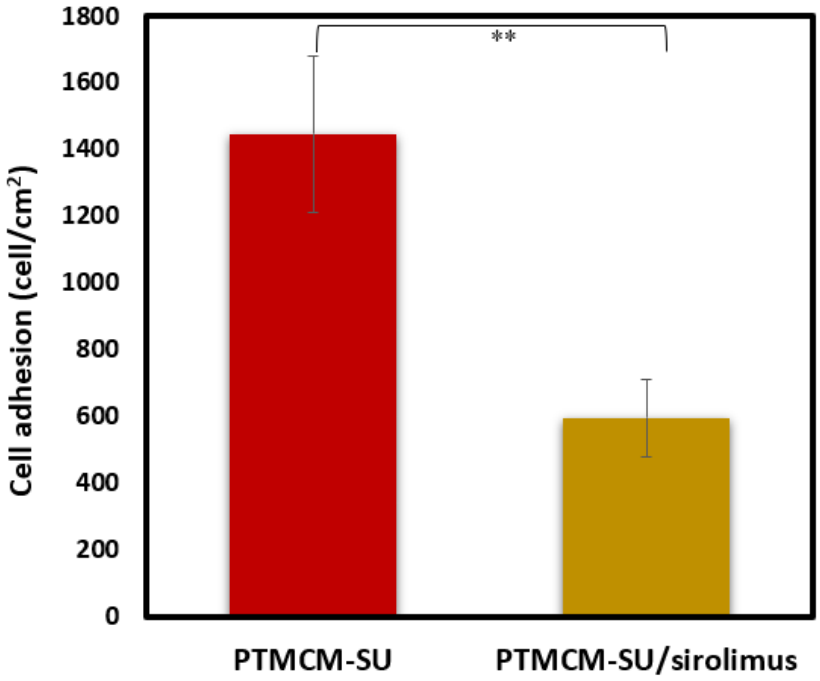

Figure 4-5. Cell adhesion of L929 cell adhesion on PTMCM-SU/SS and PTMCM-SU/sirolimus (n=5, $^{**}p<0.01$).

4.4 Conclusion

In this Chapter, ester-free urea PTMC derivatives of PTMCM-SU was chosen as sirolimus and paclitaxel carrier with the beneficial of urea group for interaction with the drugs. Both drugs were able to slower to release out by the polymer of PTMCM-SU compared to PTMCM-VB and PTMC. This is probably due to the interactions of urea group and drug that assisted the retardment of drug release. The PTMCM-SU coated with sirolimus can inhibit the growth of L929 cells from adhesion and proliferation that could be used as a prospective drug-eluting stent application to prevent any side effect of restenosis.

4.5 Supporting Information

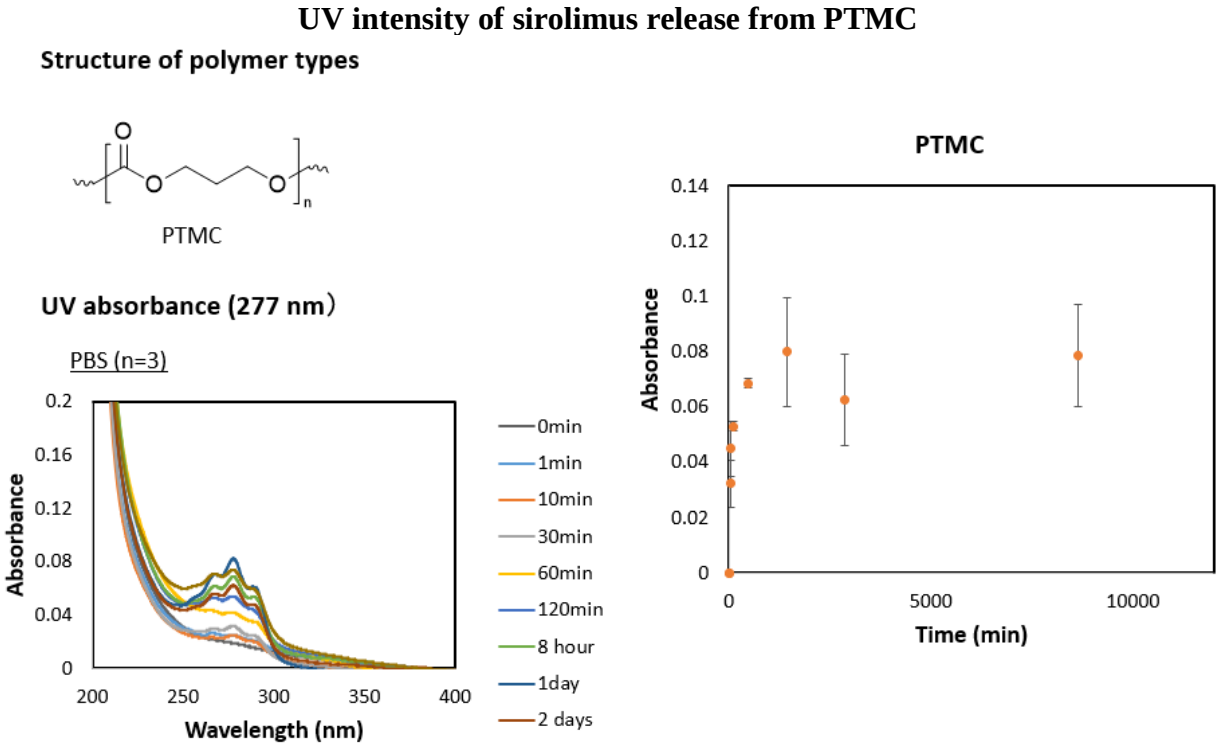

Figure S4-1. Sirolimus drug release profile from PTMC.

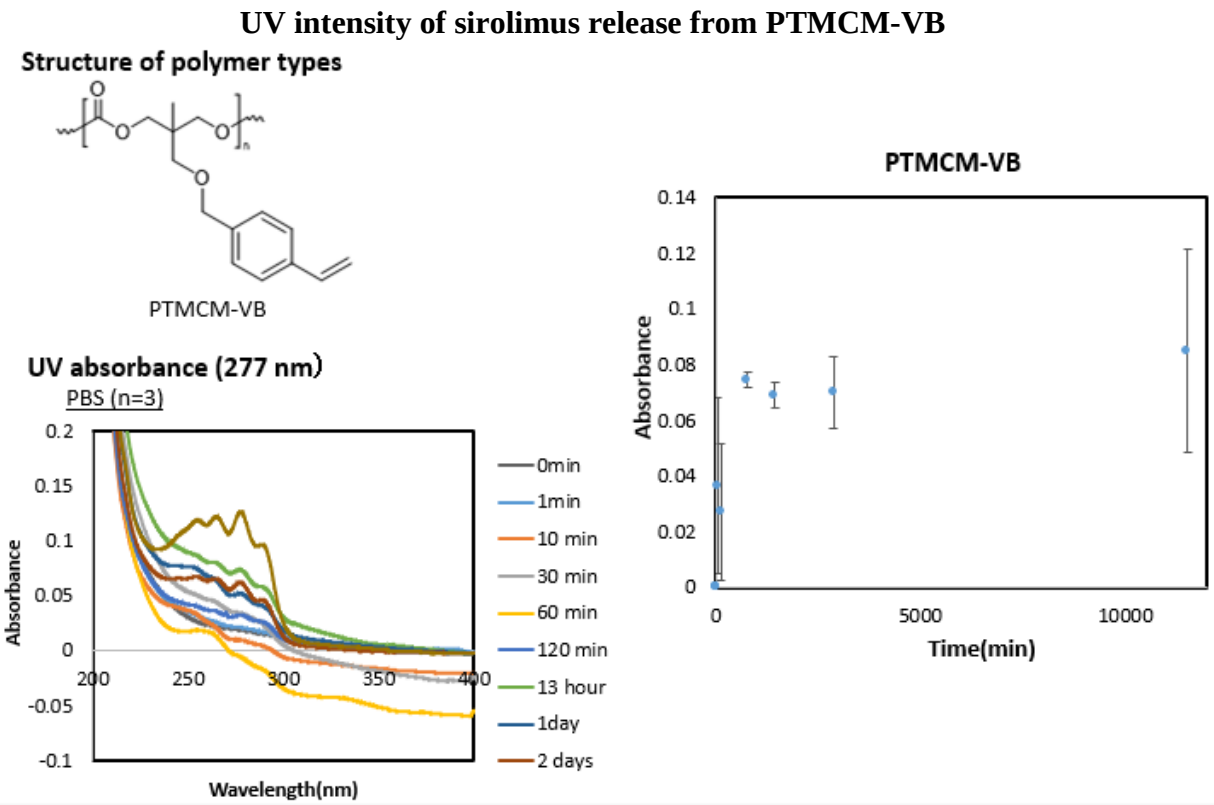

Figure S4-2. Sirolimus drug release profile from PTMCM-VB.

UV intensity of sirolimus release from PTMCM-SU

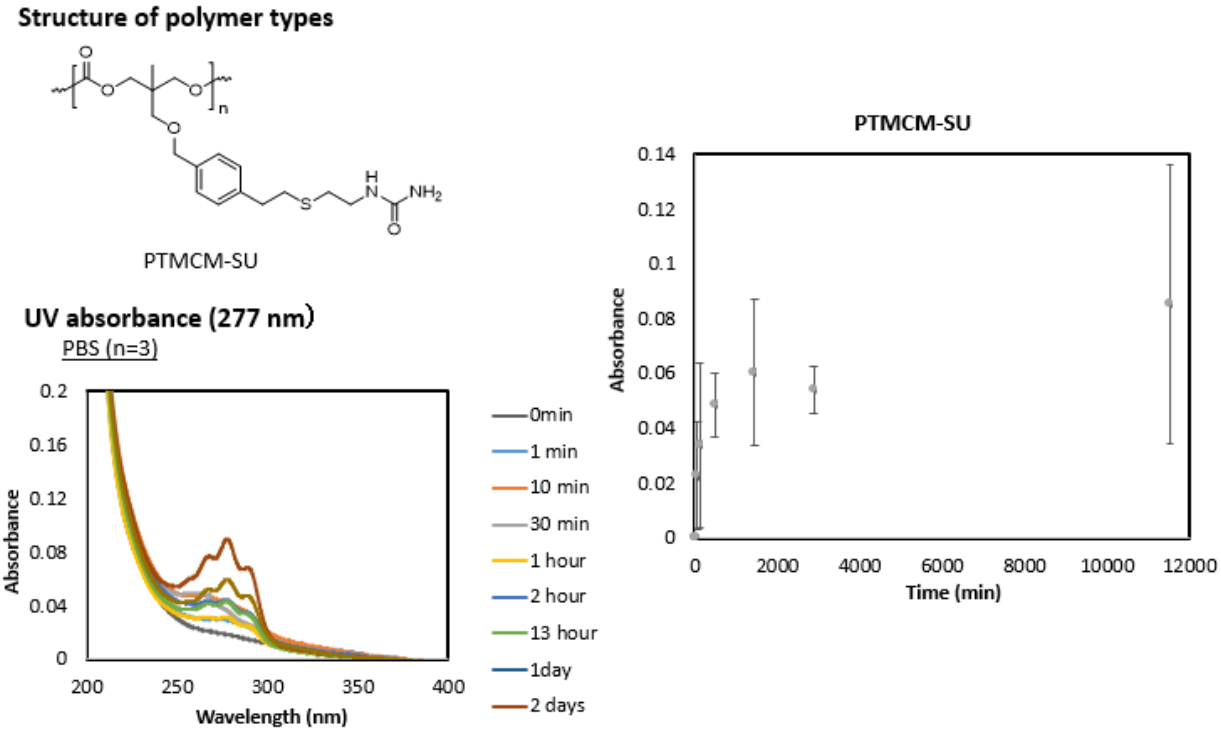

Figure S4-3. Sirolimus drug release profile from PTMCM-SU.

UV intensity of paclitaxel release from PTMC

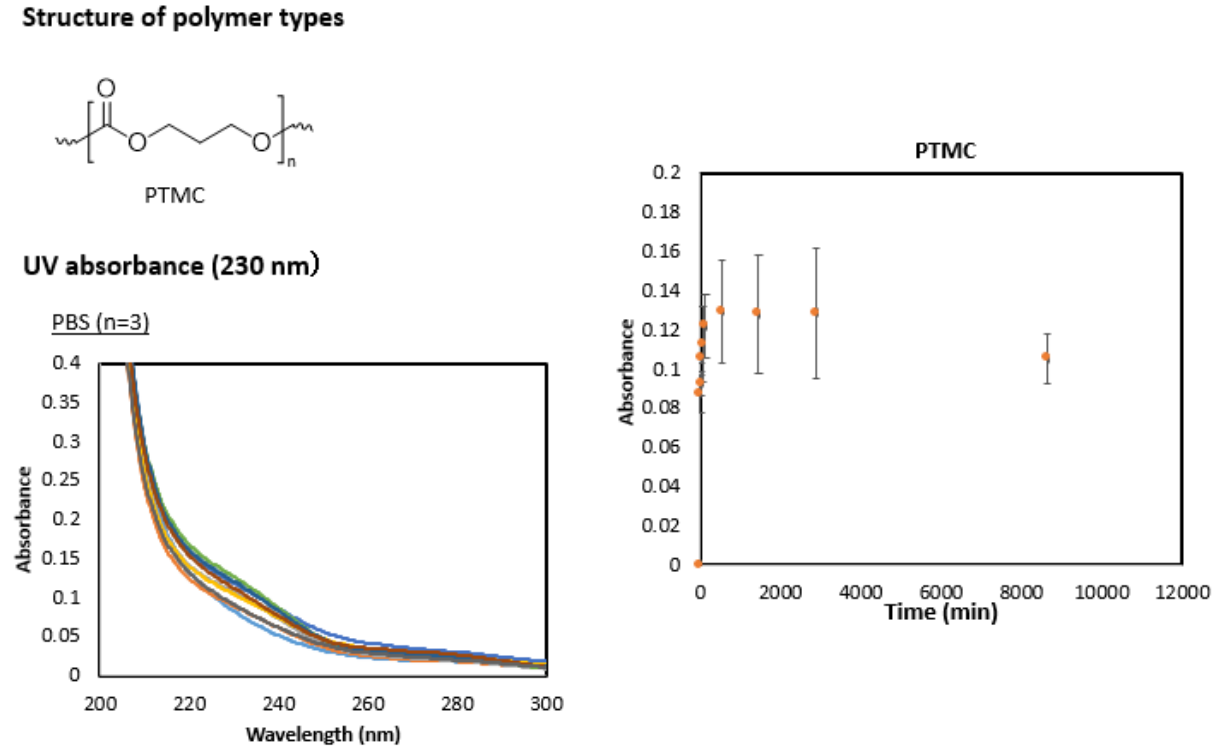

Figure S4-4. Paclitaxel drug release profile from PTMC.

UV intensity of paclitaxel release from PTMCM-VB

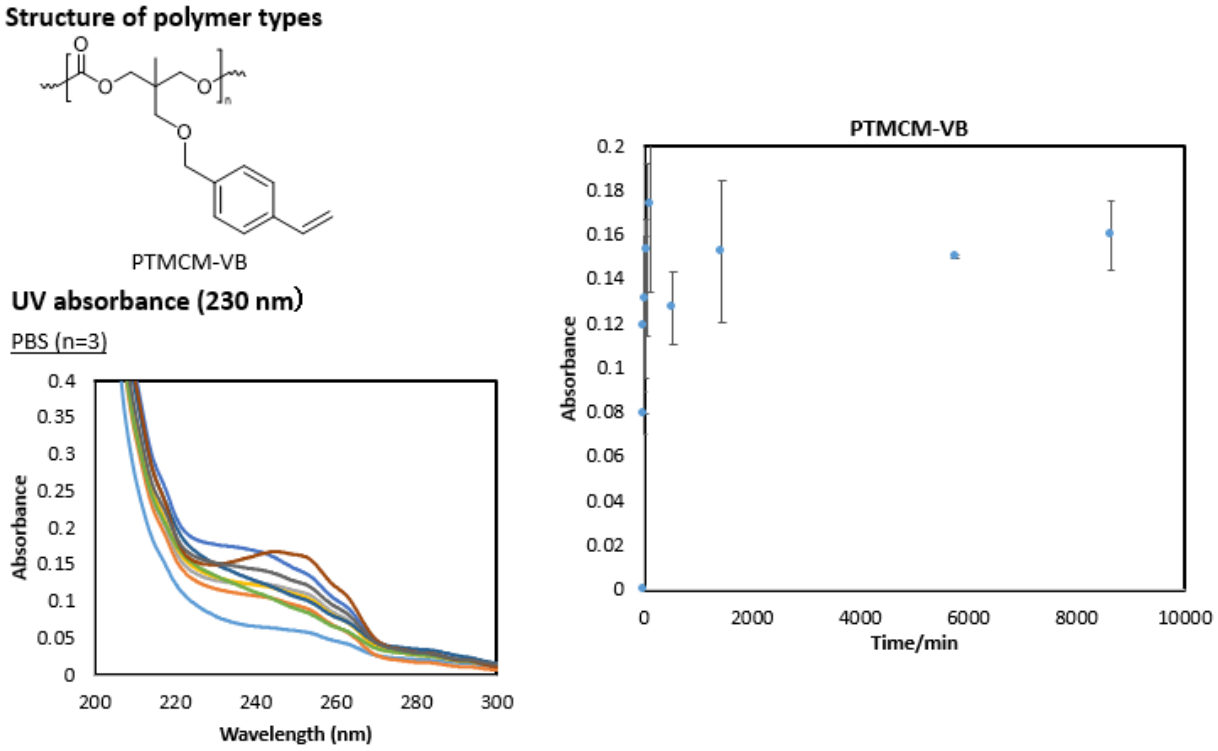

Figure S4-5. Paclitaxel drug release profile from PTMCM-VB.

UV intensity of paclitaxel release from PTMCM-VB

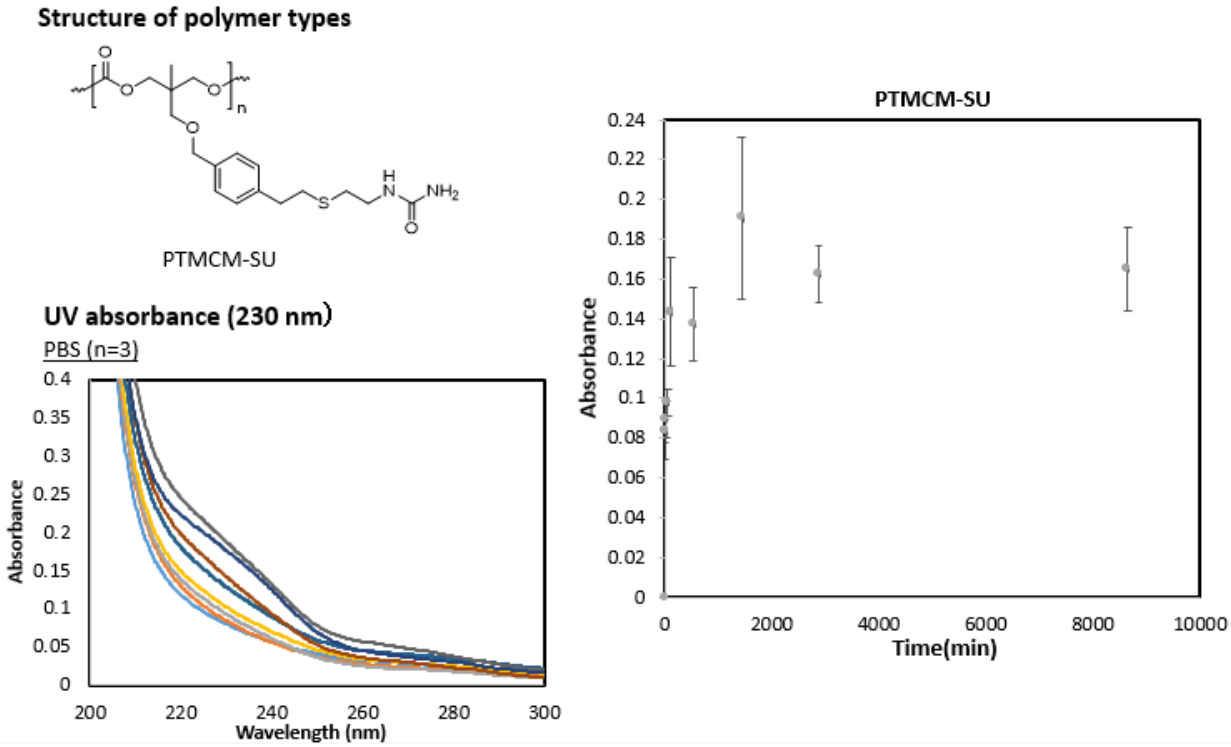

Figure S4-6. Paclitaxel drug release profile from PTMCM-SU.

Comparison of FTIR spectra between PTMCM-SU, sirolimus and PTMCM-SU/Sirolimus

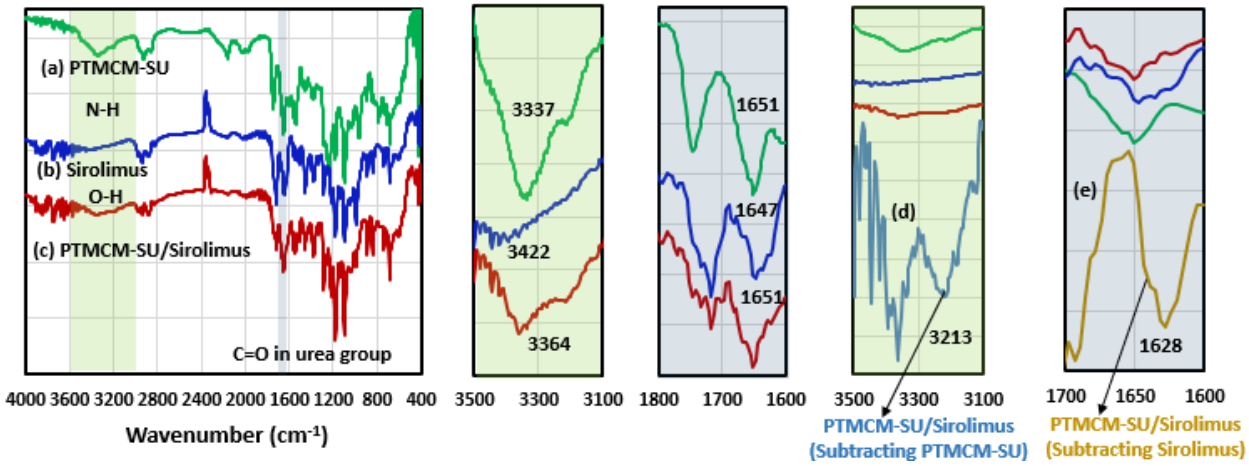

Figure S4-7. Stacked FT-IR of (a) PTMCM-SU, (b) Sirolimus, (c) PTMCM-SU/Sirolimus and sirolimus, (d) PTMCM-SU/sirolimus (Subtract PTMCM-SU), (e) PTMCM-SU/sirolimus (Subtract sirolimus).

FTIR shift of PTMCM-SU/sirolimus in the C=O region (1700cm^{-1})

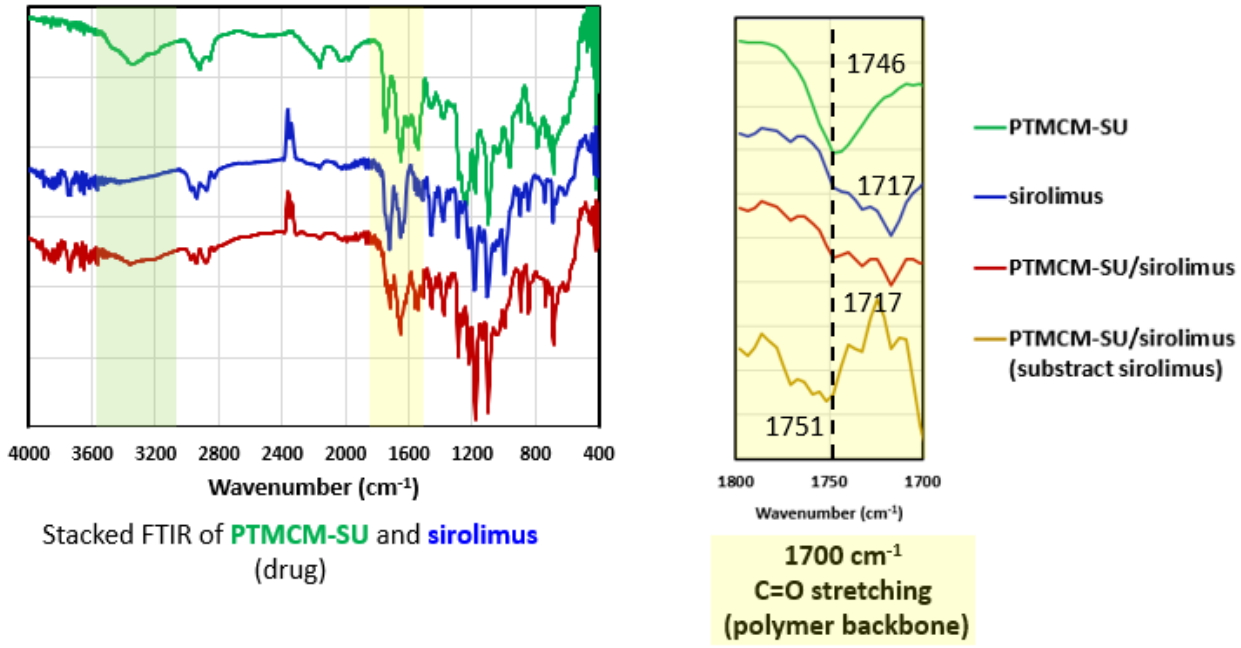

Figure S4-8. Expanded FTIR of PTMCM-SU/sirolimus in the C=O region (1700cm^{-1}).

Comparison of FTIR spectra between PTMCM-SU, paclitaxel and PTMCM-SU/paclitaxel

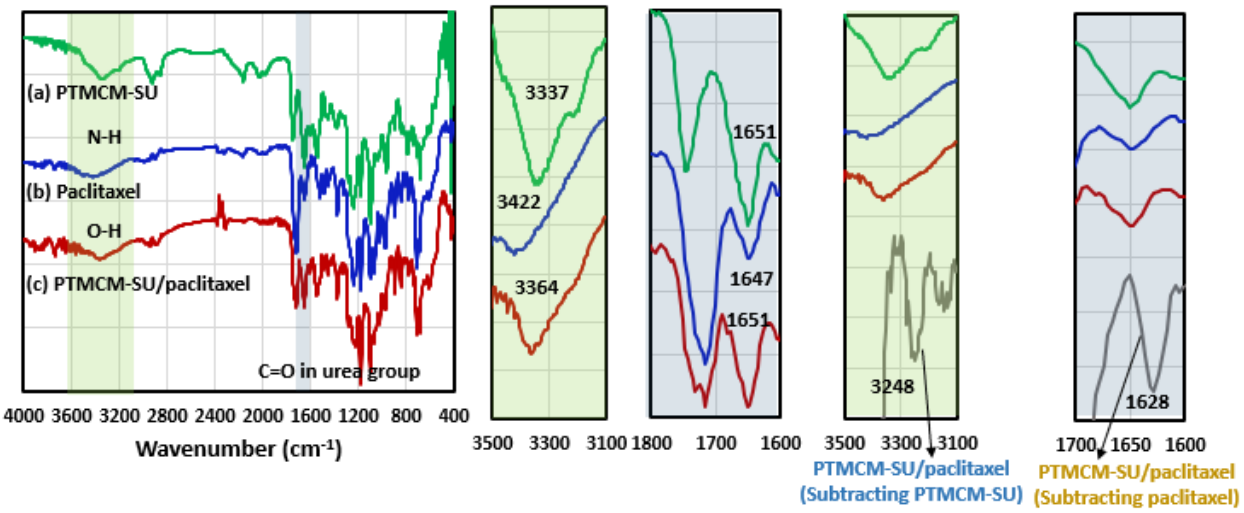

Figure S4-9. Stacked FTIR of (a) PTMCM-SU, (b) paclitaxel, (c) PTMCM-SU/paclitaxel, (d) PTMCM-SU/paclitaxel (Subtract PTMCM-SU), (e) PTMCM-SU/paclitaxel (Subtract paclitaxel).

FTIR shift of PTMCM-SU/paclitaxel in the C=O region (1700cm^{-1})

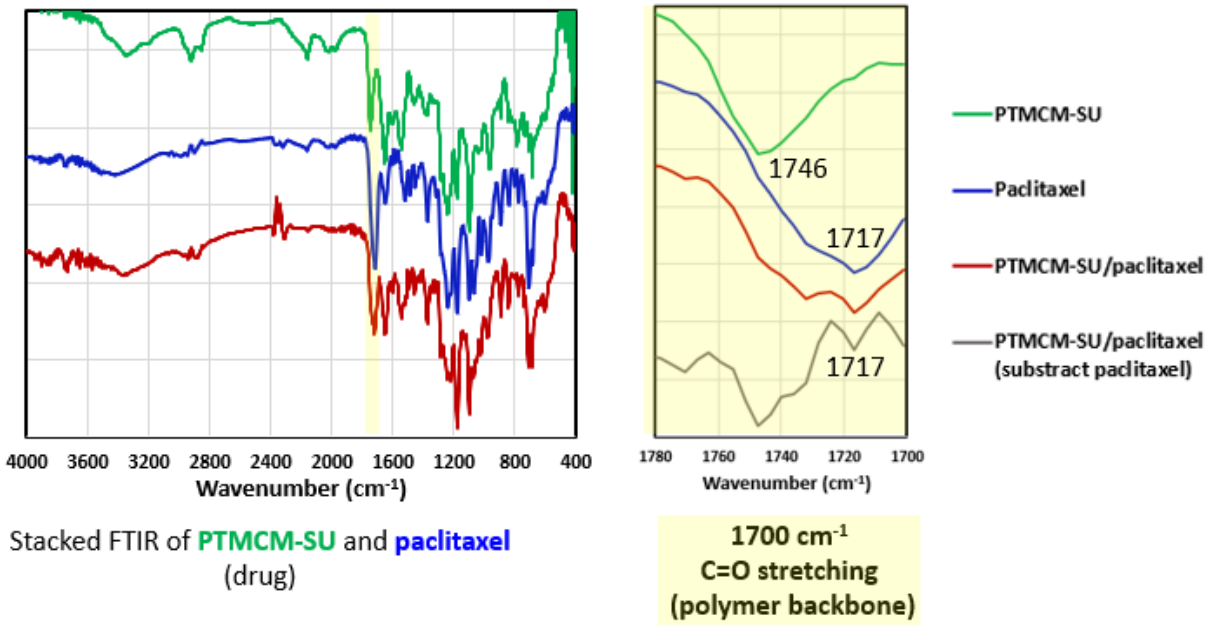

Figure S4-10. Expanded FT-IR of PTMCM-SU/paclitaxel in the C=O region (1700cm^{-1}).

4.6 References

1 S. J. Head, A. J. J. C. Bogers and A. P. Kappetein, *Curr. Opin. Pharmacol.*, **2012**, 12, 147–154.

2 R. Hou, L. Wu, J. Wang, Z. Yang, Q. Tu, X. Zhang and N. Huang, *Biomolecules*, **2019**, 9,69.

3 X. Ma, S. Oyamada, F. Gao, T. Wu, M. P. Robich, H. Wu, X. Wang, B. Buchholz, S. McCarthy, Z. Gu, C. F. Bianchi, F. W. Sellke and R. Laham, *J Pharm Biomed Anal*, **2011**, 54, 807–811.

4 F. Li, Y. Gu, R. Hua, Z. Ni, G. Zhao, *J. Drug Deliv. Sci. Technol.*, **2018**, 48, 88-95.

5 F. Ouazib, N. Bouslah Mokhnachi, N. Haddadine and R. Barille, *J. Polym. Eng.*, **2019**, 39, 534–544.

6 S. Kim, J. Tan, F. Nederberg, K. Fukushima, J. Colson, C. Yang, A. Nelson, Y. Yang, J. Hedrick, *Biomaterials*, **2010**, 31, 8063-8071.

7 S. Ellis and H. Riaz, *Cleve Clin J Med.*, **2016**, 83, 19-23.

8 R. Hou, L. Wu, J. Wang, Z. Yang, Q. Tu, X. Zhang, N. Huang, *Biomolecules*, **2019**, 9,69.

9 MS. Surapaneni, SK.Das, NG. Das, *ISRN Pharmacol.* **2012**, 623139.

10 X. Ma, S. Oyamada, F. Gao, T. Wu, MP. Robich, H. Wu, B. Buchholz, S. McCarthy, Z. Gu, CF. Bianchi, FW. Sellke, R. Laham, *J Pharm Biomed Anal.* **2012**, 5, 217.

Concluding Remark

The aim of the thesis in topic of “Syntheses and post-polymerization modification of ester-free PTMC bearing vinylbenzene derivatives and urea for clinical application” are presented with the development of new biodegradable material with low toxicity based on the ester free structures, and the advanced functionalities by post modification. I designed polymer materials by the introduction with the functional groups that contributed to intermolecular interactions, such as hydrogen bonding, $\pi - \pi$ interaction, and cycloaddition. To achieve the purpose, I prepared the three kinds of polymers using ester free PTMC derivatives by post modification.

In Chapter 1, “Synthesis and Preparation of Crosslinked Films with Ester-free Poly(trimethylene carbonate) Bearing Aromatic Urea Moiety” demonstrated the incorporation of aromatic vinyl with urea group as well as crosslinker for preparation of biodegradable polymeric film for medical application. The designed polymeric film showed increment of thermal stabilities in term of T_{10} and $T_{g.}$ The manipulation of crosslinker ratio and introduction functional group of aromatic and urea moieties resulted enhancement in mechanical properties. Also, the degradation behavior of main polymer structure provided promising stabilities against lipase. The presence of urea group induced hydrophilicity and swelling performance of designed polymer.

In Chapter 2, “Surface Coating and Characteristics of Ester-free Poly(trimethylene carbonate) Bearing an Aromatic Urea Moiety for Biomaterials Use” designed of ester-free PTMC derivatives with aromatic urea moiety as linear polymer, PTMCM-SU for biomaterials coating and its performance. Through UV irradiation pathway, PTMCM-SU was synthesized and its coating on stainless steel was studied in term of thermal performance, wettability, protein adsorption, cell adherence. After introduction of urea group, the resulted polymer possessed increased T_g = -2 °C with increased hydrophilicity with contact angle between 48 ° to 59 °. In biological response in term of protein adsorption and cell adhesion, PTMCM-SU has high affinity for the albumin as well as L929 cell adhesion.

In Chapter 3 “Synthesis of New Ester-free Poly(trimethylene carbonate) Bearing Cinnamyl Moiety for Biomaterials Applications” investigated the introduction of cinnamyl derivatives into PTMC side chain, in order to use crosslinking moiety after polymerization. Furthermore, the incorporation of cinnamyl derivative PTMC with thymol exhibited antibacterial properties against *E.coli* which promising to be use in sterile medical device. Also, electron-rich methoxy-cinnamyl PTMC derivative was able to perform cycloaddition to improve physical properties of PTMC with ease.

In Chapter 4, utilization of urea group in PTMCM-SU was motivated to be used as drug release control *via* intermolecular bonding between polymer and drug. PTMCM-SU displayed slower drug release compared to that of PTMC. Furthermore, to be used as stent application,

PTMCM-SU with promising drug release control was further incorporated with sirolimus to study cell adhesion behavior. The results indicated the suppression of cells from attached on the sample.

As described in this thesis, these PTMC derivatives bearing aromatic moieties after post modification showed improvement in physical state, thermal properties and multifunctionalities, such as drug release control, biological function, antibacterial properties. This could be prospective development for PTMC to be more practically applied in medical field. Therefore, I showed the molecular design of biodegradable polymer is vital to develop more biomaterial in pace the society need. The main objective of the thesis has found valuable characteristics for further research in more sophisticated prospects. I have published the research's outcome as a platform for exchange the knowledge and development of biodegradable polymer for future generation.

List of Publications

Chapter 1:

Lee Yae Tan, Nalinthip Chanthaset*, Shinsuke Nanto, Ryoichi Soba, Masakazu Nagasawa, Hiroshi Ohno, and Hiroharu Ajiro*

"Synthesis and Preparation of Cross-linked Films with Ester-Free Poly(trimethylene carbonate) Bearing Aromatic Urea Moiety", *Macromolecules* **2021**, 54, 12, 5518 – 5525.

Chapter 2:

Lee Yae Tan, Nalinthip Chanthaset, Hiroharu Ajiro,

"Surface Coating and Characteristics of Ester-free Poly(trimethylene carbonate) Bearing an Aromatic Urea Moiety for Biomaterials Use", *Mater. Adv.* **2022,** 3, 5578 – 5785.

Chapter 3:

Lee Yae Tan, Arif Fadlan, Nalinthip Chanthaset, Hiroharu Ajiro,

"Synthesis of New Ester-free Poly(trimethylene carbonate) Bearing Cinnamyl Moiety for Biomaterials Applications", in preparation.

Other Publications

Patent

網代広治、チャタセ ナリンティップ、吉田裕安材、リー ヤエ タン、大浦真歩、南都伸介、“管腔内留置用医療デバイスのコーティング材”、特願特願2022-001250 [国内特許]

Acknowledgements

First, I would like to express my deep gratitude to Prof. Hiroharu Ajiro, Associate Prof. Tsuyoshi Ando, Assistant Prof. Nalinthip Chanthaset, and to my advisors Prof. Hironari Kamikubo and Associate Prof. Naoki Aratani. During these 3 years, I have grateful for all the valuable guidance, either for research study or to be a better person for society. This work could not be achieved without their supervision. Also, I would like to thanks co-authors Prof. Shinsuke Nanto, Mr. Ryoichi Soba, Dr. Masakazu Nagasawa, Mr. Hiroshi Ohno, and Assist. Prof. Arif Fadlan for their consistent guidance and suggestion for my research study. Besides, I would like to thanks NAIST technicians' staff and NAIST officer for their unconditionally teaching and support during my study. I would like to lovely thanks to all the members of the Nanomaterials and Polymer Chemistry laboratory for their accompany and encouragement, especially my tutor Ms. Miyaji Yumi for helping me settle down in Japan, Ms Kamolchanok Sarisuta for always there for me. I would like to cherish all the people I have met in NAIST, the friendship and memories I will never forgot. Finally, I would like to express my eternal love to my family who made me who I am today.